Selective Modulation of PML Nuclear Bodies by Adenovirus Regulatory Proteins

DISSERTATION

with the aim of achieving a doctoral degree at the

Faculty of Mathematics, Informatics and Natural Sciences,

Department of Biology,

University of Hamburg

submitted

by

Julia Berscheminski

January 2014 in Hamburg

Tag der Disputation:	14.03.2014
Gutachter:	Prof. Dr. T. Dobner
	PD Dr. N. Fischer
Prüfungsvorsitzende:	Prof. Dr. J. Kehr

HPI Heinrich-Pette-Institut
Leibniz-Institut für Experimentelle Virologie

Carol Stocking, Ph.D.
Retrovirus Pathogenesis, Head
Phone: +49-40-48051 273
Fax: +49-40-48051 187
Email: stocking@hpi.uni-hamburg.de

Studienbüro Biologie
z.H. Frau Sült-Wüpping
MIN Fakultät
Universität Hamburg
Biozentrum Klein Flottbek
Ohnhorststr. 18
22609 Hamburg

09. Januar 2014

Sehr geehrte Damen und Herrn,

hiermit bestätige ich, dass die von Frau Julia Berscheminski mit dem Titel "Selective Modulation of PML Nuclear Bodies by Adenovirus Regulatory Proteins" vorgelegte Doktorarbeit in korrektem Englisch geschrieben ist.

Mit freundlichen Grüßen,

Carol Stocking

Dr. Carol Stocking

Leiterin der FG Retrovirus Pathogenesis
Heinrich-Pette-Institut
(Amerikanerin)

Heinrich-Pette-Institut
Leibniz-Institut für
Experimentelle Virologie

Martinistrasse 52 · 20251 Hamburg
Telefon +49 (0) 40 480 51-0
Telefax +49 (0) 40 48051-103
hpi@hpi.uni-hamburg.de

Bankverbindung
Haspa (200 505 50)
Konto 1001 315 959
www.hpi-hamburg.de

Mitglied der
Leibniz-Gemeinschaft

Declaration under oath

I hereby declare under oath that I have written the present dissertation by myself and have only used the acknowledged resources and aids.

Hamburg, 15.01.14 Signature Benchenki

Table of contents

Abbreviations

aa	amino acid
Ad	Adenovirus
APS	Ammonium persulfate
ATP	Adenosine triphosphate
B	B-Box
BRK	baby rat kidney cells
BSA	bovine serum albumin
CC	coiled-coil
CH	Cysteine Histidine
CR	conserved region
DAPI	4', 6-Diamidine-2-phenylindole dihydrochloride
dd	double-distilled
Daxx	Death-associated protein 6
DEPC	Diethylpyrocarbonate
DMEM	Dulbecco's Modified Eagle Medium
DMSO	Dimethylsulfoxide
DNA	Desoxyribonucleic acid
dNTP	Desoxyribonucleoside-5'-Triphosphate
ds	double-stranded
DTT	Dithiotreithol
E	early region
EBV	Epstein-Barr virus
ECL	Enhanced Chemiluminescence
E.coli	*Escherichia coli*
EDTA	Ethylenediaminetetraacetic acid
ETOH	Ethanol
FCS	fetal calf serum
FITC	Fluorescein isothiocyanate
ffu	Fluorescence forming units
fw	forward
HAT	Histone acetyltransferase
HCMV	Human cytomegalovirus
HDAC	Histone deacetylase

HEK	Human embryonic kidney
HP1	Heterochromatin protein 1
h p.i.	hours post infection
HRP	horse-radish peroxidase
HSV-1	Herpes simplex virus 1
HVS	Herpesvirus saimiri
ICP0	Infected Cell Polypeptide 0 protein
IFN	Interferon
Ig	Immunoglobulin
IgH	Immunoglobulin heavy chain
IgL	Immunoglobulin light chain
IP	Immunoprecipitation
kDa	Kilodalton
KSHV	Kaposi's sarcoma-associated herpesvirus
L	late region
LB	Luria Bertani
mRNA	messenger RNA
MOI	Multiplicity of infection
ND10	Nuclear domain 10
NEM	N-ethylmaleimide
NES	nuclear export signal
NLS	nuclear localization signal
nt	nucleotide
OD	optical density
ORF	open reading frame
PBS	Phosphate buffered saline
PFA	Paraformaldehyde
PIAS	Protein inhibitors of activated STAT
PML	Promyelocytic leukemia protein
PML-NB	PML nuclear body
POD	PML oncogenic domain
PVDF	Polyvinylidene fluoride
R	RING
RanBP2	Ran binding protein 2

Rb	Retinoblastoma protein
RBCC motif	RING, B-Box, coiled-coil domain
rev	reverse
RING	Really interesting new gene
RNA	ribonucleic acid
RNF4	RING finger 4
rpm	rounds per minute
RT	room temperature
SAE	SUMO activating enzyme
SDS	Sodium dodecyl sulfate
SDS-PAGE	SDS polyacrylamide gel electrophoresis
SENP	Sentrin specific protease
SIM	SUMO interaction motif
Sp100	Speckled protein 100
SUMO	Small ubiquitin related modifier
TEMED	N, N, N‘, N‘-Tetra-methylethylendiamine
TRIM	tripartite motif
Tris	Tris-(hydroxymethyl)-aminomethane
U	unit
Uba	Ubiquitin activating enzyme
vol	volume
v/v	volume per volume
w/v	weight per volume
wt	wild type

1 Abstract

PML nuclear bodies (NBs) are matrix-bound nuclear structures that have been implicated in a variety of functions, including DNA repair, transcriptional regulation, protein degradation, and tumor suppression. These domains are also known to play an essential role in antiviral host-cell defense, most presumably mediated via accumulation of SUMO-dependent and interferon-induced antiviral host factors. This likely explains why they are targeted and subsequently manipulated by numerous viral regulatory proteins. Paradoxically, the genomes of numerous DNA viruses become associated with PML-NBs, and initial sites of viral transcription/replication are often juxtaposed to these domains. To date several Ad regulatory proteins have shown association with PML-NBs, illustrating their crucial role during Ad infection, although the functional consequences of this association are still largely elusive. Particularly, the early adenoviral regulator E1B-55K has been shown to cooperate with various PML-NB-associated host factors in a SUMO-dependent manner. The aim of this work was to further elucidate the interplay between Ad regulatory proteins and PML-NBs, to unravel the enigma of these nuclear structures with respect to their role during Ad5 infection.

The first part of this work shows that the major adenoviral transactivator protein E1A-13S targets PML-NBs. Co-immunoprecipitation assays revealed that E1A-13S preferentially interacts with only one of at least six nuclear human PML isoforms, namely PML-II, which is also essential for Ad5 induced relocalization of PML-NBs into so called track-like structures. Deletion mapping located the interaction site within the E1A CR3, previously described as the transcription factor-binding region of E1A-13S. Indeed, cooperation with PML-II enhanced E1A-13S-mediated transcriptional activation. These results suggest that contrary to PML-NB-associated anti-viral defense, PML-II may support transactivation of viral gene expression.

The second part of this work unravels the role of the PML-NB-associated, alternatively spliced transcriptional regulator Sp100 during productive Ad5 infection. Knockdown of Sp100 using RNAi techniques resulted in significantly increased Ad replication, including enhanced viral gene expression. Sp100-mediated restriction of Ad growth proved to be dependent on the expression of Sp100 isoforms B, C and HMG, repressing viral gene expression at the transcriptional level. However, the Sp100A isoform enhanced transcription from viral and cellular promoters in luciferase-reporter assays. To ensure efficient viral replication, Ad has apparently evolved strategies to antagonize Sp100-

mediated restriction by alternative mechanisms. Ad5 induces relocalization of Sp100 B, C and HMG from PML-NBs, whereas Sp100A is kept in the PML tracks, which surround the newly formed viral replication centers as designated sites of active transcription. Ad-dependent loss of Sp100 SUMOylation is another crucial aspect of the virus repertoire to counteract intrinsic immunity by abrogating Sp100 association with the Heterochromatin protein 1 (HP1), likely limiting chromatin condensation. Additional data illustrate that E1B-55K interacts only with Sp100A via the C-terminal domain of E1B-55K in a SUMO-dependent manner, presumably causing the recruitment of Sp100A to PML-NBs.

Together this work provides evidence that Ad selectively counteracts antiviral responses, and at the same time benefits from proviral PML-NB-associated components by actively recruiting them to PML track-like structures, thereby creating a positive microenvironment for viral transcription and replication at these nuclear subdomains.

2 Introduction

2.1 Adenoviruses

2.1.1 Classification and pathogenesis

Adenoviruses (Ads) were first isolated from adenoid tissues and characterized in 1953 while attempting to identify the causative agents of acute respiratory infections (Hilleman & Werner, 1954; Rowe *et al.*, 1953). The isolated viruses were named *adenoviruses* in accord with the original cells from which the first virus was isolated (Enders *et al.*, 1956; Rowe *et al.*, 1953). It soon became clear, that although Ads may infect respiratory tracks, it causes only a small percentage of respiratory illness in the general population and is not the major etiologic agent of the common cold (Berk, 2007).

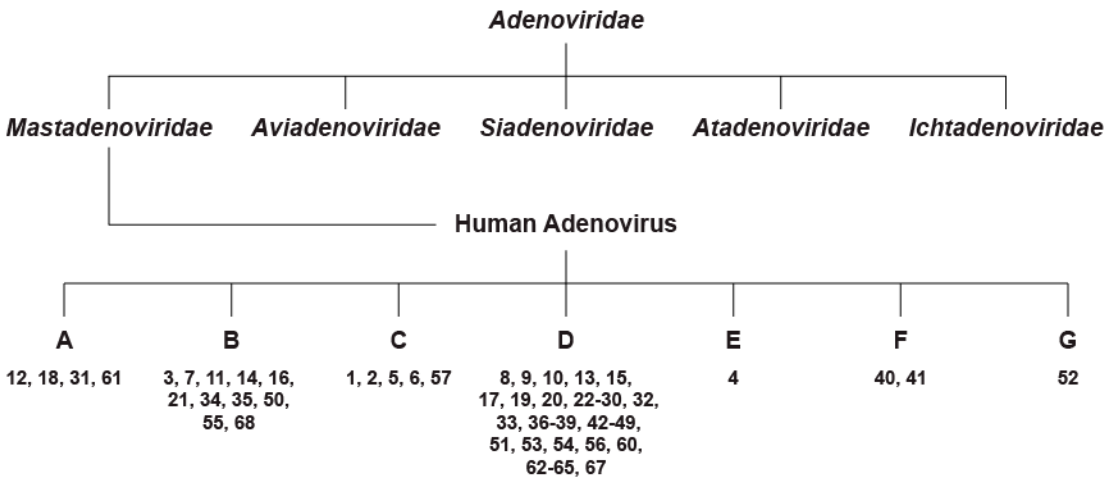

Figure 1: The family of *Adenoviridae*. Schematic representation of the family of *Adenoviridae*. Letters A-G indicate human Ad species, numbers 1-68 indicate human Ad serotypes according to Davidson *et al.* (Davison *et al.*, 2003) and the International Committee of the Taxonomy of Viruses (ICTV).

The family of *Adenoviridae* infects a wide range of vertebrate hosts and can be classified into five genera depending on their host specificity: Mastadenoviruses isolated from mammals, Aviadenoviruses isolated from birds, Siadenviruses isolated from amphibians and birds, Atadenoviruses isolated from ruminant, reptile, avian and marsupial hosts and Ichtadenoviruses isolated from fish (Benko & Harrach, 1998; Davison *et al.*, 2003; Fig. 1). Human Adenoviruses, belonging to the genus Mastadenovirus, are highly prevalent in the human population (Davison *et al.*, 2003). Historically, 51 human Ad serotypes have been clustered into six distinct species (previously called subgroups) A-F, according to their agglutination properties (Bailey & Mautner, 1994; De Jong *et al.*, 1999; Wadell, 1984). Since

then, a number of additional classification methods have been considered, such as subgrouping based on sequence similarities, oncogenicity in rodents, relatedness of tumor antigens or electrophoretic mobility of virion proteins (Berk, 2007). New Ad types have been identified by several research groups based on genomic data, including several emerging and recombinant viruses, for at total of 68 unique human Ad types (Bailey & Mautner, 1994; Buckwalter *et al.*, 2012; Davison *et al.*, 2003; Fig. 1). As Ads display a certain degree of tissue specificity, several clinical syndromes in humans are associated with a particular group of Ads causing a wide array of diseases, including pharyngitis, pneumonia, gastroenteritis, hemorrhagic cystitis or keratoconjungtivitis (Jawetz, 1959; Mautner *et al.*, 1995; Yolken *et al.*, 1982). In immunocompetent adults, Ads usually cause a mild, self-limiting local infection. However, in immunocompromised individuals, above all organ transplant recipients, HIV patients developing AIDS, and those receiving radiation and chemotherapy against tumors, Ads may cause life-threatening opportunistic infections with frequently fatal consequences (Abe *et al.*, 2003; Carrigan, 1997). Furthermore, human Ads are responsible for outbreaks in certain populations such as day care attendees and military recruits (Gaydos & Gaydos, 1995; Gray *et al.*, 2000). Especially members of species B have been frequently associated with epidemic outbreaks of systemic infections with high fever, pneumonia, gastroenteritis or central nervous system symptomatology (Louie *et al.*, 2008; Wadell, 1984; Zhu *et al.*, 2009). In infants, these infections are particularly severe and may be fatal.

2.1.2 Structure and genome organization of human Adenoviruses

Human Ads are large (~90 nm diameter) non-enveloped viruses containing a linear, double-stranded (ds) DNA genome of 26-45 kDa (Rux & Burnett, 2004; San Martin & Burnett, 2003). The genome ends harbor several inverted terminal repeats (ITR) and the 5' ends are associated with terminal proteins (TP), which serve as primers for initiating the viral DNA synthesis (Davison *et al.*, 2003). Most structural studies have focused on the closely related human adenoviruses type 2 and 5 (Ad2 and Ad5). Their icosahedral capsid shells are composed of three major proteins: 240 hexon (II) trimers, forming 20 triangular facets of the capsid surface, 12 penton base (III) pentamers, one at each of the 12 vertexes of the icosahedron and 12 Fiber (IV) trimers projecting from the penton base pentamers (Fig. 2). The C-terminal Fiber knob mediates initial attachment to host cells via high affinity interactions with the cell receptor. For most human Ad types, the Coxsackie/Adenovirus Receptor (CAR) (Bergelson *et al.*, 1997; Wu *et al.*, 2003) or CD46

(Gaggar *et al.*, 2003) serve as the major primary receptors. Additionally, the penton base protein facilitates efficient virus uptake via secondary interaction with integrins on the host cell surface (Mathias *et al.*, 1994; Wickham *et al.*, 1994; Wickham *et al.*, 1993).

The so-called minor capsid proteins IIIa, VI, VIII and IX were initially thought to function as cement proteins that help stabilizing the capsid. However, recent publications showed that apart from their structural features, they also exert crucial functions within the host cell. One example represents the minor capsid protein VI, which participates in disruption of the endosomal membrane after virus entry and plays an antagonistic role in the initial antiviral response in the cell nucleus (Schreiner *et al.*, 2012; Wiethoff *et al.*, 2005). The genome core inside the capsid is composed of the DNA, five additional proteins (V, VII, μ, IVa2, terminal protein (TP) and the viral protease (Everitt *et al.*, 1973; Vellinga *et al.*, 2005). The core polypeptides V, VII and μ condense the viral DNA into a nucleoprotein complex (Harpst *et al.*, 1977; Russell *et al.*, 1971; Russell & Precious, 1982). Protein V is able to bind protein VI and penton base suggesting a role as a linker between core and capsid (Everitt *et al.*, 1975). The viral protease plays a critical role in the assembly of the virion by processing the precursors of the structural proteins (Anderson, 1990; Webster *et al.*, 1989) and

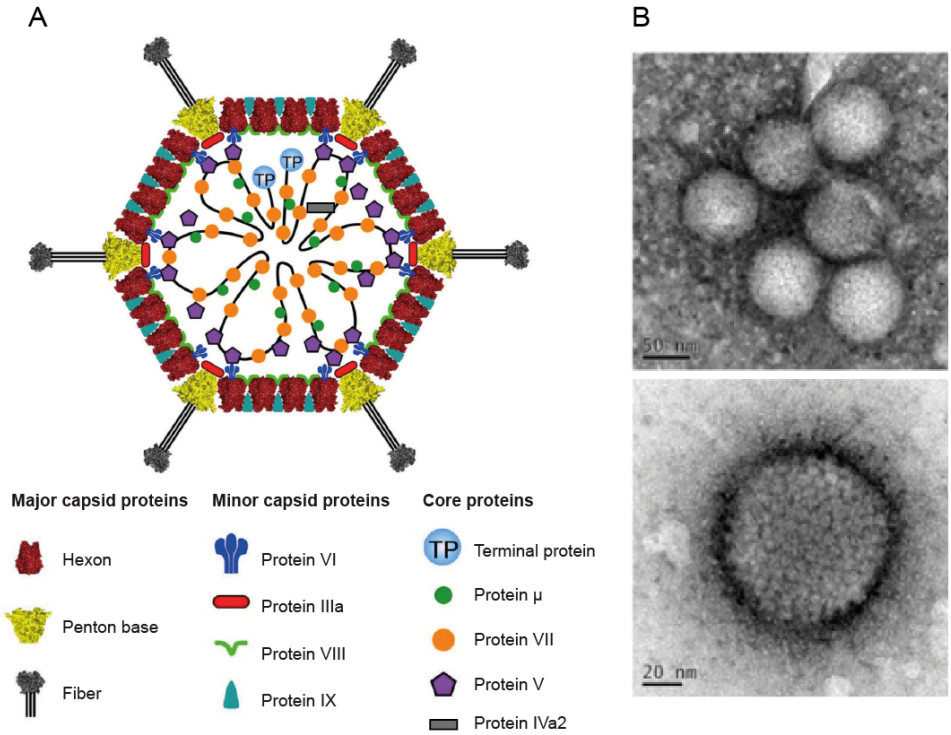

Figure 2: Adenovirus capsid structure. (A) Schematic representation of Ad5 according to Nemerow *et al.* (Nemerow *et al.*, 2009; Russell, 2009). (B) Electron microscope images illustrating the icosahedral structure of Ad5 particles (Department of Electron Microscopy, Heinrich Pette Institute, Leibniz Institute for Experimental Virology, Hamburg).

polypeptide IVa2 associates with a specific stretch of the virus DNA and participates in the DNA packaging process (Zhang *et al.*, 2001). The genome of Ad5 contains nine transcription units encoding 40 regulatory and structural proteins as well as two non-coding RNAs (virus-associated RNAs, VA-RNAs; Fig. 3). The transcription units comprise five early (E1A, E1B, E2, E3, E4), two delayed (IX, IVa2) and the major late transcription unit (MLTU) resulting in five families of late mRNA (L1-L5) after processing. Early proteins are involved in transcriptional/translational regulation, mRNA export, viral DNA replication, cell cycle control and prevention of the host antiviral response. Late units mainly encode for structural proteins but also have functions in the very early stages of infection. Apart from the VA-RNAs, all Ad5 transcription units are transcribed by the cellular RNA polymerase II (Weinmann *et al.*, 1974).

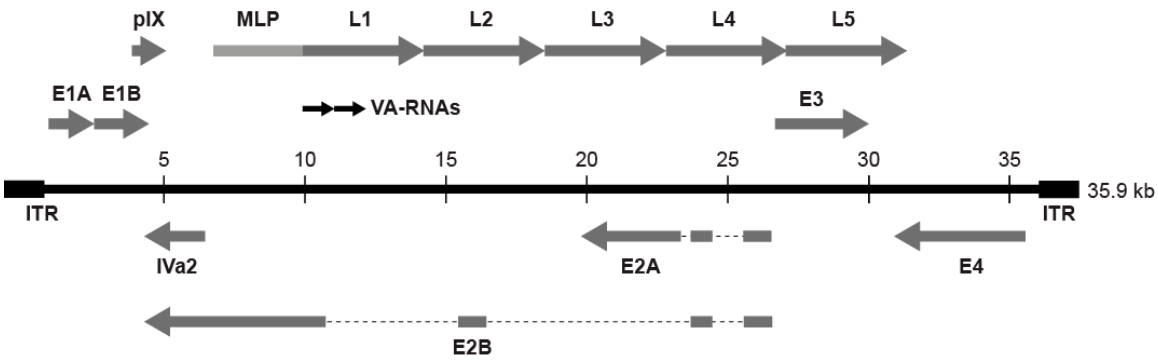

Figure 3: Genome organization of Ad5. Organization of early (E1A, E1B, E2A, E2B, E3, E4), delayed (IX, IVa2) and late (L1-L5) transcription units is indicted by arrows. E: early; L: late; ITR: inverted terminal repeat; VA-RNA: Virus-associated RNA.

2.1.3 Productive infectious cycle of human Adenoviruses

Human Ads generally infect post-mitotic resting, differentiated epithelial cells of the respiratory and gastrointestinal tracts. Additionally, several tumor and primary cell lines can be infected in tissue culture. Generally, Ads cause lytic infections in human cells, whereas infection of animal cells, in particular rodent cells, results in an abortive infection.

The adenoviral productive replication cycle is divided by convention into two phases, the early and the late phase, separated by the onset of viral DNA replication. The early events start as soon as the virus interacts with the host cell. The viral genes encoding proteins IVa2 and IX begin to be expressed at an intermediate time and thus form a delayed early category (Bridge & Pettersson, 1995).

Upon receptor-mediated internalization of the viral particle, mainly via clathrin-mediated endocytosis (Greber *et al.*, 1993; Varga *et al.*, 1991), the clathrin-coated vesicles mature to endosomes, from which the virus escapes into the cytosol by pH shift and pVI permeabilizing the endosomal membrane (Greber *et al.*, 1993; Wiethoff *et al.*, 2005). After microtubule-dependent transport to the nucleus, the subviral particle associates with the nuclear pore complex and the viral DNA/ core complex is imported into the nucleus. Subsequently, "immediate early" gene expression is initiated with E1A as the first transcription unit to be expressed (Nevins *et al.*, 1979). E1A is the major viral transcriptional activator, responsible for onset of transcription from the early transcription units E1-E4 (Winberg & Shenk, 1984). The early viral regulatory proteins ascertain an optimal environment for virus replication, with E1A/ E4 gene products inducing the host cell to enter the S-phase of the cell cycle, and E1/ E3 protecting the viral system from various antiviral defenses of the host organism, such as apoptosis, growth arrest or immune response (Berk, 2007). Proteins of the E2 region are mainly involved in viral DNA replication, encoding for the viral DNA binding protein (DBP or E2A), the viral DNA polymerase (E2B) and the terminal protein (TP; Shenk, 2001). The E4 region encodes for at least six different products transcribed from several open reading frames, namely E4orf1, E4orf2, E4orf3, E4orf4, E4orf6 and E4orf6/7, which mediate essential functions during efficient virus replication (Tauber & Dobner, 2001b).

Concomitant with the onset of viral DNA replication, the late phase of the viral replication cycle begins with expression of the major late transcription unit (MLTU), resulting in one 29 kbp precursor mRNA that is alternatively spliced (Nevins & Darnell, 1978). During the late phase of infection, host cell mRNA transport and translation are shut-off (host cell shut-off), whereas viral late mRNAs are efficiently synthesized, transported to the cytoplasm and preferentially translated (Beltz & Flint, 1979). Finally, assembly of progeny virions and packaging of viral DNA takes place, orchestrated by late (L4-100K, L4-33K, L4-22K) and early regulatory (E1B-55K, E4orf6, E2A) proteins. Depending on the cell type the viral life cycle is completed after 24-36 h with the release of up to 10^4 progeny virus particles per cell.

2.1.4 Adenovirus early regulatory proteins

2.1.4.1 Early region 1A – E1A

The E1A transcription unit is the first to be expressed after the viral chromosome entered the nucleus (Nevins *et al.*, 1979), producing two major mRNAs during the early phase of infection (Perricaudet *et al.*, 1979). Additional alternatively spliced E1A mRNA species (11S, 10S, 9S) accumulate at later time points of the infection cycle (Stephens & Harlow, 1987).

The E1A proteins are localized in both the cytoplasm and the nucleus (Rowe *et al.*, 1983; Ulfendahl *et al.*, 1987). In general, they activate viral transcription and re-program host-cell gene expression, forcing quiescent cells to enter and pass through the cell cycle, thereby providing an optimal environment for viral replication (Berk, 2005; Flint & Shenk, 1989; Gallimore & Turnell, 2001). The two early E1A polypeptides (243 and 289 aa), often referred to as the E1A-12S and E1A-13S proteins for the sedimentation coefficient of their mRNA, are identical except for an additional 46 aa segment, present only in the large E1A-13S (Perricaudet *et al.*, 1979; Fig. 4)) Comparing the E1A aa sequences of different Ad types, the two major E1A products prove to be constructed of four conserved regions (CR1-CR4), separated by less conserved domains (Kimelman *et al.*, 1985; van Ormondt *et al.*, 1980). The conserved regions and the N-terminus of E1A mediate protein-protein interactions that regulate transcription, chromatin remodeling and cell proliferation (Fig. 4). CR3, coinciding almost exactly with the unique region of E1A-13S, is particularly important for activating Ad early transcription units through interactions with the mediator complex (MED23) via its zinc-finger domain and with diverse transcription factors (TFs) via the C-terminal end of CR3 (Pelka *et al.*, 2008; Wang & Berk, 2002; Fig. 4).

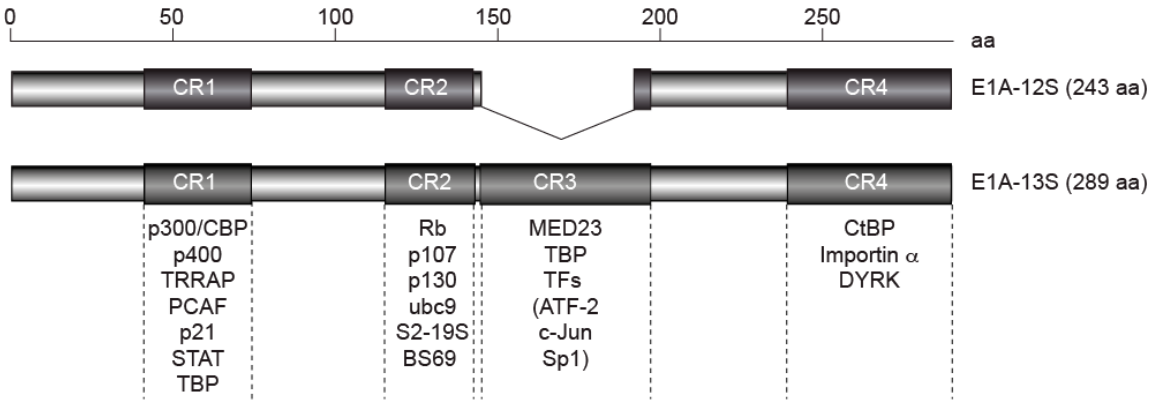

Figure 4: E1A organization and cellular proteins interacting with the conserved regions. Linear representation of E1A-12S and E1A-13S domain structure with conserved regions (Pelka *et al.*, 2008). Proteins interacting within the CRs are listed below. CR: conserved region.

E1A does not bind to DNA directly, rather it interacts with key cellular proteins, that control gene expression and cell growth to modulate their functions (Frisch & Mymryk, 2002). E1A influences a complex network of cellular pathways, including epigenetic as well as transcriptional regulators (Fig. 4), modulating approximately 70 % of all gene products (Ferrari *et al.*, 2009; Ferrari *et al.*, 2008). In this context, E1A expression alone is sufficient to immortalize non-permissive primary rodent cells and fully transform them in cooperation with a second oncogene, e.g. adenoviral E1B-55K or activated *ras* (Houweling *et al.*, 1980; Ruley, 1983). This property partly relies on its interaction with the tumor suppressor Rb (retinoblastoma protein), which was also the first identified E1A interaction partner (Whyte *et al.*, 1988). E1A interacts specifically with hypophosphorylated active Rb family members mainly through the LxCxE motif of CR2 and partly CR1, displacing the Rb proteins from transcription factors of the E2F family (Dyson *et al.*, 1992; Fattaey *et al.*, 1993; Ikeda & Nevins, 1993). This dissociation frees E2F to activate E2F-dependent transcription, including early viral transcription and causes the infected cell to enter the cell cycle (Cress & Nevins, 1996).

Other substantial E1A targets are the cellular transcriptional coactivators p300 and its closely related homolog CBP, which are recruited to numerous promoters through their association with DNA-binding TFs (Goodman & Smolik, 2000). Once recruited, p300/CBP are thought to activate transcription by acetylating histone tails or target lysines of other TFs. Interaction of E1A either inhibits or redirects the acetyltransferase activities of p300/CBP to other cellular regulatory proteins, e.g. Rb (Frisch & Mymryk, 2002; Hamamori *et al.*, 1999). Nevertheless, the interaction of E1A with p300/CBP is very complex and far from being completely understood.

2.1.4.2 Early region 1B – E1B

The early region 1B (E1B) encodes two major proteins E1B-19K and E1B-55K (Bos *et al.*, 1981; Perricaudet *et al.*, 1979), at least three splice variants and two N-terminally truncated E1B-55K polypeptides, which seem to partly share functions with the large E1B-55K protein (Kindsmuller *et al.*, 2009; Sieber & Dobner, 2007). Both major E1B proteins contribute to complete cell transformation of primary rodent cells and play important roles during infection at least in part by antagonizing apoptosis and growth arrest (Debbas & White, 1993). This is mainly achieved through direct or indirect regulation of the tumor suppressor protein p53 and/or PML-NB-associated factors. E1B-19K, a homolog of the cellular anti-apoptotic protein Bcl2, functions through modulation of pro-apoptotic

regulators, such as Bax and Bak (White, 1993; 2001). The multifunctional E1B-55K employs several mechanisms to inhibit p53 function. P53 transcriptional activation is partly inhibited via direct interaction with E1B-55K, accompanied by the tethering of the E1B-55K C-terminal repression domain to p53 target genes (Kao *et al.*, 1990; Martin & Berk, 1998; Teodoro & Branton, 1997; Yew & Berk, 1992). Additionally, E1B-55K inhibits acetylation and promotes SUMO modification of p53, thereby modulating its transcriptional activity (Liu *et al.*, 2000; Muller & Dobner, 2008; Pennella *et al.*, 2010). Nuclear-cytoplasmic relocalization induces the complete silencing of p53-dependent functions (Endter *et al.*, 2005; Endter *et al.*, 2001).

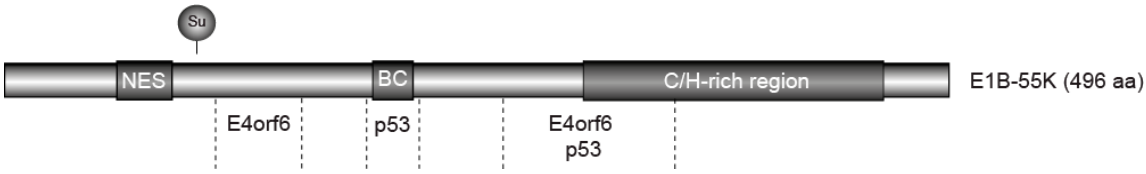

Figure 5: Schematic domain structure of Ad5 E1B-55K. BC box: Elongin B/Elongin C box; C/H-rich region: cysteine/histidine-rich region; NES: nuclear export signal; Su: SUMO conjugation motif. Interaction regions of E4orf6 and p53 are indicated below.

Besides its role as key regulator of p53, E1B-55K mediates various functions at all stages of the lytic viral life cycle, acting on transcriptional, post-transcriptional, translational and post-translational levels. E1B-55K continuously shuttles between nucleus and cytoplasm, mediated at least in part by a leucine-rich nuclear export signal (NES) and a SUMO conjugation motif (SCM) at lysine 104 (Endter *et al.*, 2005; Endter *et al.*, 2001; Kindsmuller *et al.*, 2007; Kratzer *et al.*, 2000; Fig. 5). In this context, interaction with the E4orf6 gene product seems to be essential for the proper nuclear localization and subnuclear targeting of E1B-55K (Dobbelstein *et al.*, 1997; Goodrum *et al.*, 1996; Ornelles & Shenk, 1991). Interestingly mutational inactivation of the SCM completely abrogates E1B-55K nuclear localization and its ability to transform primary baby rat kidney cells in combination with E1A (Endter *et al.*, 2001). Analysis of E1B-55K's aa sequence also revealed the presence of a putative BC-Box motif, that mediates the interaction with Elongin B/C (Blanchette *et al.*, 2008) and a RING finger domain in the C-terminal part of the polypeptide (Hartl *et al.*, 2008; Fig. 5). The RING finger motif is characterized by a defined arrangement of zinc ion-binding cysteine and histidine residues and has been shown for some other RING finger containing proteins to play a key role in the ubiquitination pathway (Borden & Freemont, 1996; Deshaies & Joazeiro, 2009), although the relevance of its presence in E1B-55K is still elusive.

2.1.4.3 Early region 4 – E4orf3 & E4orf6

The early region 4 (E4) encodes up to seven multifunctional regulatory proteins, named E4orf1 to E4orf6/7 according to the arrangement of their open reading frames. These proteins act via a complex network of interactions modulating post-translational modification, signal transduction, transcription, DNA repair, cell cycle control and apoptosis (Halbert *et al.*, 1985; Tauber & Dobner, 2001a; b). Of the several proteins encoded in E4, either E4orf3 or E4orf6 have to be present to ensure significant viral DNA replication by preventing induction of the cellular DNA damage response (Boyer *et al.*, 1999). Furthermore, E4orf3 and E4orf6 share redundant roles in late protein synthesis, late viral mRNA transport and progeny virus production (Huang & Hearing, 1989) and both support E1A/E1B-55K mediated transformation of primary rodent cells (Nevels *et al.*, 1997; Nevels *et al.*, 1999).

E4orf3 alone is necessary and sufficient to disrupt PML-NBs, inducing the formation of so-called track-like structures (Carvalho *et al.*, 1995; Doucas *et al.*, 1996; Puvion-Dutilleul *et al.*, 1995) via interaction with PML isoform II (Hoppe *et al.*, 2006; Leppard *et al.*, 2009; Leppard & Everett, 1999). The fact that this reorganization is conserved among various species of Ads (Hoppe *et al.*, 2006), suggests an important role during adenoviral infection, likely by countering of an intracellular defense mechanism (Doucas *et al.*, 1996; Everett, 2001; Everett & Chelbi-Alix, 2007). Furthermore, E4orf3 is involved in the modulation of certain transient PML-NB components, such as p53, the Mre11-Rad50-NBS1 (MRN) complex of the DNA repair machinery and the transcriptional modulator Tif1α (Araujo *et al.*, 2005; Konig *et al.*, 1999; Liu *et al.*, 2005; Stracker *et al.*, 2005; Weiden & Ginsberg, 1994; Yondola & Hearing, 2007).

E4orf6 is able to shuttle between the cytoplasm and the nucleus, mediated by an amphipathic α-helix containing a nuclear localization signal (NLS) and a nuclear export signal (NES) motif (Orlando & Ornelles, 1999; Weigel & Dobbelstein, 2000). E1B-55K and E4orf6 associate with each other and additional cellular proteins, among them Elongin B/C, Cullin5 and Rbx-1, to assemble a ubiquitin ligase complex (Sarnow *et al.*, 1984). This complex binds p53 and directs its polyubiquitination and subsequent proteasomal degradation (Cathomen & Weitzman, 2000; Harada *et al.*, 2002; Querido *et al.*, 2001; Querido *et al.*, 1997; Roth *et al.*, 1998; Steegenga *et al.*, 1998). Besides p53, E1B-55K and E4orf6 regulate the degradation of other cellular proteins, which have a detrimental effect on viral replication, such as Mre11, DNA ligase IV, Bloom Helicase, Tip60, integrin α3,

ATRX or SPOC1 (Baker *et al.*, 2007; Blanchette *et al.*, 2004; Dallaire *et al.*, 2009; Gupta *et al.*, 2013; Harada *et al.*, 2002; Orazio *et al.*, 2011; Schreiner *et al.*, 2013a; Schreiner *et al.*, 2013b; Stracker *et al.*, 2002). E4orf6 also interacts with, and inhibits, p53 without the presence of E1B-55K (Dobner *et al.*, 1996). In the late phase of infection, E1B-55K and E4orf6 act together to block cellular DNA accumulation and are involved in the transport of late viral mRNAs, while the transport of cellular transcripts is blocked (Babich *et al.*, 1983; Babiss & Ginsberg, 1984; Babiss *et al.*, 1985; Pilder *et al.*, 1986).

2.2 PML-NBs

2.2.1 Organization and functions of PML-NBs

Promyelocytic leukemia nuclear bodies (PML-NBs), also referred to as PML oncogenic domains (POD) or nuclear domain-10 (ND10) are multi-protein complexes that appear as punctate nuclear structures, interspersed between chromatin and tightly bound to the nuclear matrix (Stuurman *et al.*, 1992). Most mammalian cell nuclei typically contain 1-30 NBs with an average size of 0.2-1.0 μm, although abundance, composition, structure and function greatly depend on cell type, cell cycle stage and stress response (Ascoli & Maul, 1991; Bernardi & Pandolfi, 2007; Dyck *et al.*, 1994; Hodges *et al.*, 1998; Melnick & Licht, 1999). PML-NBs are dynamic structures with over 160 proteins known to localize to these domains either constitutively or transiently depending on different conditions, e.g. transformation, stress, interferon expression or viral infections (Nisole *et al.*, 2013; Van Damme *et al.*, 2010). Electron microscopy studies have shown that PML-NBs are composed of a ring-like structure, which does not contain detectable nuclei acids in the center of the ring, however at the periphery of the ring, PML-NBs make extensive contacts with chromatin fibers (Boisvert *et al.*, 2000; Dellaire & Bazett-Jones, 2004; Eskiw *et al.*, 2004).

The tumor suppressor PML, the transcriptional modulator Sp100, the chromatin-remodeling factor Daxx, the Bloom Helicase and the small ubiquitin-like modifier (SUMO) represent five constitutive PML-NB factors. The PML protein was initially regarded as the central component of PML-NBs as these structures do not form in $PML^{-/-}$ cells (Bernardi & Pandolfi, 2007; Gorisch *et al.*, 2004; Ishov *et al.*, 1999). Recent studies however demonstrated that the PML-NB spheres are defined by a shell of PML and Sp100 (Shen *et al.*, 2006). Besides the constitutive residents, proteins participating in diverse cellular events, such as the ubiquitin specific protease Usp7, the transcriptional regulator ATRX, the double-strand break repair protein Mre11, the tumor suppressors p53 and Rb, the

heterochromatin protein HP1 and the acetyltransferase CBP transiently localize to these nuclear subdomains. Consequently, since their discovery numerous publications have linked PML-NBs to a remarkably large number of cellular functions including transcriptional regulation, senescence, apoptosis, protein degradation, oncogenesis, epigenetic regulation and antiviral defense (Bernardi & Pandolfi, 2007; Everett & Chelbi-Alix, 2007; Negorev & Maul, 2001; Zhong *et al.*, 2000c).

2.2.2 SUMO

The small ubiquitin-like modifier (SUMO) is grouped into the family of ubiquitin-like proteins (UBL) due to similarities in sequence, structure and molecular mechanism of attachment. Mammalian cells encode four different isoforms, SUMO-1, -2, -3, and -4, although it is not clear if SUMO-4 is conjugated *in vivo* (Owerbach *et al.*, 2005). SUMO-2 and -3 are nearly identical (95 % sequence identity) and appear to act in redundant fashion, whereas they share only 50 % sequence identity with SUMO-1 and are functionally distinct (Saitoh & Hinchey, 2000). SUMO-2 and -3 can form polymeric chains due to a SUMO consensus motif in their N-terminal extensions (Tatham *et al.*, 2001; Vertegaal, 2007).

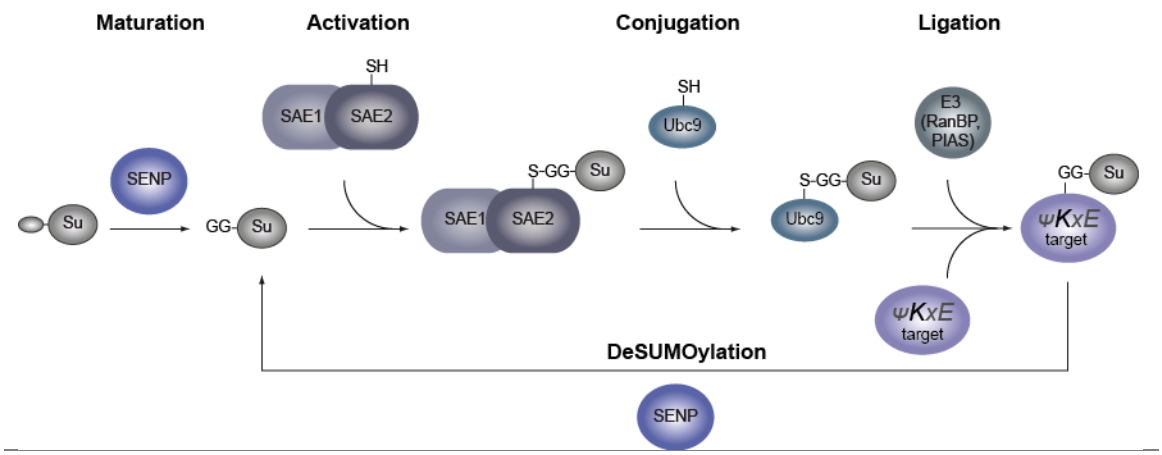

Figure 6: SUMO conjugation pathway. The SUMO precursor needs to be processed by a SUMO specific protease (SENP) to expose the di-glycine (GG) motif. Activated SUMO is conjugated to target proteins, bearing a SUMO consensus motif (ψKxE) by an enzymatic cascade involving a SUMO activating enzyme E1 (SAE1/2), a SUMO conjugating enzyme E2 (Ubc9) and typically a SUMO ligase E3 (e.g. RanBP, PIAS). SUMO can be deconjugated from the target protein by action of specific SENPs (modified from Seeler & Dejean, 2003).

All SUMO isoforms are covalently conjugated to substrates via a three-step enzymatic pathway analogous to that of ubiquitin conjugation. Similar to ubiquitin, SUMO is produced as an immature precursor with a C-terminal appendage that needs to be processed to expose the mature C-terminal di-glycine motif (Ulrich, 2009). The SUMO-

activating E1 enzyme is a heterodimer, containing SAE1/SAE2 subunits (known as Aos1/Uba2 in yeast), and catalyzes the transfer of SUMO to the catalytic cysteine of SAE2 in the initial step (Desterro *et al.*, 1999; Johnson *et al.*, 1997). In the second step, SUMO is transferred from the E1 enzyme to a cysteine residue within the SUMO conjugating enzyme Ubc9 (Desterro *et al.*, 1997; Johnson & Blobel, 1997; Okuma *et al.*, 1999). Finally, Ubc9 catalyzes the formation of an isopeptide bond between the C-terminus of SUMO and the lysine within the SUMO consensus motif ψKxE of the target protein (where ψ represents a large hydrophobic aa, and x represents any aa) (Rodriguez *et al.*, 2001). In contrast to the ubiquitin pathway no activity equivalent to an E3 ligase is absolutely required for SUMO conjugation *in vitro* but enhances the rate of conjugation and is important for substrate specificity *in vivo* (Seeler & Dejean, 2003). Both the initial processing as well as the deconjugation of SUMO is mediated by SUMO specific endopeptidases (SENPs; Hay, 2007).

SUMO proteins influence nearly every cellular process known, ranging from nucleocytoplasmic transport, transcription, protein degradation, apoptosis to DNA recombination and repair (Bossis & Melchior, 2006; Geiss-Friedlander & Melchior, 2007; Hay, 2005; 2006; Heun, 2007; Kerscher *et al.*, 2006; Melchior, 2000; Seeler & Dejean, 2003; Ulrich, 2009; Verger *et al.*, 2003). Furthermore, SUMO is also known to have implications on the subcellular localization of certain substrates, among them many PML-NB components (Shen *et al.*, 2006; Van Damme *et al.*, 2010; Zhong *et al.*, 2000a). Both the covalent conjugation of SUMO and the non-covalent interaction of SUMO with the SUMO interacting motif (SIM) of PML and associated proteins are required for formation, integrity and function of PML-NBs (Ishov *et al.*, 1999; Shen *et al.*, 2006; Zhong *et al.*, 2000a). In this context, SUMO-1 is mainly found located in the PML/Sp100 shell whereas the SUMO-2/-3 isoforms are also present in the interior of the doughnut-shaped NBs (Shen *et al.*, 2006). Since most of the enzymes involved in the SUMOylation pathway are localized at PML-NBs and up to 56 % of the PML-NB-associated proteins are modified by SUMO, these nuclear subdomains were proposed as hot spots for SUMOylation (Van Damme *et al.*, 2010). Regarding the impressive number of cellular processes regulated by this posttranslational modification, it is not surprising that many viruses frequently target and exploit the host SUMOylation system (Wimmer *et al.*, 2012).

2.2.3 PML protein

The promyelocytic leukemia (PML) gene was originally identified in acute promyelocytic leukemia (APL), where it was found fused to the retinoic acid receptor alpha gene as a result of a t(15;17) chromosomal translocation (Chang *et al.*, 1992; de The *et al.*, 1991; Kakizuka *et al.*, 1991; Koken *et al.*, 1994; Melnick & Licht, 1999; Pandolfi *et al.*, 1992; Weis *et al.*, 1994). Since than, PML was found deregulated in various cancer types and was therefore considered as a general tumor suppressor protein (Gurrieri *et al.*, 2004; Salomoni *et al.*, 2008; Salomoni & Pandolfi, 2002). In humans at least seven PML isoforms, designated PML-I to PML-VII, are expressed by alternative splicing of a single *pml* gene (Bernardi & Pandolfi, 2007; Fagioli *et al.*, 1992; Jensen *et al.*, 2001; Fig. 7). Transcription of the *pml* gene is tightly controlled by interferons and p53 (de Stanchina *et al.*, 2004; Stadler *et al.*, 1995). All PML isoforms bear the same N-terminal RBCC motif, also referred to a the tripartite motif (TRIM), consisting of the sequential organization of a RING-finger (R), two B-Boxes (B) and a coiled-coil domain (CC); hence are grouped as TRIM19 into the TRIM protein family (Bernardi & Pandolfi, 2007; Jensen *et al.*, 2001). This motif is particularly important for dimerization and localization to the PML-NBs (Kentsis *et al.*, 2002). The C-terminal region of human PML shows remarkable variability among the isoforms and accounts for isoform-specific functions (Nisole *et al.*, 2013).

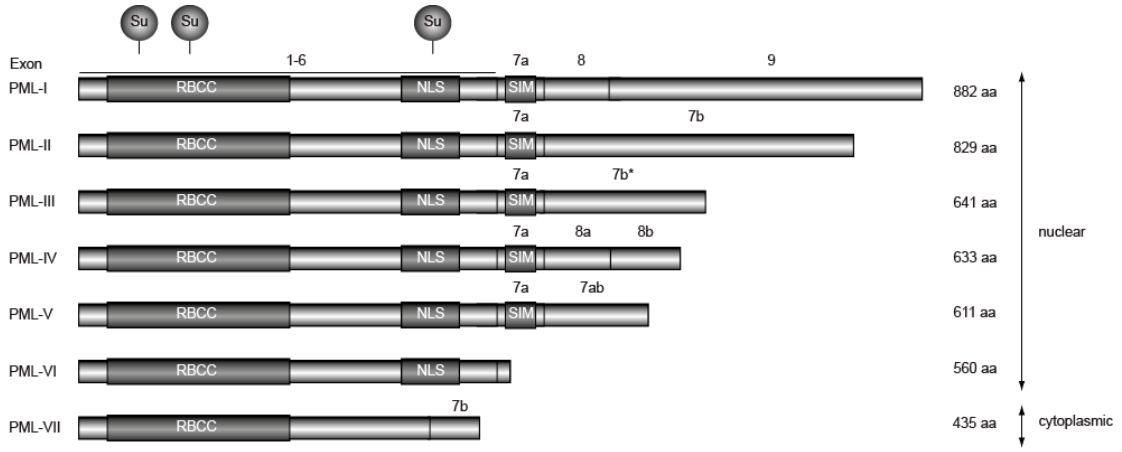

Figure 7: Major human PML isoforms. Schematic representation of the alternatively spliced human PML isoforms according to the nomenclature of Jensen *et al.* (Jensen *et al.*, 2001). Shown are the exon structure, indicated by numbers 1-9, and the domain organization of the single PML isoforms. RBCC: RING finger, B-box, coiled-coil domain; NLS: nuclear localization signal; SIM: SUMO interacting motif, Su: SUMO conjugation motif.

Additionally, PML function is modulated by posttranslational modifications, notably phosphorylation or SUMOylation (Bernardi & Pandolfi, 2007; Condemine *et al.*, 2006; Everett *et al.*, 1999; Jensen *et al.*, 2001; Muller *et al.*, 1998; Scaglioni *et al.*, 2006; Zhong *et al.*, 2000a). Phosphorylation by the Casein Kinase 2 (CK2) triggers ubiquitination and subsequent proteasomal degradation of PML (Scaglioni *et al.*, 2006). SUMO modification is particularly important, as it regulates PML localization (Duprez *et al.*, 1999) and nuclear body formation (Zhong *et al.*, 2000a). Furthermore, poly-SUMOylated PML is ubiquitinated by the RING domain-containing ubiquitin E3 ligase RNF4 and targeted for proteasomal degradation (Geoffroy *et al.*, 2010; Lallemand-Breitenbach *et al.*, 2008; Percherancier *et al.*, 2009; Tatham *et al.*, 2008). The SUMO interacting motif (SIM) is present in all PML isoforms, except in the nuclear PML-VI and the cytoplasmic PML-VII, and is required to regulate the stability of the PML-NBs and the recruitment of other SUMOylated proteins (Shen *et al.*, 2006).

2.2.4 Sp100

Sp100 (Speckled protein 100 kDa) was initially identified as an autoantigen in patients suffering from primary biliary cirrhosis (Szostecki *et al.*, 1990; Szostecki *et al.*, 1987; Szostecki *et al.*, 1992). Later studies have characterized Sp100 as an interferon-inducible transcriptional modulator, with both transcription-activating and -repressive properties (Grotzinger *et al.*, 1996; Guldner *et al.*, 1992; Lehming *et al.*, 1998).

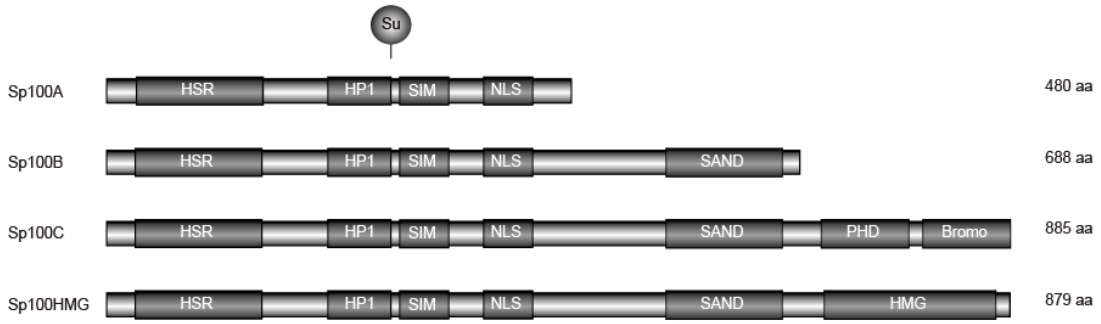

Figure 8: Major human Sp100 isoforms. Schematic representation of the alternatively spliced human Sp100 isoforms with domain organization. HSR: Homogenous staining region; HP1: Heterochromatin protein 1 interaction region; Su: SUMO conjugation motif; SIM: SUMO interacting motif; NLS: Nuclear localization signal; SAND: Sp100, AIRE-1, NucP41/45, DEAF-1-domain; Bromo: Bromo domain; PHD: Plant Homeodomain; HMG: High Mobility Group domain.

Similar to the *pml* gene, several alternatively spliced mRNAs are transcribed from the human *sp100* gene, resulting in the expression of at least four different Sp100 isoforms Sp100A, Sp100B, Sp100C and Sp100HMG (Dent *et al.*, 1996; Grotzinger *et al.*, 1996; Guldner *et al.*, 1999; Seeler *et al.*, 2001; Szostecki *et al.*, 1990; Szostecki *et al.*, 1992; Xie *et al.*, 1993; Fig. 8). All of them harbor an N-terminal HSR (homogenously stained region) domain for dimerization and localization to the PML-NBs (Sternsdorf *et al.*, 1999), but only Sp100 B, C and HMG contain a SAND (Sp100, AIRE-1, NucP41/45, and DEAF-1) domain, exhibiting high affinity to DNA with unmethylated CpGs (Bottomley *et al.*, 2001; Isaac *et al.*, 2006). Other features common to all Sp100 isoforms are a motif for interaction with members of the HP1 family, a SIM and an NLS (Seeler *et al.*, 1998; Sternsdorf *et al.*, 1999; Fig. 8). The identification of HP1 as an interaction partner of Sp100 suggested a possible involvement in control or maintenance of chromatin architecture (Seeler *et al.*, 1998). The longest isoforms Sp100C and Sp100HMG contain additional domains, that have previously shown association with chromatin (Baker *et al.*, 2008; Burnett *et al.*, 2001; Fish *et al.*, 2012; Lehming *et al.*, 1998; Seeler *et al.*, 1998), such as a Bromo-, PHD (plant-homeo-domain) and HMG (High Mobility Group) domain (Seeler *et al.*, 2001). Recent work by Newhart and coworkers showed that Sp100A increases chromatin decondensation, whereas the SAND domain in Sp100B, C and HMG promotes chromatin condensation, suggesting a differential role of these isoforms in transcriptional regulation (Newhart *et al.*, 2013). All Sp100 isoforms are posttranslationally modified by SUMO at Lysine 297 (Sternsdorf *et al.*, 1997). However, contrary to SUMOylated PML preferentially targeted to the PML-NB (Muller *et al.*, 1998), SUMO modification of Sp100 seems not to be prerequisite for nuclear body targeting (Sternsdorf *et al.*, 1999). More likely, SUMOylation of Sp100 regulates the interaction with HP1 and other non-histone chromosomal proteins (Seeler *et al.*, 2001; Seeler *et al.*, 1998), forming a chromatin-associated complex (Lehming *et al.*, 1998; Seeler *et al.*, 1998).

2.2.5 Role of PML-NBs in viral infections

From the early days of molecular characterization of PML-NBs, they have been investigated extensively with respect to their role in viral infections. DNA viruses, e.g. adeno-, herpes-, papilloma- or polyomaviruses, as well as RNA viruses frequently target PML-NBs (Table 1). Regarding the number of publications, the predominant opinion appears to be that PML-NBs mediate an intracellular antiviral defense mechanism (Everett & Chelbi-Alix, 2007; Tavalai & Stamminger, 2008). This assumption is appropriate

provided by the fact that some PML-NB-associated proteins are induced by interferon and seem to impair efficient virus replication (Chelbi-Alix *et al.*, 1998; Regad & Chelbi-Alix, 2001). Consequently, many early viral regulatory proteins target PML-NBs to counteract their antiviral properties. However, it appears to be a general feature of particularly nuclear-replicating DNA viruses that their parental genomes frequently become associated with PML-NBs, resulting in location of their initial sites of viral transcription/replication juxtaposed to these domains (Everett, 2001). Therefore, growing evidence points to the molecular mechanisms involved being more complicated.

Table 1 Overview of viruses targeting PML-NBs. Listed are human DNA and RNA viruses known to target PML-NB-associated proteins independent of its repressive or beneficial effect on virus replication. Note that only the constitutive PML-NB proteins and ATRX were taken into account. For more detailed description see review articles (Everett, 2001; Everett & Chelbi-Alix, 2007; Tavalai & Stamminger, 2008; Van Damme & Van Ostade, 2011).

Virus	Viral protein	Cellular protein	Reference
DNA Viruses			
Adenoviridae			
Ad5	E4orf3, E1B-55K, pVI, pIX	PML-II, -IV, -V, Daxx, ATRX, Sp100	(Hoppe *et al.*, 2006; Ishov & Maul, 1996; Leppard *et al.*, 2009; Leppard & Everett, 1999; Rosa-Calatrava *et al.*, 2003; Schreiner *et al.*, 2013a; Schreiner *et al.*, 2012; Schreiner *et al.*, 2010; Ullman & Hearing, 2008; Ullman *et al.*, 2007)
Herpesviridae			
EBV	BLZF-1, EBNA5, EBNA1, BNRF1, LMP1, EBNA-LP	PML-IV, Daxx, ATRX Sp100A	(Adamson & Kenney, 2001; Amon *et al.*, 2006; Bell *et al.*, 2000; Echendu & Ling, 2008; Ling *et al.*, 2005; Sides *et al.*, 2011; Sivachandran *et al.*, 2008; Sivachandran *et al.*, 2012; Tsai *et al.*, 2011; Wimmer *et al.*, 2010)
HCMV	pp71, IE1, IE2, IE72, UL35	Daxx, ATRX Sp100A	(Ahn *et al.*, 1998; Hofmann *et al.*, 2002; Kim *et al.*, 2011; Korioth *et al.*, 1996; Lee *et al.*, 2004; Reeves *et al.*, 2010; Saffert & Kalejta, 2006; Salsman *et al.*, 2011; Wilkinson *et al.*, 1998)
HSV-1	ICP0	PML-I, PML-II, Daxx, Sp100	(Burkham *et al.*, 2001; Burkham *et al.*, 1998; Chee *et al.*, 2003; Chelbi-Alix *et al.*, 1998; Cuchet *et al.*, 2011; Cuchet-Lourenco *et al.*, 2012; Everett & Maul, 1994; Everett *et al.*, 2008; Everett *et al.*, 2006; Everett & Zafiropoulos, 2004; Glass & Everett, 2013; Lukashchuk & Everett, 2010; Maul *et al.*, 1996; Meredith *et al.*, 1995; Muller & Dejean, 1999; Negorev *et al.*, 2006; Negorev *et al.*, 2009; Nojima *et al.*, 2009; Taylor *et al.*, 2000)
KSHV	BLZF-1, LANA, K-Rta	PML	(Izumiya *et al.*, 2013; Katano *et al.*, 2001; Marcos-Villar *et al.*, 2009; Szekely *et al.*, 1999; Wu *et al.*, 2001)
VZV	Orf61, Orf23	PML-IV	(Kyratsous & Silverstein, 2009; Reichelt *et al.*, 2011; Wang *et al.*, 2011)
Pappilomaviridae			
HPV	L2, E2, E4, E6-AP	PML-I-IV, Sp100, Daxx	(Bischof *et al.*, 2005; Florin *et al.*, 2002; Guccione *et al.*, 2004; Lin *et al.*, 2009; Louria-Hayon *et al.*, 2009; Nakahara & Lambert, 2007; Stepp *et al.*, 2013)
Polyomaviridae			

SV40	Large TAg	n. d.	(Ishov & Maul, 1996; Jiang *et al.*, 1996; Jul-Larsen *et al.*, 2004; Tang *et al.*, 2000)
JCV	VP1, VP2, VP3	n. d.	(Gasparovic *et al.*, 2009; Shishido-Hara *et al.*, 2012)
BK	Large TAg	n. d.	(Jiang *et al.*, 2011; Jul-Larsen *et al.*, 2004)
RNA Viruses			
Arenaviridae			
LCMV	Z-protein	n. d.	(Asper *et al.*, 2004; Borden *et al.*, 1998; Djavani *et al.*, 2001; Garcia *et al.*, 2010)
Bunyaviridae			
Hantavirus	N-protein	Daxx	(Kaukinen *et al.*, 2005; Li *et al.*, 2002)
Flaviviridae			
Dengue Virus	Capsid protein	Daxx	(Netsawang *et al.*, 2010)
HCV	Core protein	n. d.	(Herzer *et al.*, 2005)
Filoviridae			
Ebola Virus	n. d.	n. d.	(Bjorndal *et al.*, 2003)
Othomyxoviridae			
Influenza Virus A	M, NS1, NS2	PML-III, -V, -VI	(Chelbi-Alix *et al.*, 1998; Iki *et al.*, 2005)
Retroviridae			
HIV-1	n. d.	PML, Daxx	(Berthoux *et al.*, 2003; Turelli *et al.*, 2001)
HTLV-1	Tax	n. d.	(Desbois *et al.*, 1996)
HFV	Tas	PML-III	(Regad *et al.*, 2001)
Rhabdoviridae			
VSV	n. d.	PML-III	(Bonilla *et al.*, 2002; Chelbi-Alix *et al.*, 1998)
Rabies Virus	P proteins	PML-IV	(Blondel *et al.*, 2010; Blondel *et al.*, 2002)
Picornaviridae			
Poliovirus	n. d.	PML-III	(Pampin *et al.*, 2006)
EMCV	3Dpol	PML-IV	(El McHichi *et al.*, 2010; Maroui *et al.*, 2011)

3 Material

3.1 Cells

3.1.1 Bacterial strains

Strain	Genotype
DH5α	*sup*E44, Δ*lac*U169, (φ80d *lac*ZΔ *M15*), *hsd*R17, *rec*A1, *end*A1, *gyr*A96, *thi*-1, *rel*A1 (Hanahan & Meselson, 1983)

3.1.2 Mammalian cell lines

Cell line	Genotype
H1299	Human lung carcinoma cell line, p53 negative (Mitsudomi *et al.*, 1992)
H1299shSp100	H1299 cell line with shRNA against all Sp100 isoforms; shRNA 5'-GTG AGC CTG TGA TCA ATA A-3' (Everett *et al.*, 2008)
Hep PML-II	HepaRG cell line with depletion of all PML isoforms and reconstitution of EYFP-tagged PML-II isoform resistant to the shRNA by introduction of five silent point mutations in the relevant sequence; altered sequence: 5'-AGA TGC TGC AGT TAG CAA G-3' (Cuchet *et al.*, 2011)
HepaRG	Pseudoprimary human hepatoma cell line (Cerec *et al.*, 2007; Gripon *et al.*, 2002)
Hep shDaxx	HepaRG cell line with shRNA against Daxx shRNA 5'-GGA GTT GGA TCT CTC AGA A-3' (provided by Roger Everett, Glasgow/UK)
Hep shPML	HepaRG cell line with shRNA against six PML isoforms; shRNA 5'-AGA TGC AGC TGT ATC CAA G-3' (Everett *et al.*, 2006)
Hep shSp100	HepaRG cell line with shRNA against Sp100 isoforms; shRNA 5'-GTG AGC CTG TGA TCA ATA A-3' (Everett *et al.*, 2008)
HEK-293	Established Ad5-transformed, human embryonic kidney cell line stably expressing the adenoviral E1A and E1B oncoproteins (Graham *et al.*, 1977)
HeLa	Human cervix carcinoma cell line, p16 negative (Gey et al., 1952)
HeLa-Su1	HeLa cell line stably expressing His-SUMO-1 (Tatham *et al.*, 2009)
HeLa-Su2	HeLa cell line stably expressing His-SUMO-2 (Tatham *et al.*, 2009)
MEF	Mouse embryonic fibroblasts (Wang *et al.*, 1998)
U2OS	Human osteosarcoma cell line, p16 negative (Ponten & Saksela, 1967)

U2OSshDaxx	Human osteosarcoma cell line with shRNA against Daxx shRNA 5'-GGA GTT GGA TCT CTC AGA A-3' (Schreiner *et al.*, 2013a)

3.1.3 Viruses

Adenovirus	Characteristics
H5*pg*4100	Wt Ad5 containing an 1863 bp deletion (nt 28602-30465) in the E3 region (Kindsmuller *et al.*, 2007)
H5*pm*4149	Ad5 E1B-55K null mutant containing four stop codons at the aa positions 3, 8, 86 and 88 of the E1B-55K sequence (Kindsmuller *et al.*, 2007)
H5*pm*4101	Ad5 E1B-55K mutant containing three aa exchanges (L83/87/91A) within the NES of the E1B-55K sequence (Kindsmuller *et al.*, 2007)
H5*pm*4102	Ad5 E1B-55K mutant containing one aa exchange (K104R) within the SCM of the E1B-55K sequence (Kindsmuller *et al.*, 2007)
H5*pm*4150	Ad5 E4orf3 mutant with an additional thymidine at position nt 34592, causing a frame shift mutation after codon 36 (Forrester *et al.*, 2012)
H5*pm*4154	Ad5 E4orf6 null mutant containing a stop codon at aa 66 within the E4orf6 sequence (Blanchette *et al.*, 2004)
H5*dl*347	Ad5 containing a cloned segment corresponding to E1A-12S mRNA in place of the E1A gene (Winberg & Shenk, 1984)
H5*dl*348	Ad5 containing a cloned segment corresponding to E1A-13S mRNA in place of the E1A gene (Winberg & Shenk, 1984)
H5*dl*312	Ad5 lacking a large segment of the E1A gene and therefore does not produce E1A products (Winberg & Shenk, 1984)

3.2 Nucleic acids

3.2.1 Oligonucleotides

The following oligonucleotides were used for sequencing, PCR, RT qPCR and site-directed mutagenesis. All nucleotides were ordered from Metabion (Munich) and numbered according to the internal group *Filemaker Pro* database.

#	Name	Sequence	Purpose
1371	18S rRNA-fwd	5'-CGG CTA CCA CAT CCA AGG AA-3'	RT qPCR

1372	18S rRNA-rev	5'-GCT GGA ATT ACC GCG GCT-3'	RT qPCR
1686	E1A-fwd	5'-GTG CCC CAT TAA CCA GTT G-3'	RT qPCR
1687	E1A-rev	5'-GGC GTT TAC AGC TCA AGT CC-3'	RT qPCR
64	E1B bp2043-fwd	5'-CGC GGG ATC CAT GGA GCG AAG AAA CCC ATC TGA GC-3'	Sequencing
1571	E2A-fwd	5'-GAA ATT ACG GTG ATG AAC CC G-3'	RT qPCR
1572	E2A-rev	5'-CAG CCT CCA TGC CCT TCT CC-3'	RT qPCR
1470	Fiber-fwd	5'-GGA GAC AAA ACT AAA CCT GTA ACA C-3'	RT qPCR
1471	Fiber-rev	5'-TCC CAT GAA AAT GAC ATA GAG TAT GC-3'	RT qPCR
635	pcDNA3-fwd	5'-ATG TCG TAA CAA CTC CGC-3'	Sequencing
636	pcDNA3-rev	5'-GGC ACC TTC CAG GGT CAA G-3'	Sequencing
1623	PML-nuc456-rev	5'-GGA ACC ACT GGT GTG CCT CG-3'	Sequencing
1624	PML-nuc439-fwd	5'-GCT TG AGT GCG AGC AGC TCC-3'	Sequencing
1625	PML-nuc984-fwd	5'-GCT GTG CTG CAG CGC ATC CGC ACG-3'	Sequencing
1626	PML-nuc1539-fwd	5'-GGA GCA GCC CAG GCC CAG CAC C-3'	Sequencing
1627	PML-nuc2135-fwd	5'-CGG GCT TCC TGG CTG CCC TGC C-3'	Sequencing
1789	PML-I-nuc2010 fwd	5'-CTC CGC TTG CAC CCT CAA TTG C-3'	Sequencing
1790	PML-II-nuc2148 fwd	5'-CCA TCC TGC CAA TGC CCA GG-3'	Sequencing
2463	PML-II SIM-fwd	5'GGA ACG CGG TGG GGG GAT CAG CAG C-3'	Mutagenesis
2464	PML-II SIM-rev	5'-GCT GCT GAT CCC CCC ACC GCG TTC C-3'	Mutagenesis
2745	PML-II seq	5'-GGC AAG GTT GGC TCG GAG C-3'	Sequencing
2742	Sp100 seq2	5'-CTG CGA ACA AAT TGC TGT CC-3'	Sequencing

2743	Sp100 seq5	5'-TGG CAT GTG GGG GCG GCG AC-3'	Sequencing
2730	Sp100A ΔHSR-fwd	5'-GTG GCT GTG TGC AGG AAG ATG G-3'	Mutagenesis
2731	Sp100A ΔHSR-rev	5'-GAC AAA TTG CCT TCT CAA GAA AG-3'	Mutagenesis
2732	Sp100A-SIM-fwd	5'-CAG GCA TCT GAC AAA AAA GTC ATC AGC AG-3'	Mutagenesis
2733	Sp100A-SIM-rev	5'-CTG CTG ATG ACT TTT TTG TCA GAT GCC TG-3'	Mutagenesis
2199	E1AD121A-fwd	5'-GGA GGT GAT CGC TCT TAC CTG C-3'	Mutagenesis
2200	E1AD121A-rev	5'-GCA GGT AAG AGC GAT CAC CTC C-3'	Mutagenesis
2272	E1A-del1-fwd	5'-ACC CAA GGC TCT CTG CTC CGG-3'	15 aa deletions in CR2/3 of Ad5 E1A-13S
2273	E1A-del1-rev	5'-CAC GAG GCT GGC TTT CCA CCC-3'	15 aa deletions in CR2/3 of Ad5 E1A-13S
2274	E1A-del2-fwd	5'-CAC CTC CGG TAC AAG GTT TGG C-3'	15 aa deletions in CR2/3 of Ad5 E1A-13S
2275	E1A-del2-rev	5'- GAT GAA GAG GGT GAG GAG TTT GTG-3'	15 aa deletions in CR2/3 of Ad5 E1A-13S
2276	E1A-del3-fwd	5'-GGG TGG AAA GCC AGC CTC GTG G-3'	15 aa deletions in CR2/3 of Ad5 E1A-13S
2277	E1A-del3-rev	5'-GTG GAG CAC CCC GGG CAC GG-3'	15 aa deletions in CR2/3 of Ad5 E1A-13S
2278	E1A-del4-fwd	5'-AAA CTC CTC ACC CTC TTC ATC CTC-3'	15 aa deletions in CR2/3 of Ad5 E1A-13S
2279	E1A-del4-rev	5'-CAT TAT CAC CGG AGG AAT ACG GG-3'	15 aa deletions in CR2/3 of Ad5 E1A-13S
2280	E1A-del5-fwd	5'-ACC GTG CCC GGG GTG CTC C-3v	15 aa deletions in CR2/3 of Ad5 E1A-13S
2281	E1A-del5-rev	5'-ATT ATG TGT TCG CTT TGC TAT ATG AG-3'	15 aa deletions in CR2/3 of Ad5 E1A-13S
2290	E1A-del6-fwd	5'-CCC CGT ATT CCT CCG GTG ATA ATG-3'	15 aa deletions in CR2/3 of Ad5 E1A-13S
2291	E1A-del6-rev	5'-ATG TTT GTC TAC AGT CCT GTG TCT G-3'	15 aa deletions in CR2/3 of Ad5 E1A-13S

2292	E1A-del7-fwd	5'-ATA GCA AAG CGA ACA CAT AAT ATC TGG-3'	15 aa deletions in CR2/3 of Ad5 E1A-13S
2293	E1A-del7-rev	5'-CCT GAG CCC GAG CCA GAA CCG-3'	15 aa deletions in CR2/3 of Ad5 E1A-13S
2294	E1A-del8-fwd	5'-CAC AGG ACT GTA GAC AAA CAT GCC-3'	15 aa deletions in CR2/3 of Ad5 E1A-13S
2295	E1A-del8-rev	5'-CCT ACC CGC CGT CCT AAA ATG G-3'	15 aa deletions in CR2/3 of Ad5 E1A-13S
2296	E1A-del9-fwd	5'-TTC TGG CTC GGG CTC AGG CTC-3'	15 aa deletions in CR2/3 of Ad5 E1A-13S
2297	E1A-del9-rev	5'-ATC CTG AGA CGC CCG ACA TCA C-3'	15 aa deletions in CR2/3 of Ad5 E1A-13S
2298	E1A-del10-fwd	5'-TTT AGG ACG GCG GGT AGG TCT TGC-3'	15 aa deletions in CR2/3 of Ad5 E1A-13S
2299	E1A-del10-rev	5'-GAA TGC AAT AGT AGT AGT ACG GAT AGC TG-3'	15 aa deletions in CR2/3 of Ad5 E1A-13S

3.2.2 Vectors

#	Name	Purpose	Reference
136	pcDNA3	Expression vector for mammalian cells, CMV promoter	Invitrogen
138	pGL3	*Firefly*-Luciferase-Assay	Promega
129	pG4	Reporter gene expression vector for Gal4 fusions	(Sadowski & Ptashne, 1989)
180	pRL-TK	*Renilla*-Luciferase-Assay	Promega

3.2.3 Recombinant plasmids

#	Name	Vector	Insert	Reference
2	pC53SN3	pCMV/neo	Human p53	Group database
1467	pCyclin G-Luc	unknown	Cyclin G promoter reporter gene construct	G. Akusjärvi

375	pGL-GAL-TK-LUC	pGL-2	Reporter gene construct with 4 GAL4 binding sites in front of the TK promoter	Group database
2472	pHA-E1A-12S	pcDNA3	N-terminal HA-tagged Ad5 E1A-12S	This work
2809	pHA-E1A-12S-D121A	pcDNA3	N-terminal HA-tagged Ad5 E1A-12S	This work
2475	pHA-E1A-13S	pcDNA3	N-terminal HA-tagged Ad5 E1A-13S	This work
2498	pHA-E1A-13S-D121A	pcDNA3	N-terminal HA-tagged Ad5 E1A-13S	This work
2545	pHA-E1A-13S-del120-135	pcDNA3	N-terminal HA-tagged Ad5 E1A-13S	This work
2546	pHA-E1A-13S-del132-147	pcDNA3	N-terminal HA-tagged Ad5 E1A-13S	This work
2547	pHA E1A-13S-del143-157	pcDNA3	N-terminal HA-tagged Ad5 E1A-13S	This work
2548	pHA E1A-13S-del154-168	pcDNA3	N-terminal HA-tagged Ad5 E1A-13S	This work
2549	pHA-E1A-13S-del166-180	pcDNA3	N-terminal HA-tagged Ad5 E1A-13S	This work
2550	pHA-E1A-13S-del176-191	pcDNA3	N-terminal HA-tagged Ad5 E1A-13S	This work
2552	pHA E1A-13S-del188-202	pcDNA3	N-terminal HA-tagged Ad5 E1A-13S	This work
2552	pHA-E1A-13S-del198-212	pcDNA3	N-terminal HA-tagged Ad5 E1A-13S	This work
2553	pHA-E1A-13S-del209-223	pcDNA3	N-terminal HA-tagged Ad5 E1A-13S	This work
2554	pHA-E1A-13S-del109-124	pcDNA3	N-terminal HA-tagged Ad5 E1A-13S	This work
2606	pHA-E1A-13S-del182-191	pcDNA3	N-terminal HA-tagged Ad5 E1A-13S	This work
1319	pE1B-55K	pcDNA3	Ad5 E1B-55K	Group database
2194	pE1B-55K-E472A (E2)	pcDNA3	Ad5 E1B-55K	Group database

1022	pE1B-55K-K104R (SCM)	pcDNA3	Ad5 E1B-55K	Group database
1023	pE1B-55K-NES	pcDNA3	Ad5 E1B-55K	Group database
2141	pE1B-55K-R443A	pcDNA3	Ad5 E1B-55K	Group database
2140	pE1B-55K-R443in	pcDNA3	Ad5 E1B-55K	Group database
1730	pE1B-55K-C454/456S (RF6)	pcDNA3	Ad5 E1B-55K	Group database
2193	pE1B-55K-RTR	pcDNA3	Ad5 E1B-55K	Group database
2808	pE2F-1	pcDNA3	Human E2F-1	N. Fischer
1213	pG4-p300	pG4	Human p300 fused to a GAL binding domain	Group database
2425	pGL3-Basic Prom E1A	pGL3	Ad5 E1A promoter reporter gene construct	Group database
2423	pGL3-Basic Prom E2E	pGL3	Ad5 E2early promoter reporter gene construct	Group database
2425	pGL3-Basic Prom E3	pGL3	Ad5 E3 promoter reporter gene construct	Group database
2422	pGL3-Basic Prom pIX	pGL3	Ad5 pIX promoter reporter gene construct	Group database
2806	pYFP-HP1α	unknown	YFP-tagged Heterochromatin protein 1α	H. Will
2807	pYFP-HP1β	unknown	YFP-tagged Heterochromatin protein 1β	H. Will
2055	pflag-PML-I	pLKO.1.puro	Human N-terminal flag-tagged human PML-I	R. Everett
2056	pflag-PML-II	pLKO.1.puro	Human N-terminal flag-tagged human PML-II	R. Everett
2813	pflag-PML-II-SIM	pLKO.1.puro	Human N-terminal flag-tagged human PML-II	This work
2057	pflag-PML-III	pLKO.1.puro	Human N-terminal flag-tagged human PML-II	R. Everett
2058	pflag-PML-IV	pLKO.1.puro	Human N-terminal flag-tagged human PML-IV	R. Everett

2059	pflag-PML-V	pLKO.1.puro	Human N-terminal flag-tagged human PML-V	R. Everett
2060	pflag-PML-VI	pLKO.1.puro	Human N-terminal flag-tagged human PML-VI	R. Everett
2388	pflag-Sp100A	pSG5	N-terminal flag-tagged human Sp100A	H. Guldner
2811	pflag-Sp100A ΔHSR	pSG5	N-terminal flag-tagged human Sp100A	This work
2810	pflag-Sp100A-SIM	pSG5	N-terminal flag-tagged human Sp100A	This work
2389	pflag-Sp100B	pSG5	N-terminal flag-tagged human Sp100A	H. Guldner
2396	pflag-Sp100C	pSG5	N-terminal flag-tagged human Sp100A	Group database
2390	pflag-Sp100HMG	pSG5	N-terminal flag-tagged human Sp100A	H. Guldner
2076	pE4orf6-HA	pcDNA3	N-terminal HA-tagged Had5 E4orf6	Group database
2812	pH2A-prom luc	unknown	H2A promoter reporter gene construct	N. Fischer

3.3 Antibodies

3.3.1 Primary antibodies

Name	Properties	Source
2A6	Monoclonal mouse Ab; against N-terminus of Ad5 E1B-55K (Sarnow *et al.*, 1982)	Group database
3F10	Monoclonal rat Ab; against the HA-tag	Roche
4E8	Monoclonal rat Ab; against the central region of Ad5 E1B-55K	Group database
610	Polyclonal rabbit Ab; against Ad5 E1A	R. Grand
6A11	Monoclonal rat Ab; against Ad5 E4orf3	Group database
6B10	Monoclonal rat Ab; against Ad5 L4-100K	Group database

6His	Monoclonal mouse Ab; against 6xHis-tag	Clontech
β-actin (AC-15)	Monoclonal mouse Ab; against β-actin	Sigma Aldrich
B6-8	Monoclonal mouse Ab; against Ad5 E2A protein (Reich *et al.*, 1983)	Group database
DO-I	Monoclonal mouse Ab; against the N-terminal aa 11-25 of human p53	Santa Cruz
E2A	Polyclonal rabbit Ab; against Ad5 E2A-72 kDa protein	R.T. Hay
flag-M2	Monoclonal mouse Ab; against the flag-tag	Sigma Aldrich
GFP	Monoclonal rabbit Ab; against GFP epitope	Abcam
L133	Polyclonal rabbit serum; against Ad5 capsid (Kindsmuller *et al.*, 2007)	Group database
M58	Monoclonal mouse Ab; against Ad5 E1A-12S and -13S (Harlow *et al.*, 1985)	Group database
PML (NB100-59787)	Polyclonal rabbit Ab; against PML isoforms	Novus Biologicals
PML clone 36.1-104	Monoclonal mouse Ab; against mouse PML isoforms	Millipore
RSA3	Monoclonal mouse Ab; against the N-terminus of Ad5 E4orf6 and E4orf6/7 (Marton *et al.*, 1990)	Group database
GH3	Polyclonal rabbit Ab; against Sp100 isoforms	H. Will

3.3.2 Secondary antibodies

3.3.2.1 Antibodies for Western Blotting

Product	Properties	Company
HRP-Anti-Mouse IgG	HRP (horseradish peroxidase)-coupled; raised in sheep	Jackson
HRP-Anti-Rabbit IgG	HRP (horseradish peroxidase)-coupled; raised in sheep	Jackson
HRP-Anti-Rat IgG	HRP (horseradish peroxidase)-coupled; raised in sheep	Jackson
HRP-Anti-Mouse IgG light chain specific	HRP (horseradish peroxidase)-coupled; raised in sheep	Jackson

HRP-Anti-Rabbit IgG light chain specific	HRP (horseradish peroxidase)-coupled; raised in sheep	Jackson
HRP-Anti-Rat IgG light chain specific	HRP (horseradish peroxidase)-coupled; raised in sheep	Jackson

3.3.2.2 Antibodies for immunofluorescence staining

Product	Properties	Company
Cy3-Anti-Mouse IgG	Affinity purified, Cy3-coupled; raised in donkey (H + L)	Dianova
Cy3-Anti-Rabbit IgG	Affinity purified, Cy3-coupled; raised in donkey (H + L)	Dianova
Cy3-Anti-Rat IgG	Affinity purified, Cy3-coupled; raised in donkey (H + L)	Dianova
Alexa 488 Anti-Mouse IgG	Alexa 488 antibody raised in goat (H + L; $F(ab')_2$ Fragment)	Invitrogen
Alexa 488 Anti-Rabbit IgG	Alexa 488 antibody raised in goat (H + L; $F(ab')_2$ Fragment)	Invitrogen

3.4 Standards and markers

Product	Company
1 kb/ 100bp DNA ladder	New England Biolabs
PageRuler Plus Prestained Protein Ladder	Pierce

3.5 Commercial systems

Product	Company
Dual-Luciferase Reporter Assay System	Promega
Plasmid Purification Mini, Midi und Maxi Kit	Qiagen
Protein Assay	BioRad
QuikChange Site-Directed Mutagenesis Kit	Stratagene

SuperSignal West Pico Chemiluminescent Substrate	Pierce

3.6 Chemicals, enzymes, reagents, equipment

Chemicals, enzymes and reagents used in this study were obtained from Agilent, Applichem, Biomol, Merck, New England, Biolabs Roche and Sigma Aldrich. Cell culture materials, general plastic material as well as equipment were supplied by BioRad, Biozym, Brand, Engelbrecht, Eppendorf GmbH, Falcon, Gibco BRL, Greiner, Hartenstein, Hellma, Nunc, Pan, Sarstedt, Protean, Schleicher & Schuell, VWR and Whatman.

3.7 Software and databases

Software	Purpose	Source
Acrobat 9 Pro	PDF data processing	Adobe
BioEdit 7.0.5.2	Sequence data processing	Open Software (provided by Ibis Therapeutics Carlsbad)
CLC Main Workbench 5.0	Sequence data processing	CLC bio
Endnote X4	Reference management	Thomson
Filemaker Pro 11	Database management	FileMaker, Inc.
Gene Tools	Quantification of DNA/protein bands	SynGene
Illustrator CS5	Layout processing	Adobe
Photoshop CS5	Image processing	Adobe
PubMed	Literature database, open sequence analysis software	Open Software (provided by NCBI)
Word 2011	Text processing	Microsoft

4 Methods

4.1 Bacteria

4.1.1 Culture and storage

For liquid *E.coli* culture, sterile LB medium containing the appropriate antibiotic (100 µg/ml ampicillin; 50 µg/ml kanamycin) was inoculated with a single bacteria colony. Cultures were incubated at 30 °C/37 °C at 200 rpm in an *Inova 4000 Incubator* (New Brunswick) over night. If necessary, bacteria concentrations were determined by measuring the optical density (OD) at 600 nm (*SmartSpec Plus;* BioRad) against plain medium.

For single colony selection, bacteria were plated on 100 mm dishes containing LB medium with 15 g/l agar and the appropriate antibiotics (100 µg/ml ampicillin; 50 µg/ml kanamycin) before incubation at 30 °C/37 °C over night. Solid plate cultures can be stored for several weeks at 4 °C sealed with Parafilm (Pechiney Plastic Packaging). Liquid cultures were centrifuged briefly at 4000 rpm for 5 min (*Multifuge 3 S-R*; Heraeus) at RT. The bacteria pellets were then resuspended in 1.0 ml LB medium containing 50 % sterile glycerol and transferred into *CryoTubes* (Nunc). These glycerol cultures can be stored at -80 °C for years.

LB Medium	10 g/l	Trypton
	5 g/l	Yeast extract
	5 g/l	NaCl
		(Autoclaved)

Antibiotic solution	50 mg/ml	Ampicillin
	10 mg/ml	Kanamycin
		(Sterile filtered; storage at -20 °C)

4.1.2 Chemical transformation of *E.coli*

1 µl β-Mercaptoethanol (1.2 M) and 1-10 µl diluted plasmid DNA (~200 ng) were transferred into a 15 ml *Falcon 2059* tube together with 100 µl of chemically competent DH5α bacterial cells. After 30 min on ice, the heat shock was performed by incubating the bacteria in a water bath at 42 °C for 45 s. The cells were immediately chilled on ice for 2 min before addition of 1 ml LB medium without antibiotics, followed by incubation for 1 hour at 37 °C and 220 rpm in an *Inova 4000 Incubator* (New Brunswick). The bacteria were pelleted (4000 rpm; 3 min; *Cryo centrifuge 5417R*, Eppendorf), resuspended in 100 µl LB,

plated on LB agar containing appropriate antibiotics and incubated at 30 °C/37 °C over night.

4.2 Mammalian cells

4.2.1 Cultivation

Adhesive mammalian cells were grown as monolayers on polystyrene cell culture dishes (12-well/6-well/100 mm/150 mm tissue culture dishes; Sarstedt/Falcon) in *Dulbecco's Modified Eagle Medium* (DMEM; Sigma) containing 0.11 g/l sodium pyruvate, 10 % FCS (Pan) and 1 % of penicillin/streptomycin solution (1000 U/ml penicillin & 10 mg/ml streptomycin in 0.9 % NaCl; Pan). For cultivation of hepatoma cell lines (Hep parental; Hep shSp100; Hep shPML) the medium was additionally supplemented with 5 µg/ml bovine insulin (Sigma) and 0.5 µM hydrocortisone (Sigma). The cells were incubated at 37 °C in Heraeus incubators with 5 % CO_2 atmosphere. To split confluent cells, the medium was removed, cells were washed once with sterile PBS and incubated with trypsin/EDTA (Pan) for 3-5 min at 37 °C. Trypsin activity was inactivated by adding standard culture medium and detached cells were transferred to a 50 ml tube following 3 min centrifugation at 1500 rpm (*Multifuge 3S-R*; Heraeus). The supernatant was removed and cells were resuspended in an appropriate amount of culture medium. Depending on the experimental conditions, cells were counted and seeded in a definite amount for further experiments as described in 4.2.3 or split in an appropriate ratio (1:2-1:20).

PBS		
	140 mM	NaCl
	3 mM	KCl
	4 mM	Na_2HPO_4
	1.5 mM	KH_2PO_4
		(pH 7.0-7.7; autoclaved)

4.2.2 Storage

For long-time storage of mammalian cell lines, subconfluent cultures were trypsinized and pelleted as described previously (4.2.1). The cells were resuspended in pure FCS and transferred to *CryoTubes* (Nunc). The samples were frozen slowly using a *Mr. Frosty* freezing container (Nalgene Labware) before storage in liquid nitrogen. For re-cultivation, cells were rapidly thawed in a water bath at 37 °C and immediately resuspended in pre-warmed culture medium. Cells were pelleted once by centrifugation to remove the DMSO

containing medium, resuspended in 1 ml of fresh culture medium, seeded in an appropriate cell culture dish and incubated at standard conditions (4.2.1).

4.2.3 Determination of cell number

Cells were trypsinized, pelleted and resuspended in an appropriate volume of fresh medium (4.2.1). 50 µl cell suspension were mixed with 50 µl Trypan Blue solution and placed in a *Neubauer cell counter* (C. Roth). After determination of the mean number of cells in 16 small squares using a *Leica DMIL* light microscope, the total number of viable cells was calculated by applying the following formula:

cell number/ml = counted cell x 2 (dilution factor) x 10^4

Trypan blue solution	0.15 %	Trypan Blue
	0.85 %	NaCl

4.2.4 Transfection with Polyethylenimine

In general DNA was introduced into mammalian cell lines using a linear 25 kDa polyethylenimine (PEI; Polysciences). PEI was dissolved in ddH_2O at a concentration of 1 mg/ml, neutralized with 0.1 M HCl (pH of 7.2), sterile filtered (0.2 µm pore size), aliquoted and stored at -80 °C. The cells were seeded in 12-/6-well or 100 mm tissue culture dishes 24 h before transfection. The transfection solution composed of a mixture of DNA, PEI and pre-warmed DMEM without supplements in a ratio of 1:10:100 was vortexed and incubated for 20 min at RT. The culture medium of the cells was replaced by fresh DMEM without supplements before application of the transfection solution. After incubation of the cells for 6-8 h at standard conditions, transfection mixture was replaced by standard culture medium since PEI is toxic to mammalian cells. Transfected cells were harvested 24-72 h post transfection (p. t.).

4.2.5 Cell harvesting

Harvesting of transfected or infected adherent mammalian cells was performed with cell scrapers before transfer into 15 ml tubes and centrifugation at 2000 rpm for 3 min at RT (*Multifuge* 3 S-R; Heraeus). After removing the supernatant, the cell pellet was washed once with PBS and stored at –20 °C for following experiments.

4.3 Adenovirus

4.3.1 Infection with adenovirus

In general, mammalian cells were infected at a confluency of approximately 60-80 %. The cells were washed once with PBS before applying fresh medium without supplements. Virus dilutions were prepared in an appropriate volume of DMEM without supplements and added to the cells. Following formula was used for determination of the volume of virus stock solution:

$$\textit{volume virus stock solution } (\mu l) = \frac{\textit{multiplicity of infection (MOI)} \times \textit{total cell number}}{\textit{virus titer (focus forming units (ffu)}/\mu l)}$$

After an incubation of 2 h at standard culture conditions the infection medium was replaced with standard culture medium. The infected cells were harvested at desired time points post infection according to the experimental setup.

4.3.2 Propagation and storage of high-titer virus stocks

150 mm cell culture dishes containing 60 % confluent HEK-293 cells were infected with established laboratory virus stocks at an MOI of 5 ffu/cell as described in 4.3.1. 3-5 days post infection cells were harvested, pelleted (2000 rpm, 5 min, RT; *Multifuge 3 S-R*; Heraeus), washed once with PBS and resuspended in an appropriate volume of DMEM without supplements (~1 ml/150 mm dish). Cells were broken up and viral particles were released by freezing in liquid nitrogen followed by rapid thawing in a water bath at 37 °C. At least three subsequent freezing/thawing cycles were performed before pelleting the cell debris at 4500 rpm for 10 min (*Multifuge 3 S-R*; Heraeus). The virus-containing supernatant was mixed with sterile glycerol to a final concentration of 10 % (v/v) and kept at -80 °C for long-time storage or at 4 °C for short-time storage.

4.3.3 Titration of virus stocks

Virus titer determination is based on the number of *fluorescent forming units* (ffu) after immunofluorescence staining of the adenoviral DNA binding protein (DBP; Reich *et al.*, 1983). Therefore, each virus stock was diluted with DMEM by a factor of 10^2 - 10^6 to infect $1x10^6$ HEK-293 cells/6-well with each virus dilution. 20 h p.i. the cells were washed once with PBS and fixed by applying ice-cold methanol for 15 min at -20 °C. The methanol was then removed, the cells were air dried at RT and non-specific antibody binding sites were blocked with TBS-BG for 1 hour at RT on an orbital shaker (GFL). Each well was incubated for 2 h in an antibody solution containing the E2A (DBP) specific antibody B6-8

(1:10 in TBS-BG), washed three times for 10 min with TBS-BG before adding *Alexa Fluor* 488-coupled secondary antibody (Invitrogen; 1:500 in TBS-BG) for 2 h at RT. Finally, the secondary antibody was removed, each well was washed three times for 10 min with TBS-BG and infected cells were counted using a fluorescence microscope (Leica). The total number of infectious particles was calculated as the mean value of at least three independent countings taking into account the infected cell numbers, virus dilutions and microscope magnification.

TBS-BG		
	20 mM	Tris-HCl (pH 7.6)
	137 mM	NaCl
	3 mM	KCl
	1.5 mM	$MgCl_2$
	0.05 % (v/v)	Tween20
	0.05 % (w/v)	Sodium azide
	5 % (w/v)	Glycine
	5 % (w/v)	BSA

4.4 DNA techniques

4.4.1 Preparation of plasmid DNA from *E.coli*

0.5 l of LB medium supplemented with the appropriate antibiotics was inoculated with 200-500 µl of a pre-culture derived from a single bacteria colony. After incubation for 16-20 h at 30 °C/37 °C (*Inova 4000 Incubator*; New Brunswick), the bacteria were pelleted at 6000 rpm for 10 min (*Avanti J-E*; Beckman & Coulter). Plasmid DNA was extracted according to the manufacturer´s protocol using a *MaxiKit* (Qiagen). For analytical purposes bacteria from 1 ml liquid cultures were harvested (4000 rpm, 5 min; *Eppendorf 5417R*) in 1.5 ml reaction tubes and resuspended in 300 µl *resuspension buffer P1* (Qiagen). The bacteria were lysed by adding 300 µl *lysis buffer P2* (Qiagen) followed by 5 min incubation at RT and addition of 300 µl *neutralization buffer P3* (Qiagen). After an additional 5 min incubation at -20 °C, salts and cellular debris were pelleted by centrifugation at 14000 rpm for 10 min (*Eppendorf 5417R*). The supernatant was transferred into a new 1.5 ml reaction tube together with 1 volume isopropanol and 0.1 volumes 3 M NaAc and DNA was precipitated by centrifugation at 14000 rpm for 30 min (*Eppendorf 5417R*). The DNA pellet was washed once with 1 ml 75 % (v/v) ethanol, again centrifuged at 14000 rpm for 5 min (*Eppendorf 5417R*), air dried and rehydrated in an appropriate volume of ~20-50 µl ddH_20.

4.4.2 Quantitative determination of nucleic acid concentrations

For determination of DNA/RNA concentrations a *NanoDrop* spectrophotometer (PEQLAB) was used at a wavelength of 260 nm. DNA purity was assessed by calculation of the OD_{260}/OD_{280} ratio, which should be located at 1.8 for highly pure DNA and at 2.0 for highly pure RNA.

4.4.3 Agarose gel electrophoresis

Analytical and preparative agarose gels were prepared by dissolving agarose (*Seakem LE agarose*; Biozym) in TBE buffer to a final concentration of 0.6-1.2 % (w/v) depending on the size of the analyzed DNA fragments. Agarose was melted by heating in a microwave (Moulinex) and Ethidium bromide was added to a final concentration of 0.5 µg/ml before pouring the liquid agarose solution in an appropriate gel tray. DNA samples were mixed with 6 x *Loading Buffer* and subjected to agarose gel electrophoresis at a voltage of 5-10 V/cm gel length. DNA was visualized by applying UV light at 312 nm using the *G:BOX transilluminator system* (SynGene). To minimize harmful UV irradiation for preparative purposes, agarose gels were supplemented with 1 mM guanosine. The DNA was extracted from the gel slices by centrifugation at 20000 rpm for 2 h (*RC 5B Plus*; Sorvall), precipitated with isopropanol from the obtained supernatant, washed, dried and rehydrated as described for plasmid DNA in 4.4.1.

5 x TBE	450 mM	Tris (pH 7.8)
	450 mM	Boric Acid
	10 mM	EDTA
6 x loading buffer	10 mM	EDTA
	50 % (v/v)	Glycerol
	0.25 % (w/v)	Bromphenol blue
	0.25 % (w/v)	Xylen Cyanol

4.4.4 Polymerase chain reaction (PCR)

For standard amplification of a DNA template, a 50 µl PCR reaction was prepared by mixing 25 ng DNA template, 125 ng forward primer, 125 ng reverse primer, 1 µl dNTP mixture (dATP, dTTP, dCTP, dGTP; each 1 mM), 5 µl 10 x PCR reaction buffer and 5 U Taq-polymerase (Roche) in a 0.2 ml PCR tube. Following PCR program was performed using a thermocycler (*Flexcycler*; Analytic Jena):

DNA denaturation	1 min	95 °C
Primer annealing	45 sec	55 – 70 °C
Extension	1 min/kb	72 °C
		(25-30 cycles)
Final extension	10 min	72 °C
Storage	∞	4 °C

DNA denaturation, primer annealing and extension were performed for 25-30 cycles. To determine PCR efficiency 5 µl PCR reaction were analyzed by gel electrophoresis (4.4.3).

4.4.5 Site-directed mutagenesis

Plasmid mutations were inserted using the *In vitro QuickChange Site-Directed Mutagenesis* (Agilent) according to the manufacturer´s instructions. Forward and reverse primers were designed with the desired mutations and ordered from Metabion (Munich). Depending on the introduced mutation the PCR program was as follows:

DNA denaturation	1 min	95 °C
Primer annealing	45 sec	55 °C
Extension	45 min/kb	68 °C
		(12-16 cycles)
Final extension	10 min	68 °C
Storage	∞	4 °C

DNA denaturation, primer annealing and extension were performed for 12-16 cycles. To determine PCR efficiency 10 µl PCR reaction were analyzed by gel electrophoresis (4.4.3). The remaining 40 µl of PCR product were incubated with 1 µl restriction enzyme *DpnI* (New England Biolabs) for 1 h at 37 °C to remove methylated template DNA. 10 µl were transformed into chemical competent DH5α (4.1.2), single clones were picked, cultured in 5-10 ml LB medium (4.1.1) and prepared plasmid DNA (4.4.1) was analyzed by restriction digest (4.4.7), agarose gel electrophoresis (4.4.3) and sequencing (4.4.9).

4.4.6 Cloning of DNA fragments

4.4.7 Enzymatic DNA restriction

For analytical restriction digestions 1 µg DNA was incubated with 3-10 U of the appropriate restriction enzyme for 2 h at 37 °C. For preparative restriction digests, 20 µg DNA were incubated with 50 U restriction enzyme for at least 3 h at 37 °C. If necessary, multiple consecutive enzymatic restrictions were carried out, following separation by preparative agarose electrophoresis (4.4.3) and/or isopropanol precipitation (4.4.1).

4.4.8 Ligation

Enzymatically restricted DNA fragments or PCR products synthesized for deletion mutant generation were first purified by agarose gel electrophoresis (4.4.3) or isopropanol precipitation (4.4.1). After restriction, the DNA fragments were dephosphorylated using 5 U Antarctic phosphatase (New England Biolabs) at 37 °C for 30 min to prevent re-circularization of the vectors. For generation of deletion mutants, 10 µl PCR, 2 µl Buffer A, 20 pmol ATP and 1.5 µl PK were mixed with ddH_2O to a final volume of 20 µl and incubated for 1 h at 37 °C in order to phosphorylate the DNA ends. For ligation of an insert into a vector DNA, 20-100 ng vector DNA were mixed with the insert DNA in a ratio of 1/3 together with 2 µl 2 x ligation buffer, 1 U *T4 DNA ligase* (Roche) and ddH_2O to a final volume of 20 µl. For ligation of deletion mutants 200 ng of phosphorylated PCR product were used. Ligation was performed for 30 min at 25 °C. Finally, the ligation product was transformed into chemical competent *E.coli* (4.1.2), single clones were picked, cultured in 5-10 ml LB medium (4.1.1) and prepared plasmid DNA was analyzed by restriction digestion (4.4.7), agarose gel electrophoresis (4.4.3) and sequencing (4.4.9).

4.4.9 DNA sequencing

For DNA sequencing 0.5-1.0 µg of DNA and 20 pmol of sequencing primer were mixed with ddH_2O in a total volume of 7 µl. Sequencing was performed by Seqlab (Göttingen).

4.5 RNA techniques

4.5.1 Preparation of total RNA from mammalian cells

Mammalian cells were seeded in 100 mm cell culture dishes, treated and harvested according to the experimental setup. The cell pellet was lysed in 100 µl RIPA buffer supplemented with protease inhibitors for 2 min on ice before centrifugation at 500 g for 5 min (4 °C; *Eppendorf 5417R*). The supernatant was discarded and the remaining nuclei pellet was resuspended in *Trizol reagent* (Invitrogen). After 5 min incubation at RT, 200 µl

Chloroform (Sigma) was added, vortexed shortly and incubated for another 3 min at RT. Cell debris was pelleted at 12000 g for 15 min at 4 °C (*Eppendorf 5417R*) and the RNA containing supernatant was transferred into a new 1.5 ml reaction tube to precipitate the RNA with 600 µl isopropanol at 12000 g for 15 min (4 °C; *Eppendorf 5417R*). The RNA pellet was washed once with 1 ml 75 % (v/v) EtOH (7500 g, 15 min, 4 °C; *Eppendorf 5417R*), air-dried and re-hydrated in 20 µl DEPC-treated H_2O at 55 °C for 10 min. The amount of total RNA was determined with the *NanoDrop* spectrophotometer (PEQLAB; 4.4.2). RNA was stored at -20 °C or subjected to reverse transcription for quantitative RT-PCR (4.5.2).

4.5.2 Quantitative reverse transcription (RT)-PCR

1 µg of RNA was reverse transcribed using the *Reverse Transcription System* (Promega). Quantitative reverse transcription (RT)-PCR was performed with a first-strand method in a *Rotor-Gene 6000* (Corbett Life Sciences) in 0.5 ml reaction tubes containing a 1/50 dilution of the cDNA template, 10 pmol/µl of each synthetic oligonucleotide primer and 5 µl/sample *SensiMix SYBR* (Bioline). The PCR conditions were as follows: 10 min at 95 °C, followed by 40 cycles of 30 s at 95 °C, 30 s at 62 °C, and 30 s at 72 °C. The average threshold cycle (CT) value was determined from triplicate reactions, and levels of viral mRNA relative to cellular 18S rRNA were calculated. The identities of the products obtained were confirmed by melting curve analysis.

4.6 Protein methods

4.6.1 Preparation of total cell lysates

Unless otherwise indicated, all total cell lysates were prepared with the highly stringent RIPA lysis buffer to ensure proper solubilisation of matrix-associated proteins, such as PML or Sp100 and to eliminate unspecific or weak protein interactions. Cells were harvested as described in 4.2.5 and cell pellets were resuspended in 100-500 µl (depending on pellet size) ice-cold RIPA lysis buffer. RIPA buffer was freshly supplemented with 1 mM DTT, 0.2 mM PMSF, 1 mg/ml pepstatin A, 5 mg/ml aprotinin, 20 mg/ml leupeptin, 25 mM iodacetamide and 25 mM N-ethylmaleimide. To ensure efficient cell disruption, lysates were incubated on ice for 30 min and vortexed every 10 min before sonification (40 pulses; output 0.80; 0.8 Impulse/s; *Branson Sonifier 450*) to shear genomic DNA. Cell debris and insoluble components were pelleted (14000 rpm, 5 min, 4 °C; *Eppendorf 5417R*) and the protein concentration of the supernatant was determined by spectrophotometry (4.6.2).

Finally, proteins were denatured by addition of 5 x SDS sample buffer and subsequent boiling at 95 °C for 3 min. Protein lysates were stored at -20 °C until analysis by SDS-PAGE/immunoblotting (4.6.5; 4.6.6).

RIPA	50 mM	Tris-HCl (pH 8.0)
	150 mM	NaCl
	5 mM	EDTA
	1 % (v/v)	Nonidet P-40
	0.1 % (w/v)	SDS
	0.5 % (w/v)	Sodium Desoxycholate
5 x SDS sample buffer	100 mM	Tris-HCl (pH 6.8)
	10 % (w/v)	SDS
	200 mM	DTT
	0.2 % (w/v)	Bromphenol blue

4.6.2 Quantitative determination of protein concentrations

Protein concentrations of total cell lysates were determined by measuring the absorption of protein-bound chromogenic substrate at 595 nm using the Bradford-based *BioRad Protein-Assay* (Bradford, 1976). For each sample 1 µl protein lysate was mixed with 800 µl ddH_2O and 200 µl *Bradford Reagent* (BioRad), incubated for 5 min at RT and measured in a *SmartSpec Plus* spectrophotometer (BioRad) at 595 nm against a blank. Protein concentrations were determined by interpolation from a standard curve with BSA (concentrations of 1-16 µg/ µl; New England Biolabs).

4.6.3 Immunoprecipitation

For immunoprecipitation equal amounts (0.5 mg-2 mg) of total cell lysates (4.6.1) were pre-cleared by addition of protein A- or protein G-sepharose (Sigma-Aldrich) for 1 h at 4 °C in a rotator (GFL). Simultaneously, 1 µg purified antibody or 100 µl/mg sepharose for hybridoma supernatant were coupled to 3 mg of sepharose/IP. Antibody-coupled sepharose beads were washed three times with 1.0 ml of lysis buffer and added to the pre-cleared protein lysate in a 1.5 ml reaction tube after clearing by centrifugation (600 g, 5 min, 4 °C; *Eppendorf 5417R*). Immunoprecipitation was performed at 4 °C in a rotator (GFL) for 1-2 h. Sepharose beads with precipitated protein complexes were pelleted (600 g, 5 min, 4 °C; *Eppendorf 5417R*) before washing three times with 1.0 ml RIPA lysis buffer. Finally, an

appropriate volume of *2 x SDS sample buffer* was added to the samples before boiling them at 95 °C for 3 min. Eluted protein samples were stored at -20 °C until further analysis.

2 x SDS sample buffer		
	100 mM	Tris-HCl (pH 6.8)
	4 % (w/v)	SDS
	200 mM	DTT
	0.2 % (w/v)	Bromphenol blue
	20 %	Glycerol

4.6.4 Denaturing purification and analysis of - conjugates

HeLa cells stably expressing 6His-SUMO-1 or 6His-SUMO-2 were infected/transfected with the appropriate virus/expression vector. 48 h later, cells were harvested, washed once with 1 x PBS and lysed in 5 ml Guanidinium containing lysis buffer. 10 % of the cells were lysed with RIPA Buffer for total protein analysis (4.6.1). Lysates in Guanidinium buffer were incubated for 6 h at 4 °C with 25 µl Ni-NTA agarose (Qiagen) prewashed with lysis buffer. The slurry was washed once with lysis buffer; then once with each wash buffer pH 8.0/ pH 6.3. 6His-SUMO conjugates were eluted with 40 µl elution buffer and subsequent boiling at 95 °C for 5 min. After denaturation, proteins were separated by SDS-PAGE and visualized by immunoblotting.

Guanidinium lysis buffer		
	6 M	Guanidinium-HCl
	0.1 M	Na_2HPO_4
	0.1 M	NaH_2PO_4
	10 mM	Tris-HCl (pH 8.0)
	20 mM	Imidazole
	5 mM	β-Mercaptoethanol

Wash buffer pH 8.0		
	8 M	Urea
	0.1 M	Na_2HPO_4
	0.1 M	NaH_2PO_4
	10 mM	Tris-HCl (pH 8.0)
	20 mM	Imidazole
	5 mM	β-Mercaptoethanol
		Protease inhibitors

Wash buffer pH 6.3		
	8 M	Urea
	0.1 M	Na_2HPO_4

	0.1 M	NaH_2PO_4
	10 mM	Tris-HCl (pH 6.3)
	20 mM	Imidazole
	5 mM	β-Mercaptoethanol
		Protease inhibitors
Elution buffer	200 mM	Imidazole
	0.1 % (w/v)	SDS
	150 mM	Tris-HCl (pH 6.8)
	30 % (v/v)	Glycerol
	720 mM	β-Mercaptoethanol
	0.01 % (w/v)	Bromphenol blue

4.6.5 SDS polyacrylamide gel electrophoresis (SDS-PAGE)

Protein samples were separated according to their molecular weights by SDS-PAGE (Biometra). Polyacrylamide gels were made using 30 % acrylamide/bisacrylamide solution (37.5:1 *Rotiphorese Gel 30*; Roth) diluted to the final concentration of 8 %-15 % with ddH_20. The gels were run at 20 mA/gel in TGS-buffer. The *PageRuler Prestained Protein Ladder Plus* (Fermentas) was used for protein weight comparison.

5 % stacking gel	17 % (v/v)	Acrylamide solution (30 %)
	120 mM	Tris-HCl (pH 6.8)
	0.1 % (w/v)	SDS
	0.1 % (w/v)	APS
	0.1 % (v/v)	TEMED
8 % separating gel	27 % (v/v)	Acrylamide solution (30 %)
	250 mM	Tris-HCl (pH 8.8)
	0.1 % (w/v)	SDS
	0.1 % (w/v)	APS
	0.6 % (v/v)	TEMED
10 % separating gel	34 % (v/v)	Acrylamide solution (30 %)
	250 mM	Tris-HCl (pH 8.8)
	0.1 % (w/v)	SDS
	0.1 % (w/v)	APS
	0.6 % (v/v)	TEMED

12 % separating gel	40 % (v/v)	Acrylamide solution (30 %)
	250 mM	Tris-HCl (pH 8.8)
	0.1 % (w/v)	SDS
	0.1 % (w/v)	APS
	0.6 % (v/v)	TEMED
15 % separating gel	50 % (v/v)	Acrylamide solution (30 %)
	250 mM	Tris-HCl (pH 8.8)
	0.1 % (w/v)	SDS
	0.1 % (w/v)	APS
	0.6 % (v/v)	TEMED
TGS buffer	25 mM	Tris
	200 mM	Glycine
	0.1 % (w/v)	SDS

4.6.6 Western Blotting

Equal amounts of protein samples were separated by SDS-PAGE and transferred onto nitrocellulose (Whatman) or polyvinylidene fluoride (PVDF) membranes using the *Trans-Blot Electrophoretic Transfer Cell* System (BioRad) in Towbin-buffer. Gels and membranes were soaked in Towbin-buffer, placed between two soaked blotting papers (Whatman) and two blotting pads in a plastic grid. The electrophoretic transfer was performed in a blotting tank filled with Towbin-buffer at 400 mA for 90 min. To saturate non-specific antibody binding sites, the membranes were incubated for 2 h at RT or over night at 4 °C in PBS-Tween containing 5 % (w/v) non-fat dry milk (Frema) on an orbital shaker (GFL). Afterwards, the blocking solution was discarded, membranes were washed briefly to remove remaining blocking solution and incubated for 2 h at RT with the primary antibody diluted in PBS-Tween. The primary antibody dilutions were established for each individual antibody. To reduce the background signal, some primary antibody solutions were supplemented with 1-3 % (w/v) non-fat dry milk (Frema). After primary antibody incubation, the membranes were washed three times for 10 min and incubated for 2 h at RT in PBS-Tween with the HRP coupled secondary antibody (1:10000; Amersham) containing 5 % (w/v) non-fat dry milk (Frema) before three final washes in PBS-Tween for 15 min. Protein bands were visualized by enhanced chemiluminescence using *SuperSignal West Pico Chemiluminescent Substrate* (Pierce) according to the manufacturer´s instructions and

detected by X-ray films (*RP New Medical X-Ray Film*; CEA) using a *GBX Developer* (Kodak). X-ray films were scanned, cropped using *Photoshop CS5* (Adobe) and figures were prepared using *Illustrator CS5* (Adobe).

Towbin buffer	25 mM	Tris-HCl (pH 8.3)
	200 mM	Glycine
	0.05 % (w/v)	SDS
	20 % (v/v)	Methanol
PBS-Tween	0.1 % (v/v)	Tween20
		In 1x PBS

4.6.7 Indirect immunofluorescence

For indirect immunofluorescence cells were grown on glass coverslips and transfected/infected according to the experimental setup. Cells were fixed with 4 % PFA at 4 °C for 20 min and permeabilized with PBS containing 0.5 % (v/v) Triton X-100 for 30 min at RT. To visualize intranuclear E1A staining, the cells were extracted with CSK buffer adapted from Carvalho *et al.* for 1-3 min (Carvalho *et al.*, 1995). Otherwise cells were permeabilized by incubation with PBS-Triton for 10 min. After 1 h blocking in TBS-BG buffer, coverslips were treated for 1 h with the primary antibody diluted in PBS, washed three times with TBS-BG buffer, followed by incubation with the corresponding Alexa488 (Invitrogen) or Cy3-conjugated (Dianova) secondary antibodies. Coverslips were washed three times with TBS-BG buffer, mounted in *Glow medium* and digital images were acquired with a confocal laser-scanning microscope (*Zeiss-CLSM-510*). Images were cropped using Adobe *Photoshop CS5* and assembled with *Adobe Illustrator* CS5.

CSK buffer	10 mM	Hepes (pH 6.8)
	100 mM	NaCl
	300 mM	Sucrose
	3 mM	$MgCl_2$
	2 mM	EDTA
	0.1 mM	PMSF
	0.5 %	Triton X-100
PBS-Triton	0.5 mM	Triton X-100
		in PBS

4.7 Reporter gene assay

For quantitative determination of promoter activities, the *Dual-Luciferase Reporter Assay System* (Promega) was used according to the manufacturer´s protocol. Promoter activity was determined by the expression of *Firefly* luciferase (*Photinus pyralis*) under the control of a promoter of interest and normalized to *Renilla* luciferase (*Renilla reniformis*) expression, which is under the control of the herpes simplex virus thymidine kinase (HSV-TK) promoter and served as an internal transfection control. Subconfluent cells were transfected in 6-well/12-well dishes according to the experimental setting. 24 h post transfection cells were harvested by applying 300 µl/100 µl *passive lysis buffer* (Promega) per 6-well/12-well respectively and incubating for 15 min at RT on an orbital shaker (GFL). 5 µl of lysate was subjected to sequential measuring of *Firefly* (10 sec) and *Renilla* luciferase activity (10 sec) in a *Lumat LB 9507 luminometer* (Berthold Technologies).

5 Results

5.1 Interaction of E1A with PML

5.1.1 E1A-13S localizes to endogenous PML in transiently transfected cells

E1A has been described to localize to PML-NBs, although reports proposed different functions of E1A-12S and E1A-13S during adenoviral infection (Carvalho *et al.*, 1995). In this context, both E1A isoforms were expressed separately and their localization was visualized with respect to endogenous PML-NBs.

Both isoforms localized to the nucleus in large amounts (Fig. 9A; g, k), whereas PML exhibited the characteristic punctate nuclear staining (Fig. 9A; f, j). Consistent with published results E1A-12S as well as E1A-13S relocalized PML-NBs, causing them to appear bigger in size and lower in number (Eskiw *et al.*, 2003).

A

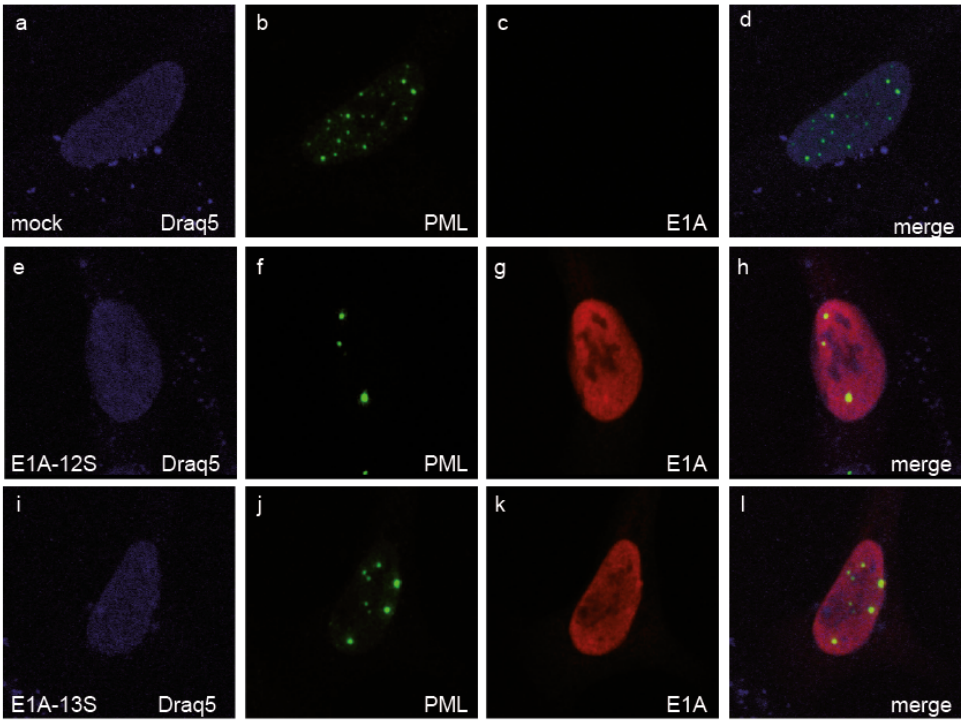

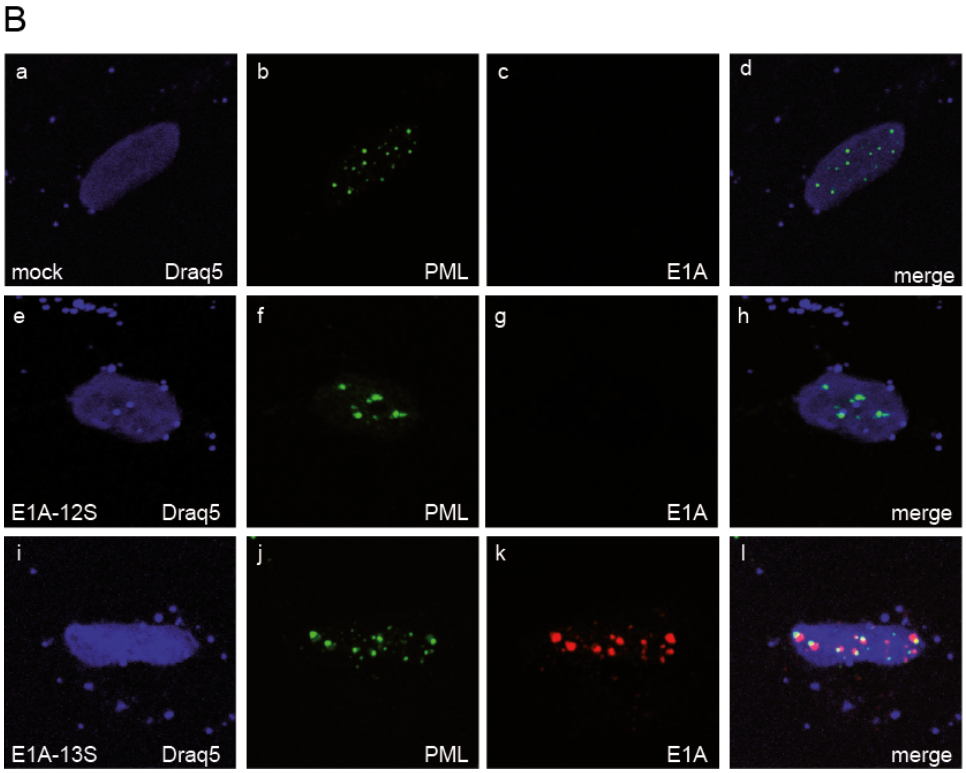

Figure 9: E1A-13S colocalizes with endogenous PML in transiently transfected cells. HepaRG cells were transfected with 3 µg of pHA-E1A-12S or pHA-E1A-13S, fixed with 4 % PFA 48 h post transfection and double-labeled with mAb M-58 (α-E1A) and pAb NB 100-59787 (α-PML). (B) HepaRG cells were extracted with cytoskeleton buffer prior to fixation with 4 % PFA. In A and B primary Abs were detected with Alexa488 (α-PML; green) and Cy3 (α-E1A; red) conjugated secondary Abs. For nuclear staining the DNA intercalating dye Draq5 (Biostatus) was used. Representative α-E1A (Ac, g, k; Bc, g, k) and α-PML (Ab, f, j; Bb, f, j) staining patterns of at least 50 analyzed cells are shown. Overlays of single images (merge) are shown in Ad, h, i; Bd, h, i (magnification x 7600).

Since the high amounts of intranuclear E1A rendered it very difficult to spot any distinct staining patterns, the cells were pre-extracted prior to fixation (Fig. 9B; Carvalho *et al.*, 1995). After pre-extraction, E1A-13S accumulated in several brightly stained nuclear aggregates juxtaposed to endogenous PML in ~30 % of the transfected cells (Fig. 9B, i-l). For the smaller E1A-12S isoform no staining juxtaposed to PML could be observed (Fig. 9B, e-h). These observations are consistent with previous reports showing that transcriptionally active proteins often tend to associate with the nuclear matrix (Nardozza *et al.*, 1996).

5.1.2 E1A-13S localizes to PML-NBs during adenoviral infection

Detailed studies have revealed an astonishing amount of cross-talk between adenoviral proteins in the modulation of host cell factors, e.g. PML and PML-associated proteins.

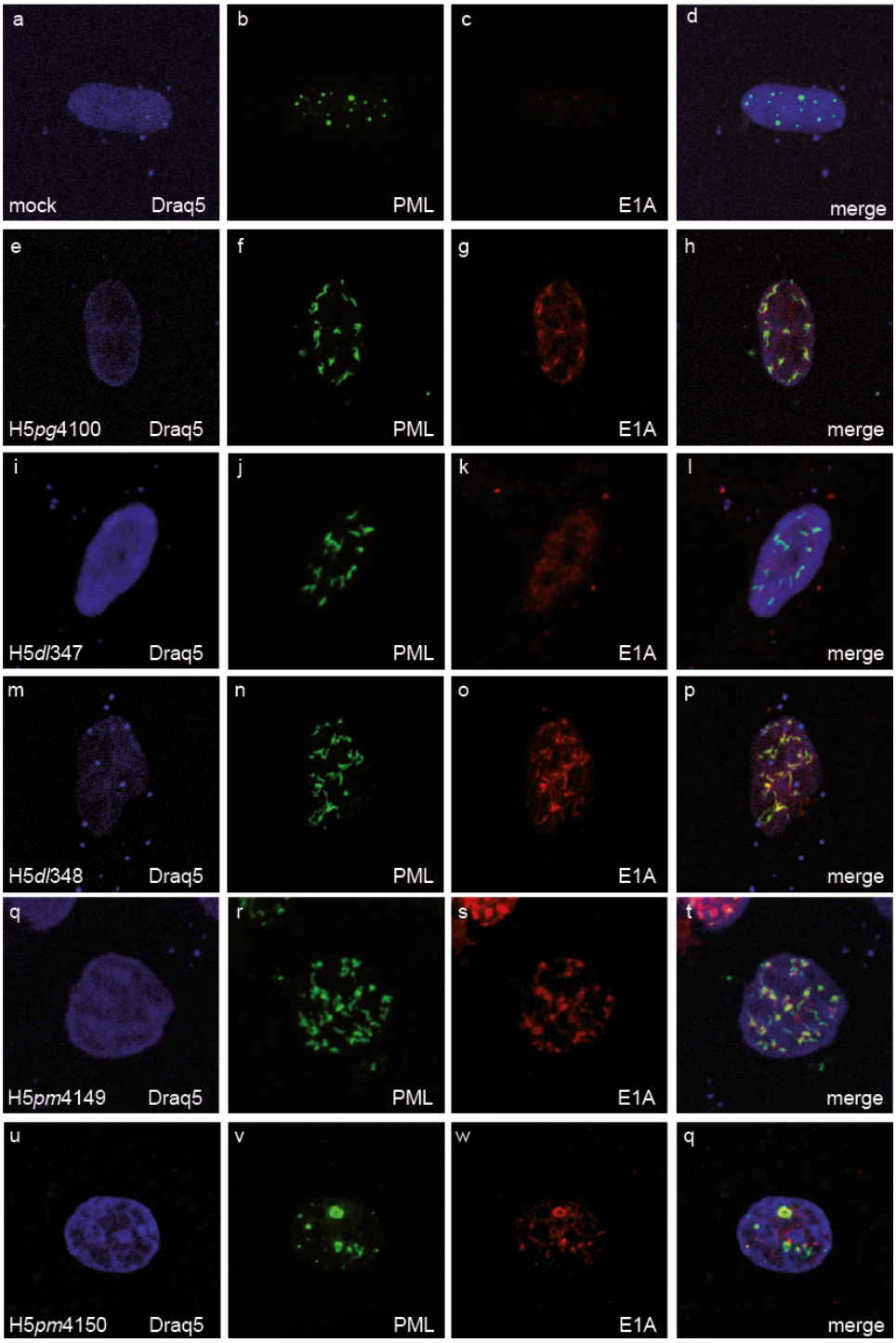

Figure 10: E1A-13S colocalizes with endogenous PML in infected cells. Human hepatocytes (HepaRG) were infected with wt (H5*pg*4100) or mutant viruses (H5*dl*347, H5*dl*348; H5*pm*4149, H5*pm*4150) at a multiplicity of 50 ffu/cell and fixed with 4 % PFA 24 h p.i. The cells were extracted with cytoskeleton buffer prior to fixation and double-labeled with mAb M-58 (α-E1A) and pAb NB 100-59787 (α-PML). Detection of primary Abs and nuclear staining was performed as in Fig. 9. Representative α-E1A (red; c, g, k, o, s, w) and α-PML (green; b, f, j, n, r, v) staining patterns of at least 50 analyzed cells are shown. Overlays of the single images (merge) are shown in d, h, i (magnification x 7600).

Previously published data illustrate that the viral protein E4orf3 is necessary and sufficient to disrupt the structure of cellular PML-NBs during Ad5 infection (Carvalho *et al.*, 1995; Hoppe *et al.*, 2006; Leppard & Everett, 1999; Puvion-Dutilleul *et al.*, 1995). In addition, viral early E1B-55K protein has been shown to interact and functionally cooperate with PML-NBs (Leppard & Everett, 1999; Schreiner *et al.*, 2010; Wimmer *et al.*, 2010). To evaluate whether other adenoviral proteins interfere with, or alter the cooperation between E1A and PML, the localization during productive Ad5 infection was analyzed (Fig. 10). HepaRG cells were infected with wt virus (H5*pg*4100) and virus mutants expressing E1A-12S (H5*dl*347) or E1A-13S (H5*dl*348). To exclude expression of other adenoviral proteins mediating PML interaction, viruses lacking E1B-55K (H5*pm*4149) or E4orf3 (H5*pm*4150) were included as controls.

As expected, PML was relocalized (Fig. 10a, 10f, 10j, 10n, 10r) into so-called track-like structures in infected cells. The virus mutant lacking E4orf3 protein (H5*pm*4150) was no longer able to relocalize PML-NBs, although their shape was different from the punctate staining in mock-infected cells (Fig. 10a; 10v). We detected E1A co-localization with PML track-like structures in wt virus (H5*pg*4100) as well as H5*dl*348-infected cells expressing only E1A-13S (Fig. 10g; 10o), whereas E1A-12S (H5*dl*347) was distributed much more diffusely in the host-cell nuclei (Fig. 10k). E1A also localized to PML after infection with virus lacking E4orf3 or E1B-55K (Fig. 10t; 10q) implying that E1A-13S localizes to PML-NBs independently of E4orf3 or E1B-55K expression.

5.1.3 E1A-13S interacts with human PML-II isoform in transient transfections

Human cells express at least seven distinguishable PML isoforms of which PML-I to -VI possess a nuclear localization sequence (Jensen *et al.*, 2001). To ascertain whether E1A specifically interacts with different PML isoforms, human cells were transfected with E1A-13S or E1A-12S and plasmids encoding human PML isoforms I to VI.

Precipitating flag-tagged PML and subsequently staining for E1A revealed a highly specific interaction between E1A-13S and PML isoform II (Fig. 11D, lane 4). E1A-12S could not be co-precipitated with any PML isoform (Fig. 11B), although the steady-state levels showed equal amounts of transfected PML and E1A isoforms (Fig. 11A, 11C).

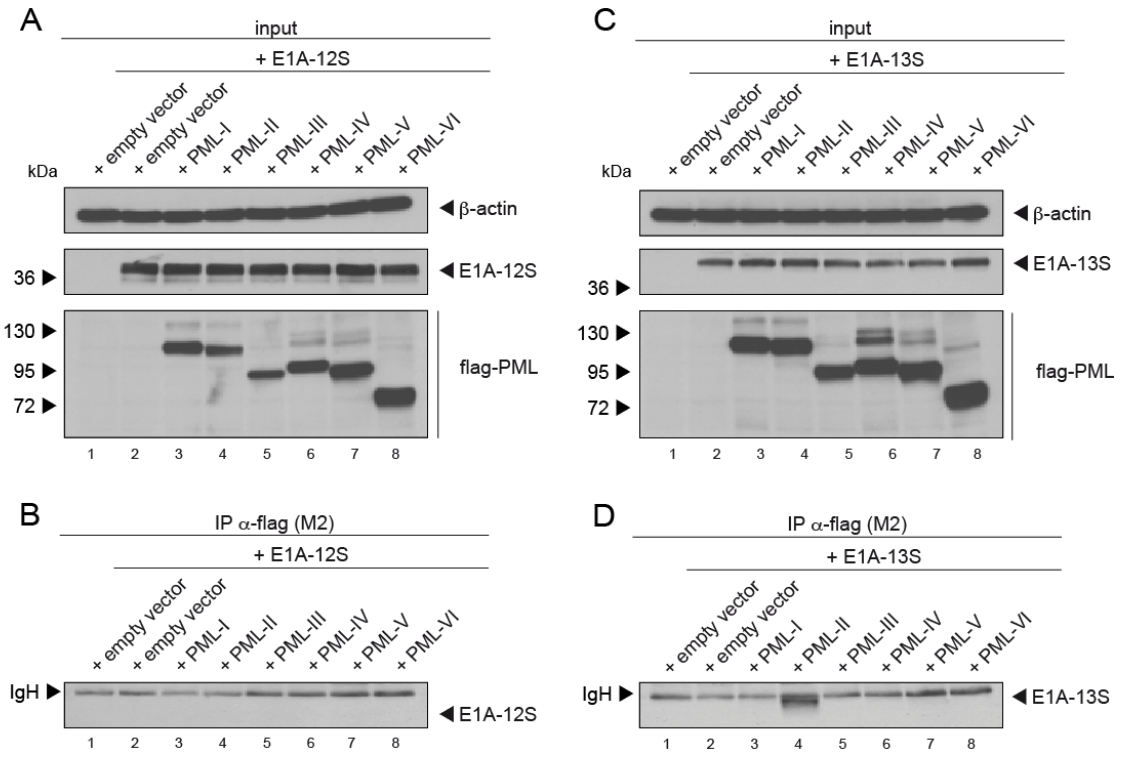

Figure 11: E1A-13S binds a specific PML isoform in transiently transfected H1299 cells. Subconfluent H1299 cells were transfected with 3 µg of pHA-E1A-12S or pHA-E1A-13S and 5 µg of different lentiviral constructs encoding N-terminal flag-tagged human PML isoforms I to VI, harvested after 48 h and total cell extracts were prepared. Immunoprecipitation of flag-PML was performed using mAb flag-M2 (α-flag), and proteins were visualized by immunoblotting. Input levels in total cell-lysates (A, C) and co-precipitated proteins (B, D) were detected using mAb 610 (α-E1A), mAb flag-M2 (α-flag) and mAb AC-15 (α-β-actin). Molecular weight in kDa is indicated on the *left*, while the relevant proteins are labeled on the *right*. Note that heavy chains (IgH) are detected at 55 kDa in B and D.

5.1.4 Mutation screening of E1A-13S revealed PML-II interaction within CR3

Since E1A-13S differs from E1A-12S in only CR3, composed of 46 aa, we assumed that PML-II binding depends on this or adjacent regions in the E1A protein. To more precisely identify the binding domain required for E1A-13S/PML-II interaction, E1A-13S mutants with overlapping 14-16 aa deletions spanning the proposed region were constructed (Fig. 12A). Although the E1A-13S mutants had slightly altered gel migration properties, input levels of E1A-13S and PML-II were equal in the co-immunoprecipitation assays (Fig. 12B). These experiments revealed that deletion mutant no. 7 (E1A-13SΔ176-191; Fig. 12A) exhibits strongly impaired PML-II binding properties (Fig. 12C, lane 11).

To further narrow down the interaction region, a shorter deletion mutant E1A-13SΔ182-191 was constructed (Fig. 13A). This mutant showed deficiency of PML-II binding similar to E1A-13SΔ176-191 (data not shown).

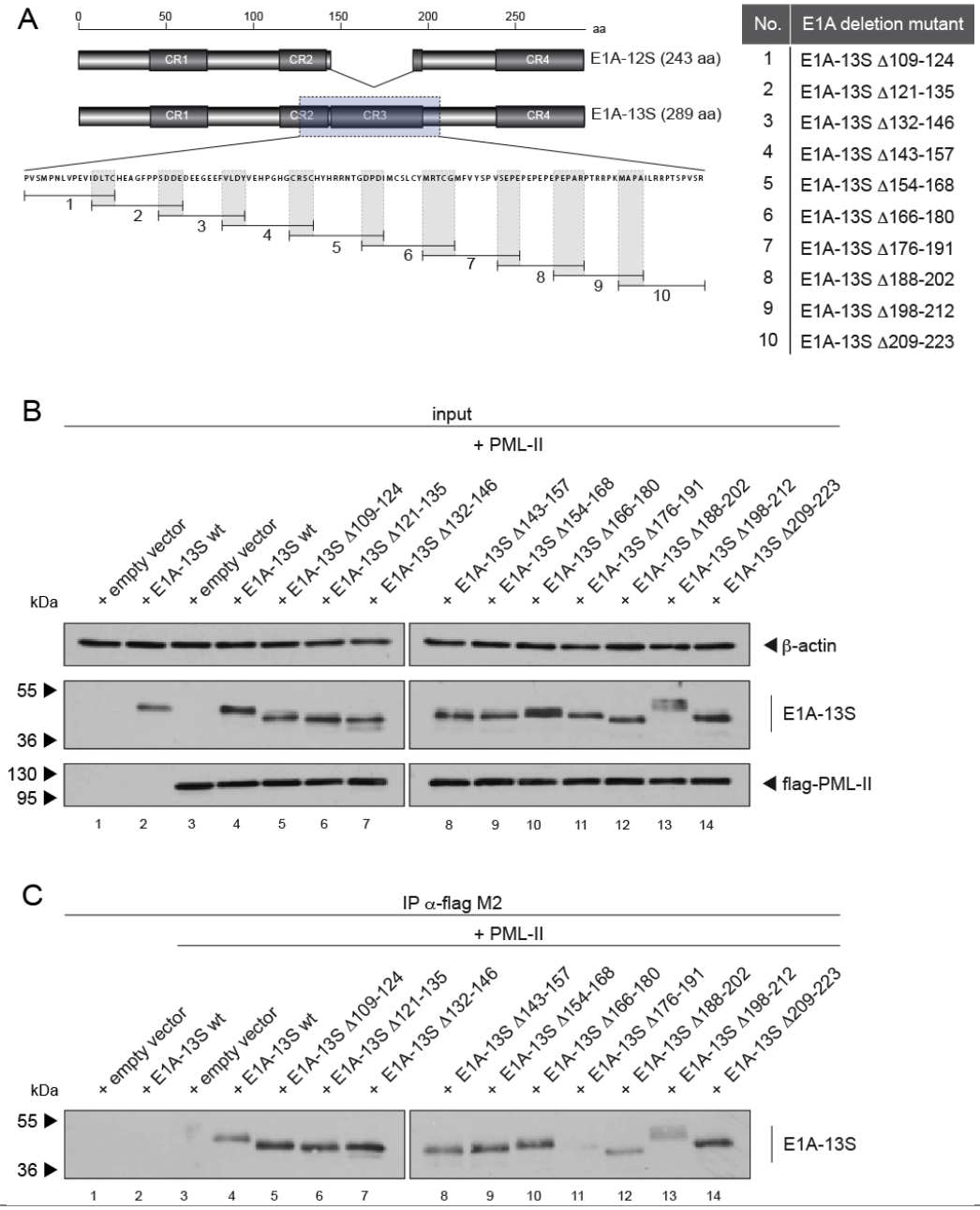

Figure 12: Mapping experiments identified an E1A mutant defective in binding PML-II. (A) Overlapping deletions of 14-16 aa spanning CR3 and adjacent regions are shown below the schematic representation of E1A-12S and E1A-13S protein structures. Detailed aa deletions of each mutant are listed on the *right*. (B, C) Subconfluent H1299 cells were transfected with 3 µg of pHA-E1A-13S wt or pHA-E1A-13S deletion mutants and 3 µg of pflag-PML-II, harvested after 48 h, before preparing total cell extracts. Co-immunoprecipitation assays were performed as described in Fig. 11. Note the different E1A-13S deletion mutants show different mobilities. Molecular weights in kDa are indicated on the *left*, relevant proteins on the *right*.

5.1.5 E1A-13S interacts with endogenous PML

Next, we verified our observations by co-immunoprecipitation experiments with endogenous PML. Therefore, human H1299 cells were transfected with E1A-12S, E1A-13S, or E1A-13SΔ182-191, or infected with wt virus (H5*pg*4100), and virus mutants expressing only E1A-12S (H5*dl*347), only E1A-13S (H5*dl*348), or no E1A protein (H5*dl*312) as a negative control (Fig. 13B).

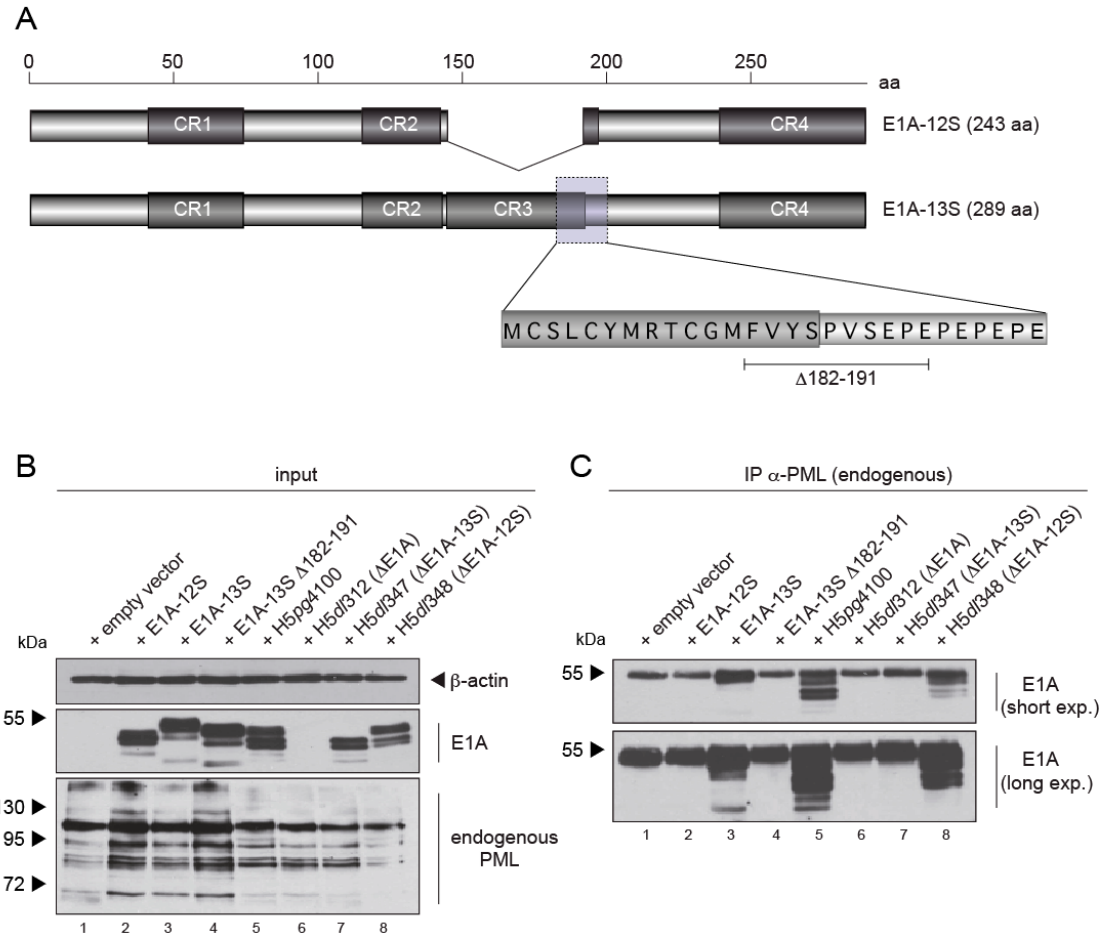

Figure 13: Interaction with PML-II depends on a highly conserved transcription factor-binding region within CR3. (A) The schematic representation of E1A-12S and E1A-13S with the enlarged interaction region depicted below. Mapped is the newly constructed PML-II/E1A-binding mutant 13SΔ182-191 with a shorter deletion as the previously identified 13SΔ176-191. (B, C) Subconfluent H1299 cells were transfected with 3 µg of pHA-E1A-12S, pHA-E1A-13S and pHA-E1A-13SΔ182-191, or infected with wt virus (H5*pg*4100) or virus mutants (H5*dl*312, H5*dl*347, H5*dl*348). The cells were harvested 48 h after transfection or 24 h. p.i. and total cell extracts were prepared. Immunoprecipitation of endogenous PML was performed using pAb NB100-59787 (α-PML), proteins were resolved on 10 % SDS-PAGE and visualized by immunoblotting. Steady-state expression levels of total cell lysates (input) and co-precipitated proteins (IP) were detected using mAb 610 (α-E1A), pAb NB100-59787 (α-PML) and mAb AC-15 (α-β-actin). Molecular weights in kDa on the *left*, corresponding proteins on the *right*.

After precipitating endogenous PML and subsequent staining for E1A, a specific interaction of endogenous PML with transfected E1A-13S as well as viral E1A in H5*pg*4100- and H5*dl*348-infected cells (Fig. 13C, lanes 3, 5 and 8) could be detected. In contrast, E1A-12S, deletion mutant E1A-13SΔ182-191, and viral E1A encoded by the virus mutant lacking E1A-13S (H5*dl*347) could not be precipitated with endogenous PML (Fig. 13C).

In sum, interaction of E1A-13S with PML could be mapped to aa 182-191 at the end of the CR3 of E1A-13S. This binding region (aa 182-191) is highly conserved in different Ad types and has previously been identified as the variable transcription factor binding domain, or promoter-targeting domain of E1A-13S (Liu & Green, 1994; Pelka *et al.*, 2008; Webster & Ricciardi, 1991).

5.1.6 E1A-13S and PML cooperation impacts viral and cellular transcription

PML-NBs have been implicated in regulating transcription (Zhong *et al.*, 2000b). Furthermore, it is known that several viral genomes including Ad DNA localize close to PML-NBs in order to start transcription and replication (Ishov & Maul, 1996; Regad & Chelbi-Alix, 2001). Therefore, E1A likely affects transcriptional regulation from adenoviral promoters in cooperation with PML-II.

To address this idea, luciferase reporter assays were performed after transfecting luciferase-dependent plasmids encoding adenoviral promoters (Schreiner *et al.*, 2012) together with E1A-13S and PML-II (Fig. 14). PML-II alone was not able to stimulate transcription from Ad5 E2 early promoter, whereas E1A-13S activated luciferase activity from this promoter 10-fold. Furthermore, PML-II efficiently stimulated transcription from the Ad5 promoter when co-expressed with E1A-13S. This was further verified by the positive correlation between increasing levels of expressed PML-II and activated transcription at constant E1A-13S levels (Fig. 14B). As a control E1A-12S and E1A-13SΔ182-191 were included in this reporter gene assay. Neither E1A-12S nor E1A-13SΔ182-191 stimulated transcription from the adenoviral promoter in combination with equal amounts of PML-II (Fig. 14B).

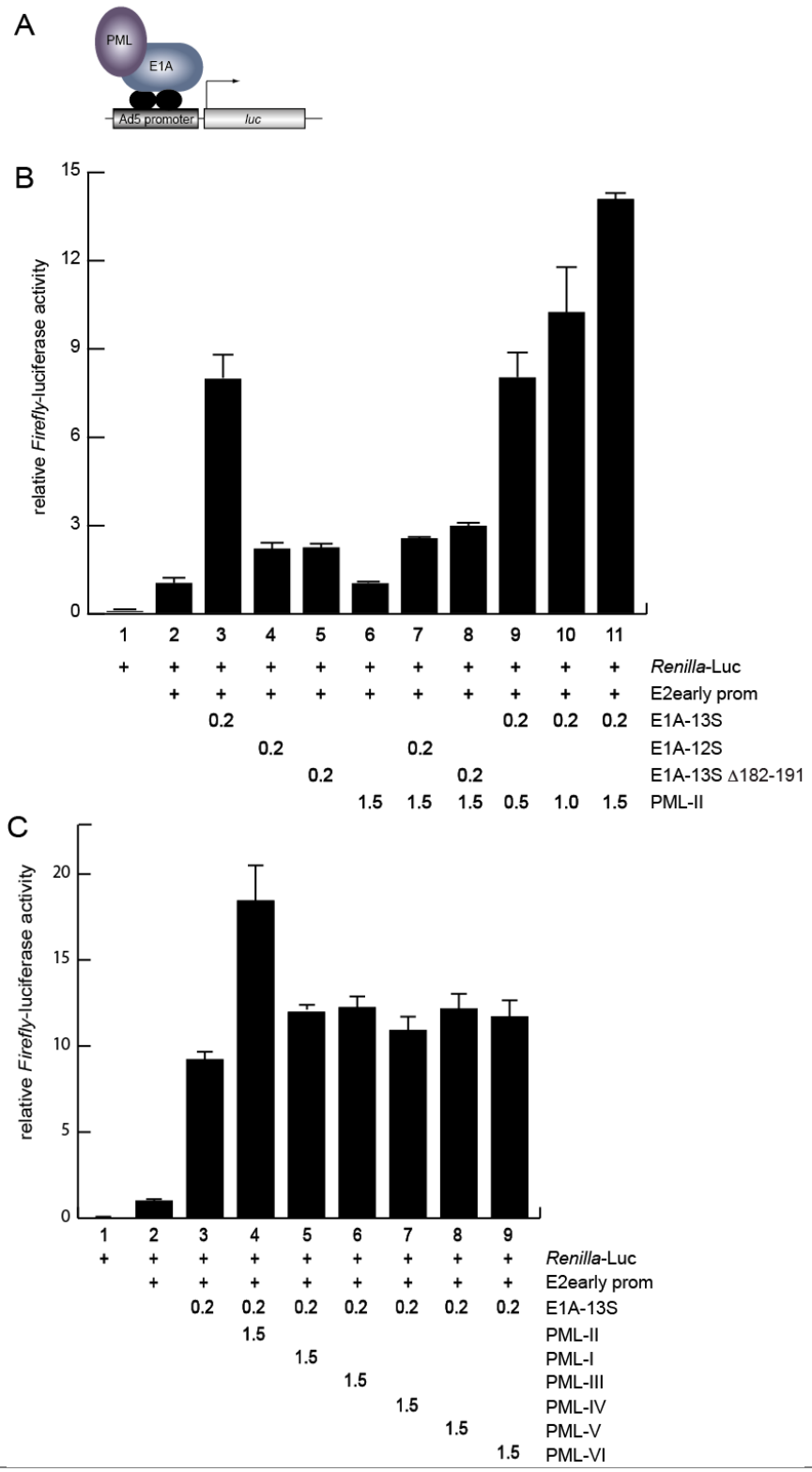

Figure 14: PML stimulates E1A-13S-dependent transcriptional activation of adenoviral E2 early promoter. (A) Schematic representation of the luciferase reporter assay: the luciferase gene is under the control of the Ad5 promoter, which is bound and activated by a complex of E1A-13S and PML-II. (B) H1299 cells were transfected with 0.2 µg of pRL-TK (*Renilla*-Luc), 0.5 µg pGL3-Basic Prom E2E (E2early-promoter), 0.2 µg pHA-E1A (HA-E1A-12S, HA-E1A-13S, HA-E1A-13SΔ182-191) and increasing amounts of pflag-PML-II in the combinations indicated (+). 24 h post transfection total cell extracts were prepared and luciferase activity was determined. The mean

and standard deviations are presented for three independent experiments. (C) H1299 cells were transfected with 0.2 µg of pRL-TK (*Renilla*-Luc), 0.5 µg pGL3-Basic Prom E2E (E2early-promoter), 0.2 µg pHA-E1A-13S and 1.5 µg pflag-PML-I to VI in the combinations indicated. 24 h post transfection total cell extracts were prepared and luciferase activity was determined. The mean and standard deviations are presented for three independent experiments.

Recently, Pelka *et al.* reported that the cellular transcription factor p300 binds E1A-13S within the CR3 region, and is recruited to Ad promoters during infection (Pelka *et al.*, 2009). p300 possesses intrinsic acetyltransferase activity and is therefore an important transcriptional co-activator; it is recruited to gene promoters via its association with numerous DNA-binding transcription factors (Goodman & Smolik, 2000). PML was also found to interact with p300/CBP and regulate transcription (von Mikecz *et al.*, 2000). In this context, we tested whether E1A-13S and PML-II affect p300 co-activator function. Luciferase reporter assays with a GAL4-responsive promoter and p300 fused to a GAL4 DNA-binding domain, in combination with E1A-13S and PML-II were performed (Fig. 15). PML-II alone only slightly stimulated transcription from the GAL4 promoter, whereas E1A-13S enhanced p300 transcriptional activity two-fold. Consistent with the observations above, co-expression of E1A-13S with PML-II strongly stimulated the luciferase activity from the GAL-4 promoter. Co-transfection of increasing PML-II amounts further stimulated p300-dependent transcriptional activation (Fig. 15B). On the other hand, co-expression of PML-II together with E1A-13SΔ182-191 did not activate transcription from the GAL-4 promoter (Fig. 15B).

Additionally, the reporter gene assays shown in Figs. 14 and 15 were performed with the other nuclear PML isoforms. The results showed that other PML isoforms do positively affect E1A-dependent transactivation although to a lesser extend compared to PML-II (Fig. 14C and 15C).

Taken together, our data on transcriptional regulation suggest that PML-II is a dose-dependent co-activator of E1A-13S-dependent transactivation. PML-II is not only able to modulate transcription from Ad5 promoters in combination with E1A-13S, but also stimulates cellular gene expression by affecting key cellular co-activators such as p300.

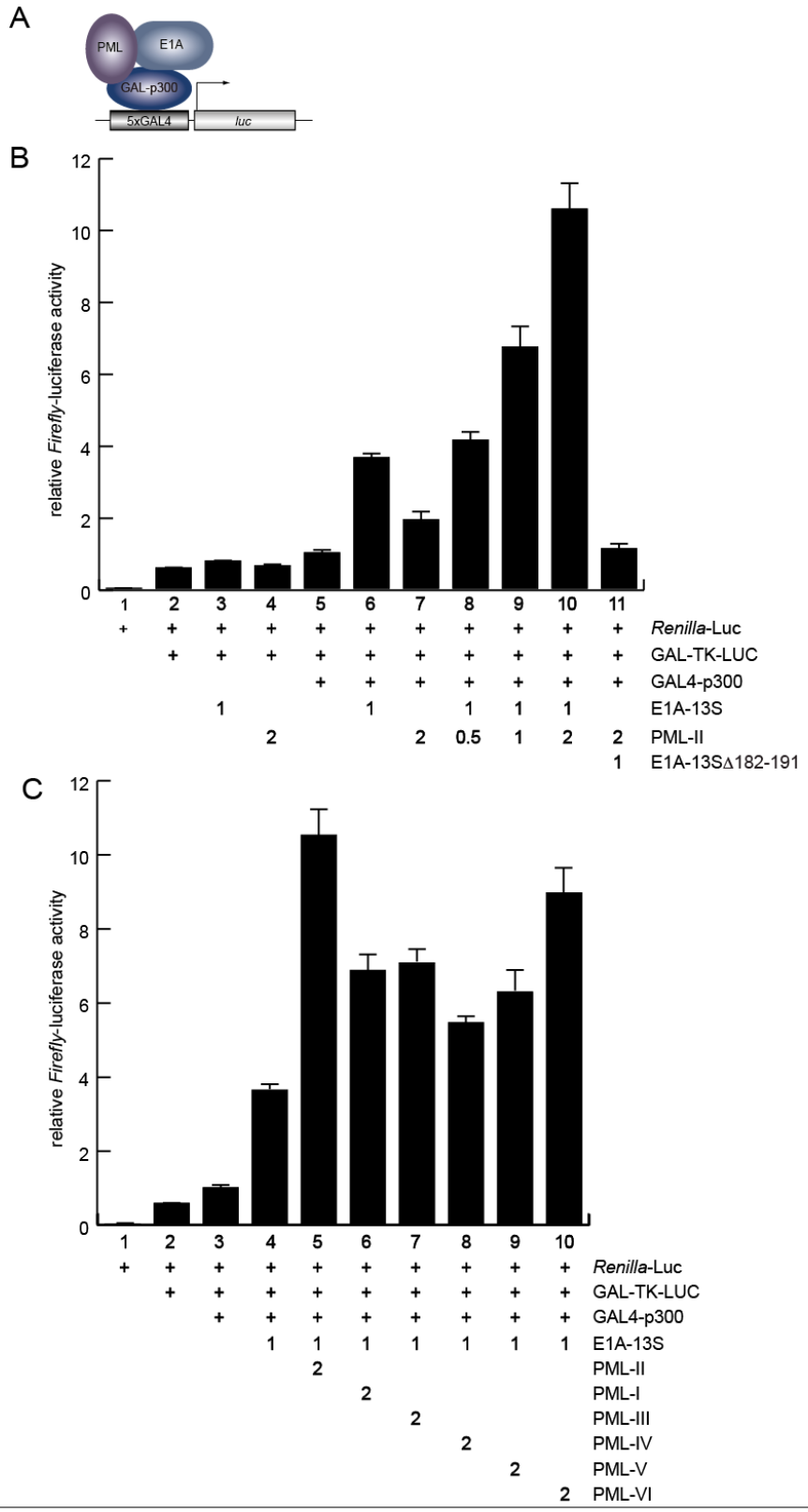

Figure 15: E1A-13S and PML cooperate to stimulate p300 transcriptional coactivation. (A) Schematic presentation of the luciferase reporter assay: the luciferase gene is under the control of a promoter containing 4 GAL4 sequences, which is bound and activated by a complex of GAL-p300, E1A-13S and PML-II. (B) H1299 cells were transfected with 0.2 µg of pRL-TK (*Renilla*-Luc), 0.5 µg pGL-GAL-TK-LUC, 0.5 µg pG4-p300, 1 µg pHA-E1A (HA-E1A-13S, HA-E1A-13SΔ182-191) and increasing amounts of pflag-PML-II in the combinations indicated (+). 24 h post transfection

total cell extracts were prepared and luciferase activity was determined. The mean and standard deviations are presented for three independent experiments. (C) H1299 cells were transfected with 0.2 µg of pRL-TK (*Renilla*-Luc), 0.5 µg pGL-GAL-TK-LUC, 0.5 µg pG4-p300, 1 µg pHA-E1A-13S and 2 µg pflag-PML-I to VI in the combinations indicated. 24 h post transfection total cell extracts were prepared and luciferase activity was determined. The mean and standard deviations are presented for three independent experiments.

5.1.7 PML-II positively regulates adenovirus progeny production in human cells

To reveal the effect of PML-II on the production of adenoviral progeny, virus growth was determined in HepaRG cell lines in which endogenous PML was knocked-down (Hep shPML) and sh-RNA resistant PML-II isoform was reconstituted (Hep PML-II; Cuchet *et al.*, 2011). In accordance with recent reports, PML-knockdown showed a modest effect on adenovirus replication compared to the parental cell line (Schreiner *et al.*, 2010; Ullman & Hearing, 2008). However, reconstitution of the single isoform PML-II enhanced virus yield 3.5-fold compared to the parental cell line (Fig. 16). Consistent with the data obtained from the reporter assays, this strongly indicates that PML-II is a positive regulator of Ad5 replication in human cells. To further test the positive effect of PML-II, early Ad5 gene expression was monitored in an abortive infection in PML null mouse embryonic fibroblasts (PML -/- MEFs). In this context, time course experiments in PML -/- MEFs compared to PML +/+ MEF cells were performed. We observed a delay in the protein expression of E2A (Fig. 17A) as well as reduced E2A mRNA expression in MEF cells without PML (Fig. 17B).

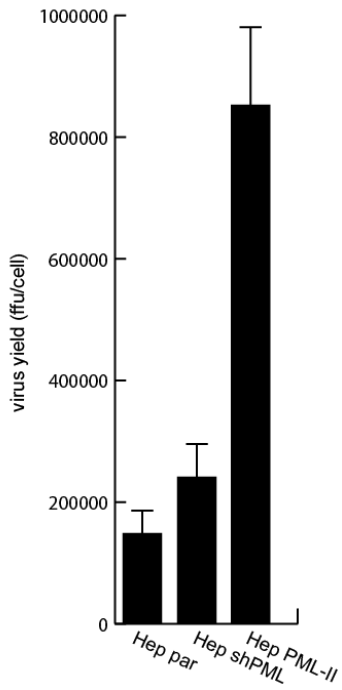

Figure 16: PML-II positively regulates adenovirus progeny production in human cells. Parental HepaRG (Hep par), Hep shPML and Hep PML-II cells were infected with wt H5*pg*4100 at a multiplicity of 50 ffu/cell. Viral particles were harvested 48 h p.i. and virus yield was determined by quantitative E2A immunofluorescence staining on HEK-293 cells.

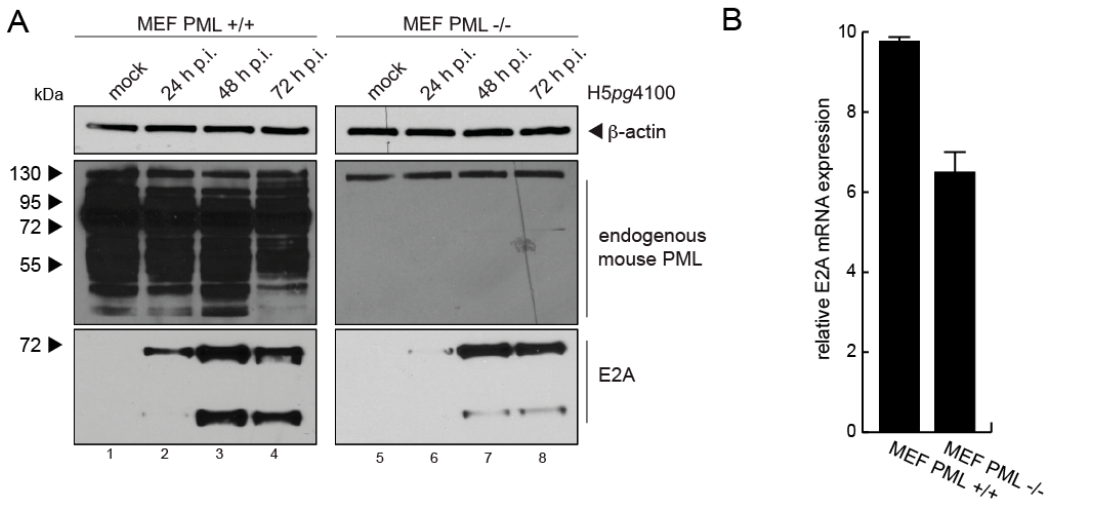

Figure 17: Ad5 E2A is delayed in an abortive infection in PML null mouse embryonic fibroblasts. (A) Subconfluent parental MEF (PML +/+) or PML knock-out MEF (PML -/-) cells were infected with wt virus H5*pg*4100 at a multiplicity of 50 ffu/cell. The cells were harvested 24, 48 and 72 h. p.i. and total cell extracts were prepared. Steady-state expression levels of total cell lysates were detected using mAb 610 (α-E1A), mAb B6 (α-E2A), mAb clone 36.1-104 (α-PML) and mAb AC-15 (α-β-actin). Molecular weights in kDa on the *left*, corresponding proteins on the *right*. (B) Subconfluent parental MEF (PML +/+) or PML knock-out MEF (PML -/-) cells were infected with wt virus H5*pg*4100 at a multiplicity of 50 ffu/cell. The cells were harvested 24 h p.i., total RNA was extracted, reverse transcribed, and quantified by RT-PCR analysis using primers specific for E2A. The data were normalized to 18S rRNA levels.

5.1.8 Transcriptional co-activation by PML does not depend on its SIM

The capability of PML to form NBs, their dynamic behavior and mode of function is mainly based on SUMOylation of the PML protein (Duprez *et al.*, 1999; Shen *et al.*, 2006; Zhong *et al.*, 2000a). The PML SUMO interacting motif (SIM) is required to form PML-NBs when exogenously expressed in PML -/- cells, and enables PML to interact non-covalently with SUMOylated proteins including PML itself (Shen *et al.*, 2006).

This raised the question whether the PML-SIM, necessary for interaction with other SUMOylated factors in the PML-NBs, plays a role in transcriptional activation of Ad promoters by PML-II in the presence of E1A-13S (Fig. 18A). Therefore, a PML-II mutant with a non-functional SIM was generated. Interestingly, this mutant stimulated E1A-13S-dependent transcription from the Ad5 E2 early promoter more efficient than PML-II wt (Fig. 18B).

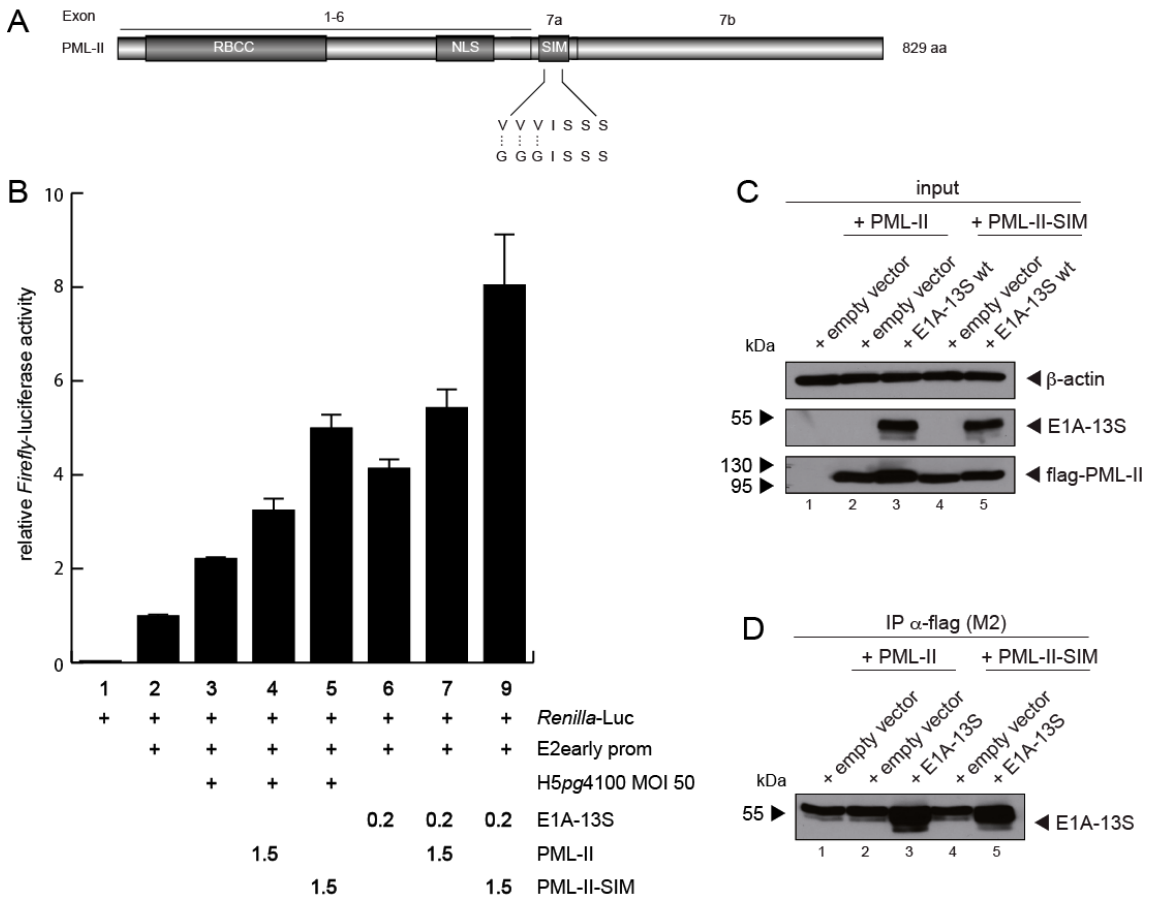

Figure 18: SIM of PML is not important for stimulating E1A-13S-dependent transcriptional activation. (A) The schematic representation of PML-II isoform showing the SIM amino acid sequence. Shown is the newly constructed PML-II-SIM construct with introduced mutations. (B) H1299 cells were transfected with 0.2 µg pRL-TK (*Renilla*-Luc), 0.5 µg pGL-Basic Prom E2E (E2early promoter), 0.2 µg pHA-E1A-13S, 1.5 µg pflag-PML-II and pflag-PML-II-SIM in the combinations indicated (+). 24 h post transfection total cell extracts were prepared and luciferase activity was determined. The mean and standard deviations are presented for three independent experiments. (C, D) Subconfluent H1299 cells were transfected with 3 µg of pHA-E1A-13S and 5 µg of pflag-PML-II or pflag-PML-II-SIM, harvested after 48 h and total cell extracts were prepared. Co-immunoprecipitation assays were performed as described in Figure 11. (C) Input levels in total cell lysates and (D) co-precipitated proteins. Molecular weights in kDa are on the *left*, while relevant proteins are indicated on the *right*.

It was also tested whether the PML-II-SIM mutant affected E1A-13S binding properties. PML-II-SIM and wt PML-II were expressed at equal amounts (Fig. 18C) and co-immunoprecipitation experiments showed no differences in binding capabilities between PML-II wt and PML-II-SIM (Fig. 18D, lanes 3 and 5).

5.2 Sp100 isoform-specific regulation of Ad5 gene expression

5.2.1 Sp100 depletion promotes Ad progeny production and protein synthesis

To analyze the effect of Sp100 on Ad progeny production, a lentivirus expressing shRNA (shSp100) was used to deplete Sp100 cellular protein from human HepaRG and H1299 cells prior to wt virus infection. Sp100 was efficiently depleted in both cell lines as shown by immunofluorescence and western blot analysis (Fig. 19A, C, D, F). Nevertheless, the knock down did not substantially affect the growth rate of the cells (Fig. 19B, E), although a slightly reduced growth rate could be observed for H1299 shSp100 cells after three days of cultivation (Fig. 19E).

Compared to the parental cell lines, knockdown of Sp100 increased the production of infectious virus particles by two-fold 24 h p.i. in both human cell lines (Fig. 20A, B). Sp100's repressive effect was somewhat less 48 h p.i. in HepaRG cells (Fig. 20), whereas the two-fold increase in progeny virions remained unaltered in H1299 cells (Fig. 20B). Therefore, the data indicate that Sp100 is a negative regulator of Ad progeny production.

Next, expression of viral early and late proteins in HepaRG and H1299 cells was monitored at different time points after infection. Consistent with previous reports, Sp100 depletion did not affect the expression of PML. However, expression of particularly Ad5 early proteins E1A, E1B-55K, E2A, and E4orf6 increased substantially in Sp100-depleted cells compared to the parental cells (Fig. 20C, D). This effect could be observed in both HepaRG and H1299 cells. Together, these data point to Sp100 being a negative regulator of Ad replication during infection. Interestingly, Mre11 and p53 protein levels were higher in the parental cells compared to the shSp100 cells (Fig. 20C, D).

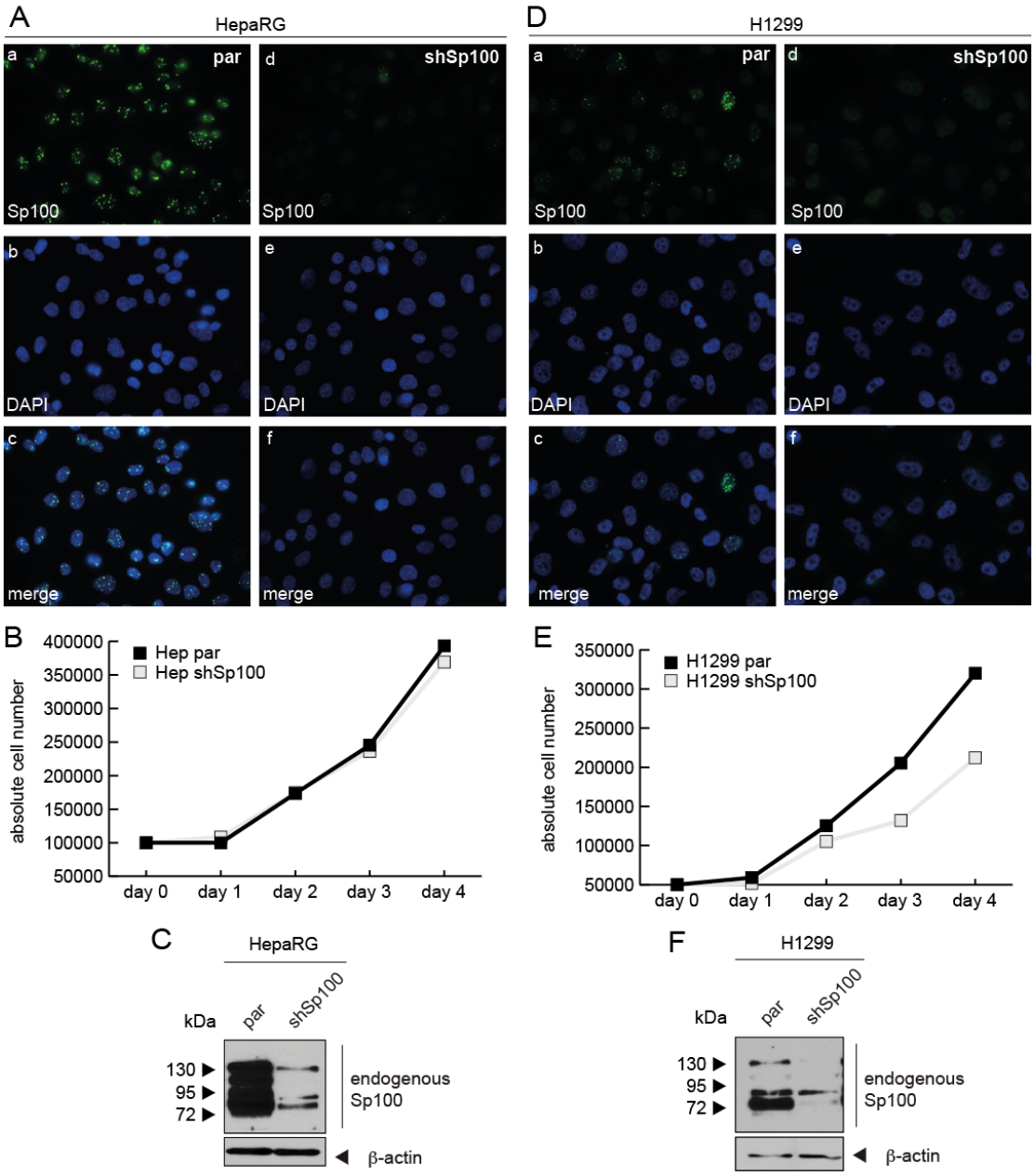

Figure 19: Depletion of Sp100 in HepaRG and H1299 cells. (A) HepaRG parental and shSp100 cells were fixed with 4 % PFA, labeled with pAb GH3 (α-Sp100) and detected with Alexa488 (α-Sp100; green) conjugated secondary Abs. Nuclei are labeled with DAPI. Representative α-Sp100 (green; Aa, Ad), DAPI (blue; Ab, Ae) staining patterns and overlays of the single images (merge; Ac, Af) are shown (magnification x 7600). (B) Total cell numbers of parental and shSp100 HepaRG cells were determined at indicated time points. (C) Total cell extracts of parental and shSp100 HepaRG cells were prepared, proteins were separated by SDS-PAGE and subjected to immunoblotting using pAb GH3 (α-Sp100) and mouse mAb (α-β-Ac-15). (D) H1299 parental and shSp100 cells were fixed with 4 % PFA, labeled with pAb GH3 (α-Sp100) and detected with Alexa488 (α-Sp100; green) conjugated secondary Abs. Nuclei are labeled with DAPI. Representative α-Sp100 (green; Da, Dd), DAPI (blue; Db, De) staining patterns and overlays of the single images (merge; Dc, Df) are shown (magnification x 7600). (E) Total cell numbers of parental and shSp100 H1299 cells were determined at indicated time points. (F) Total cell extracts of parental and shSp100 HepaRG cells were prepared, proteins were separated by SDS-PAGE and subjected to immunoblotting using pAb GH3 (α-Sp100) and mouse mAb (α-β-Ac-15).

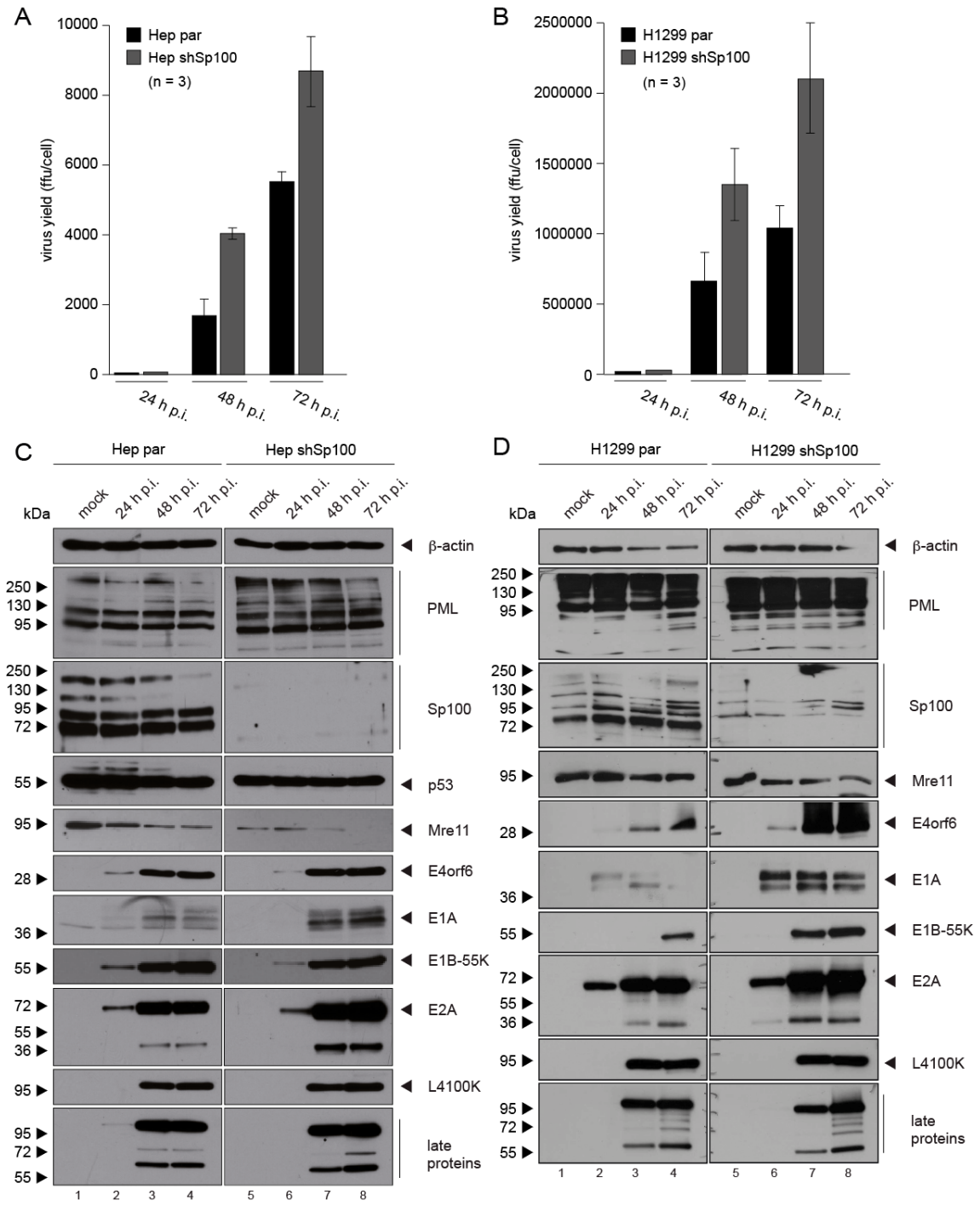

Figure 20: Sp100 depletion promotes Ad progeny production and early viral protein synthesis. (A) HepaRG parental (Hep par) and shSp100 cells were infected with wt virus H5*pg*4100 at a multiplicity of 50 ffu/cell per cell. Viral particles were harvested 24, 48 and 72 h p.i. and virus yield was determined by quantitative E2A-72K immunofluorescence staining of HEK-293 cells. (B) H1299 parental (H1299 par) and shSp100 cells were infected with wt H5*pg*4100 at a multiplicity of 20 ffu/cell per cell. Virus yield was determined as in (A). The results represent the averages from three independent experiments and error bars indicate the standard error of the mean. (C) HepaRG parental and shSp100 cells were infected as in (A) and proteins from total cell extracts were separated by SDS-PAGE and subjected to immunoblotting using pAb NB 100-59787 (α-PML), pAb GH3 (α-Sp100), rabbit mAb α-Mre11, mouse mAb M-58 (α-E1A), B6-8 (α-E2A), 2A6 (α-E1B-55K), RSA3 (α-E4orf6), and rabbit antiserum L133 to Ad capsid. (D) H1299 parental

and shSp100 cells were infected as in (B) and proteins from total cell extracts were separated by SDS-PAGE and subjected to immunoblotting using the same antibodies as in (C).

5.2.2 High molecular weight Sp100 species are reduced during Ad infection.

Since fewer high molecular weight Sp100 moieties were observed in late stages of infection (Fig. 20 C and D), it was tested whether this is triggered by the early viral proteins E1B-55K, E4orf6 or E4orf3. Sp100 protein levels were analyzed 48 h p.i. in wt- and mutant virus-infected cells lacking E4orf3 (H5*pm*4150), E1B-55K (H5*pm*4149) or E4orf6 (H5*pm*4154; Fig. 21A). Slower migrating Sp100 species (indicated by **) dramatically decreased in cells infected with either the wt or E4orf3 deficient virus (Fig. 21A, lanes 2 and 3). In contrast, levels of these Sp100 moieties were comparable in non-infected and infected cells lacking E1B-55K or E4orf6 expression (Fig. 21A, lanes 1, 4 and 5). Interestingly, a slightly slower migrating band (indicated by *; between 95 and 130 kDa) was detected in wt as well as all mutant virus infected cells (Fig. 21A, lanes 2 to 5).

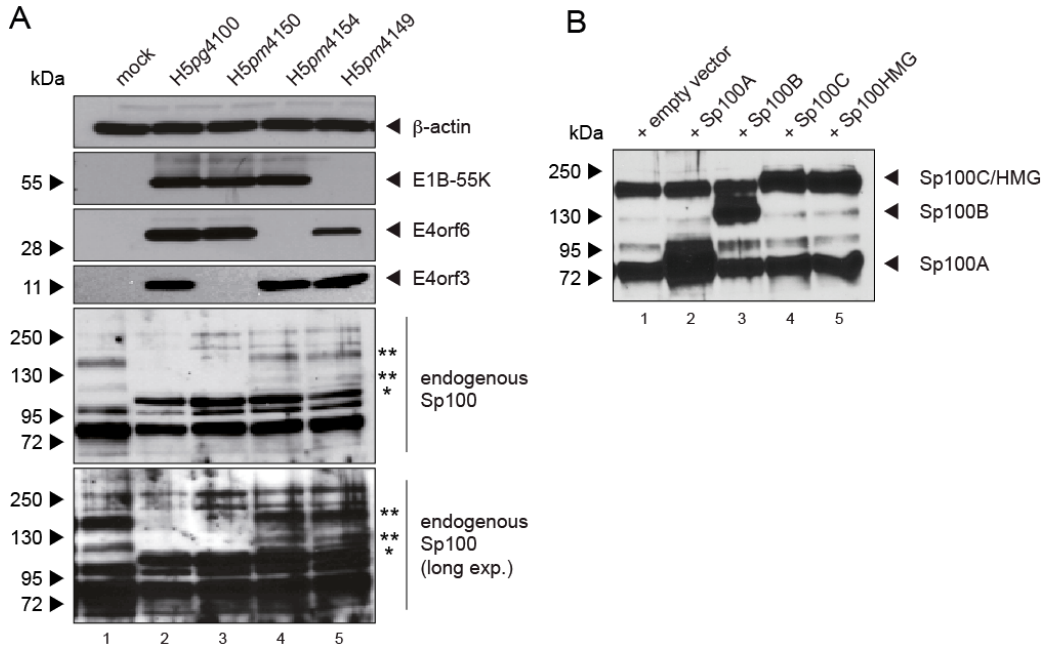

Figure 21: Sp100 depletion promotes Ad progeny production and early viral protein synthesis. A) H1299 cells were infected with wt (H5*pg*4100) or mutant viruses lacking E4orf3 (H5*pm*4150), E4orf6 (H5*pm*4154) or E1B-55K (H5*pm*4149) at a multiplicity of 20 ffu/cell. 48 h p.i. total cell extract proteins were separated by SDS-PAGE and subjected to immunoblotting using pAb GH3 (α-Sp100), mAb 2A6 (α-E1B-55K), mAb RSA3 (α-E4orf6) and mAb 6A11 (α-E4orf3). (B) H1299 cells were transfected with 5 µg of pflag-Sp100A, B, C or HMG. Cells were harvested 48 h post transfection, total cell extracts were prepared and subjected to immunoblot analysis. Input levels of Sp100 were detected using pAb GH3 (α-Sp100). Molecular weights in kDa are indicated on the *left*, relevant proteins on the *right*.

These observations imply that reductions in Sp100 protein level depend on E1B-55K and E4orf6 during Ad infection.

To assign the identified slower migrating Sp100 moieties to specific Sp100 isoforms, transfected flag-tagged Sp100A, B, C, HMG gel migrating properties were compared with those of endogenous Sp100 (Fig. 21B). Each band appearing in the endogenous Sp100 could be assigned to the transfected Sp100 isoforms, implying that the slower migrating Sp100 isoforms may represent Sp100B, C and HMG.

5.2.3 Sp100B, C and HMG are relocalized from PML-NBs to viral replication centers during infection

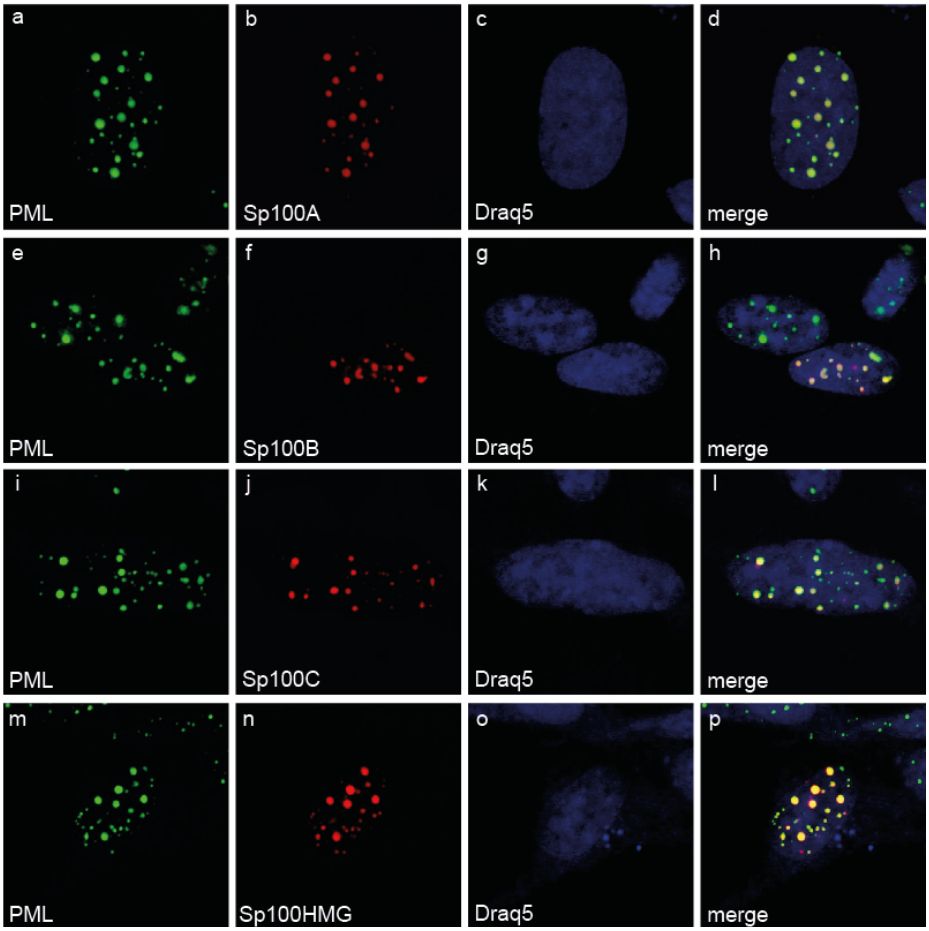

Figure 22: Localization of Sp100 isoforms in non-infected cells. HepaRG cells were transfected with 1.5 µg of pflag-Sp100A, B, C or HMG. Cells were fixed 48 h post transfection with 4 % PFA and double-labeled with mAb flag-M2 (α-flag) and pAb NB 100-59787 (α-PML). Primary Abs were detected with Cy3 (α-flag; red) and Alexa488 (α-PML; green) conjugated secondary Abs. The DNA intercalating dye Draq5 (Biostatus) was used for nuclear staining. Representative α-PML (green; a, e, i, m) and α-flag-Sp100 (red; b, f, j, n) staining patterns of at least 50 analyzed cells are shown. Overlays of the single images (merge) are shown in d, h, l, p (magnification x 7600).

Humans are so far known to express at least four different Sp100 isoforms: Sp100A, Sp100B, Sp100C and Sp100HMG (Fig. 8). To investigate the intracellular localization of the different Sp100 isoforms in non-infected HepaRG cells, single flag-tagged Sp100 isoforms were transfected prior to immunofluorescence analysis. Co-staining of flag-tagged Sp100 isoforms with endogenous PML revealed localization of all Sp100 isoforms to PML-NBs. Although some PML-NBs seemed to lack particularly flag-Sp100B, C and HMG staining and higher expression levels induced the formation of larger nuclear aggregates with an increased intensity of diffuse nuclear labeling, mild overexpression resulted in co-localization in at least 50 % of the detected PML-NBs (Fig. 22 d, h, l, p). These observations correspond with the reports of Seeler and coworker (Seeler *et al.*, 2001).

In 1995, Doucas *et al.* described the relocalization of endogenous Sp100 during Ad infection (Doucas *et al.*, 1996). In the early phase, PML and Sp100 are reorganized into track-like structures prior to Sp100 being sequestered to the early viral replication centers. Therefore, it was evaluated whether Sp100 colocalization to Ad-induced PML tracks, or juxtaposition to viral replication centers is affected in an isoform-dependent manner. HepaRG cells were transfected with the single Sp100 isoforms and superinfected with Ad5 wt virus (Fig. 23). Sp100A, B, C and HMG were detected at PML-NBs in non-infected cells (Fig. 22; d, h, l, p). 24 h p.i. PML was relocalized into track-like structures as described previously (Fig. 23A; a, e, i, m; Leppard *et al.*, 2009; Leppard & Everett, 1999).

Intriguingly, we detected only the Sp100A isoform efficiently colocalizing with the PML-containing tracks (Fig. 23A; d). In contrast, Sp100B, Sp100C and Sp100 HMG formed dot-like structures not associated with PML (n=50; Fig. 23A; h, l, p). After late replication centers marked by the Ad5 DNA binding protein E2A (Fig. 23B; a, e, i, m) have been established 48 h p.i., the majority of Sp100A was still retained in the PML tracks. Our data reveal that a substantial number of these Ad-induced tracks were closely associated with the outer rim of the viral replication centers (Fig. 23B; b, d and enlarged merge), whereas Sp100B, C and HMG accumulated entirely in the replication centers (Fig. 23B; h, l, p). In sum, these observations imply that contrary to Sp100A, isoforms B, C and HMG are separated from the PML tracks during Ad infection. This is likely due to different protein properties conferred by the additional C-terminal domains, e.g. the SAND domain.

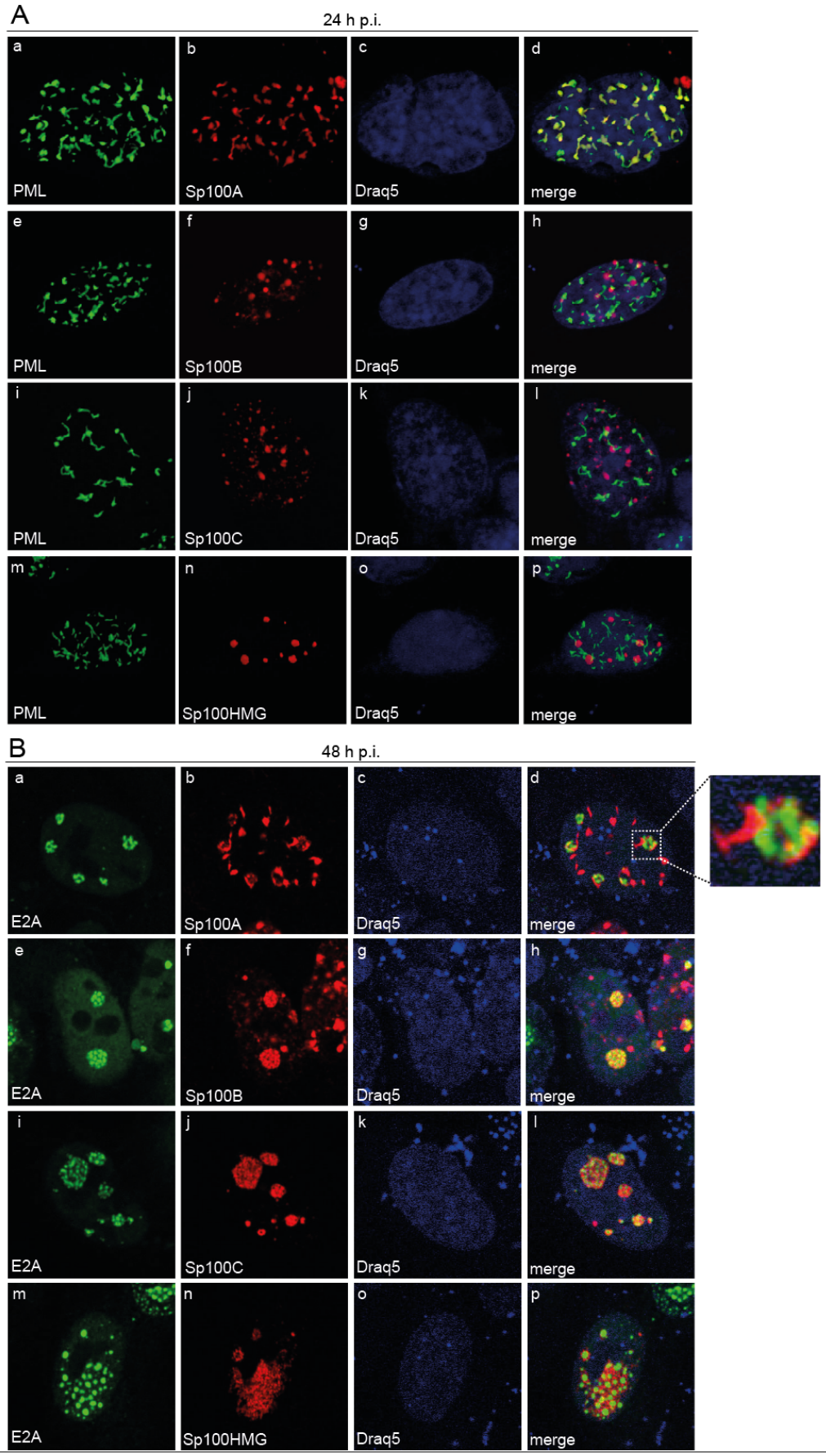
A
24 h p.i.
a
PML
b
Sp100A
c
Draq5
d
merge
e
PML
f
Sp100B
g
Draq5
h
merge
i
PML
j
Sp100C
k
Draq5
l
merge
m
PML
n
Sp100HMG
o
Draq5
p
merge
B
48 h p.i.
a
E2A
b
Sp100A
c
Draq5
d
merge
e
E2A
f
Sp100B
g
Draq5
h
merge
i
E2A
j
Sp100C
k
Draq5
l
merge
m
E2A
n
Sp100HMG
o
Draq5
p
merge

Figure 23: Ad-dependent relocalization of Sp100 B, C and HMG from PML-NBs to viral replication centers. HepaRG cells were transfected with 1.5 µg of pflag-Sp100A, B, C or HMG and superinfected with wt virus (H5*pg*4100) at a multiplicity of 50 FFU/cell 8 h post transfection. (A) The cells were fixed with 4 % PFA 24 h p.i. and double-labeled with mAb flag-M2 (α-flag) and pAb NB 100-59787 (α-PML). (B) The cells were fixed with 4 % PFA 48 h p.i. and double-labeled with mAb flag-M2 (α-flag) and rabbit mAb α-E2A. Primary Abs were detected with Cy3 (α-flag; red) and Alexa488 (α-PML/E2A; green) conjugated secondary Abs. The DNA intercalating dye Draq5 (*Biostatus*) was used to stain cell nuclei. Representative α-PML (green; Aa, Ae, Ai, Am), α-E2A (green; Ba, Be, Bi, Bm) and α-flag-Sp100 (red; Ab, Af, Aj, An, Bb, Bf, Bj, Bn) staining patterns of at least 50 analyzed cells are shown. Overlays of the single images (*merge*) are shown in d, h, l, p (magnification x 7600).

5.2.4 SUMO-2-chains of Sp100A are shortened during Ad5 infection

Since Ad apparently manipulates association of Sp100 isoforms with PML-NBs, it was monitored next whether SUMO modification of Sp100A is altered during infection since SUMO is an important determinant of subnuclear localization. First, HeLa cells expressing His-SUMO-1/-2 were transfected with Sp100A and superinfected with Ad5 wt 8 h post transfection (Fig. 24A, B). Immunoblotting of Ni-NTA-purified His-SUMO conjugates (Fig. 24A) and crude lysates (Fig. 24B) revealed that Sp100A SUMO-2 modification is reduced during Ad infection (Fig. 24A, lane 6). However, SUMO-1 conjugation on Sp100A is not affected at this time point (Fig. 24A, lane 4). A similar effect could be observed for endogenous Sp100 (Fig. 25B, lane 6).

To investigate whether the reduction of high molecular weight forms of SUMO-2 modified Sp100A depends on the viral early proteins E1B-55K, E4orf6 and/or E4orf3, His-SUMO-2 conjugates were purified (Ni-NTA) after Sp100A transfection and superinfection with wt or mutant Ad5 viruses lacking either E1B-55K (H5*pm*4149), E4orf6 (H5*pm*4154) or E4orf3 (H5*pm*4150; Fig. 24C, 24D). Significantly less high molecular weight SUMO-2 modified forms of Sp100A were detected with all viruses, irrespective of E4orf3, E1B-55K or E4orf6 expression. These results confirm that the reduced slower-migrating Sp100 bands shown in Fig. 21 are unlikely SUMO-modified Sp100 species.

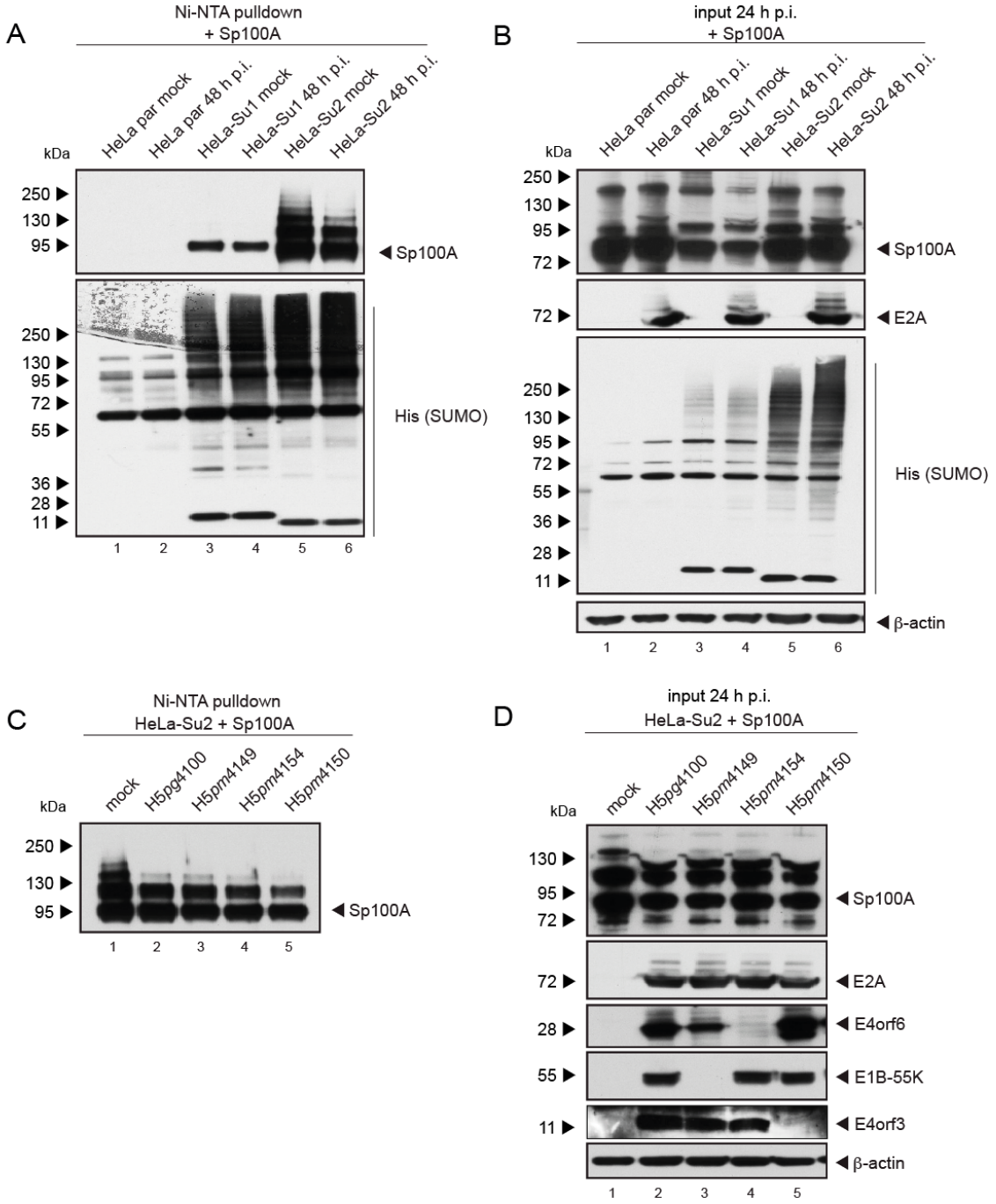

Figure 24: SUMO-2 chains of Sp100A are shortened during Ad infection. (A-D) Parental HeLa cells and HeLa cells stably expressing 6His-SUMO-1 (HeLa-Su1) or 6His-SUMO-2 (HeLa-Su2) were transfected with 2 µg of pflag-Sp100A and superinfected with wt virus (H5*pg*4100) (A, B) or mutant viruses lacking E4orf3 (H5*pm*4150), E4orf6 (H5*pm*4154) or E1B-55K (H5*pm*4149) (C, D) at a multiplicity of 20 ffu/cell 8 h *post* transfection as indicated. 48 h *post* transfection whole-cell lysates were prepared with Guanidinium Chloride buffer, subjected to Ni-NTA purification of 6His-SUMO conjugates and fractionated on a 4–12 % gradient gel before immunoblot analysis. Input levels of total cell lysates (B, D) and Ni-NTA purified proteins (A, C) were detected using pAb GH3 (α-Sp100), mAb B6 (α-E2A), mAb 6xHis and mAb AC-15 (α-β-actin), mAb 2A6 (α-E1B-55K), mAb RSA3 (α-E4orf6) and mAb 6A11 (α-E4orf3). Molecular weights in kDa are indicated on the *left*, relevant proteins on the *right*.

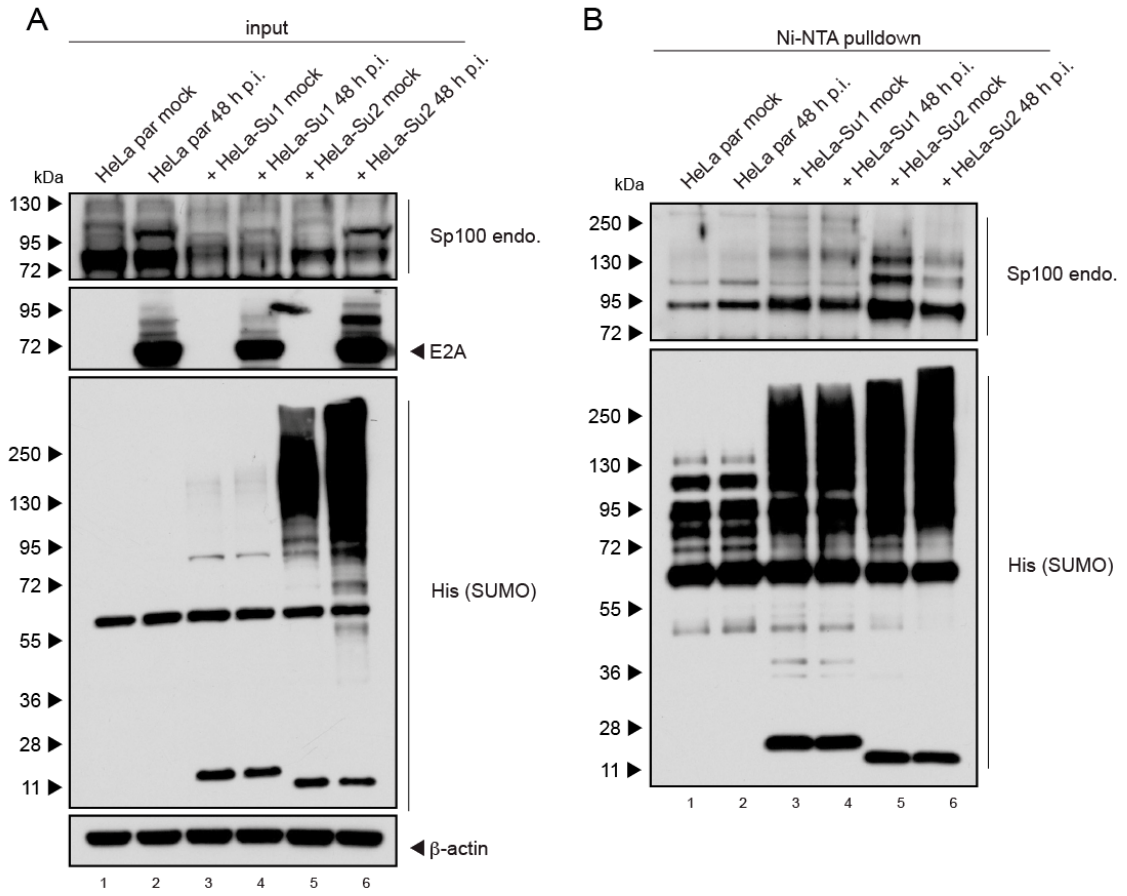

Figure 25: SUMO-2 chains of endogenous Sp100 are shortened during Ad infection. (A, B) Parental HeLa cells and HeLa cells stably expressing 6His-SUMO-1 (HeLa-Su1) or 6His-SUMO-2 (HeLa-Su2) were infected with wt virus (H5*pg*4100) at a multiplicity of 20 ffu/cell 8 h post transfection as indicated. Whole-cell lysates were prepared with Guanidinium Chloride buffer, subjected to Ni-NTA purification of 6His-SUMO conjugates and fractionated on a 4–12 % gradient gel before immunoblot analysis. Input levels of total cell lysates (A) and Ni-NTA purified proteins (B) were detected using pAb GH3 (α-Sp100), mAb B6 (α-E2A), mAb 6xHis and mAb AC-15 (α-β-actin). Molecular weights in kDa are indicated on the *left*, relevant proteins on the *right*.

It has previously been shown that the viral early protein E1A represses SUMO modification of the retinoblastoma protein and interacts with the SUMO conjugating enzyme Ubc9 to likely interfere with polySUMOylation (Ledl *et al.*, 2005; Yousef *et al.*, 2010). Therefore, we tested if E1A triggers reduced SUMO-2 modification of Sp100 (Fig. 26). As a control, we included the Ubc9 binding mutants of the two major Ad5 E1A proteins E1A-12S and E1A-13S (E1A-12S-D121A; E1A-13S-D121A) with a point mutation in the conserved Ubc9 interacting motif EVIDLT. This mutation has previously been shown to prevent E1A interaction with Ubc9 (Fig. 26; Yousef *et al.*, 2010). Analysis of Ni-NTA purified SUMO-2 conjugates after co-expression of Sp100A with E1A-13S, E1A-13S-D121A, E1A-12S and E1A-12S-D121A revealed that both wt E1A isoforms, but not the Ubc9 binding mutants (E1A-13S-D121A and E1A-12S-D121A), repressed SUMO-

2 modification of Sp100A (Fig. 26B). The slight reduction in steady state levels of Sp100A after co-transfection with wt E1A-12S/E1A-13S indicates that SUMO modification may affect stability of Sp100 (Fig, 26A, lanes 2 and 4). Endogenous PML was included as a control, but we could neither detect a change in steady state levels nor a significant change in SUMO modification, implying a specific effect on Sp100. As transfection of E1A12S/13S alone did not completely abolish Sp100 SUMO modification, it is likely that other viral regulatory proteins affect SUMO modification of Sp100 during infection.

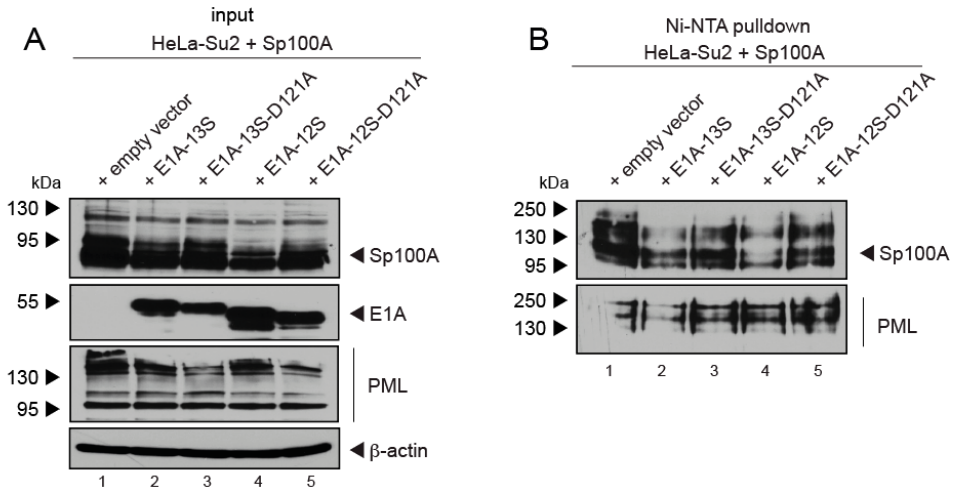

Figure 26: SUMO-2 chains of Sp100A are shortened during Ad infection depending on E1A. HeLa cells stably expressing 6His-SUMO-2 (HeLa-Su2) were transfected with 2 µg of pflag-Sp100A and 3 µg pHA-E1A-13S/HA-E1A-12S/HA-E1A-13S-D121A/HA-E1A-12S-D121A. 48 h post transfection whole-cell lysates were prepared with Guanidinium Chloride buffer, subjected to Ni-NTA purification of 6His-SUMO conjugates and fractionated on a 4–12 % gradient gel before Immunoblot analysis. Input levels of total cell lysates (A) and Ni-NTA purified proteins (B) were detected using pAb GH3 (α-Sp100), pAb PML NB100-59787, mAb M-58 (α-E1A) and mAb AC-15 (α-β-actin). Molecular weights in kDa are indicated on the *left*, relevant proteins on the *right*.

5.2.5 HP1α interaction with Sp100A is reduced during Ad5 infection

Sp100 has been shown to interact with HP1 via its PxVxL motif (Seeler *et al.*, 1998). Overexpressed or IFN-induced Sp100 enhances recruitment of endogenous HP1 protein to PML-NBs, mainly localizing to the interior of these subdomains (Lang *et al.*, 2010). Additionally, the Sp100 SCM (SUMO conjugation motif) is located close to the HP1 interaction motif (Fig. 27A); and SUMOylated Sp100 is known to stabilize its binding to HP1 *in vitro* (Seeler *et al.*, 2001). To test whether Ad mediated loss of Sp100A-SUMO-2 affects the HP1 interaction *in vivo*, binding assays were performed in infected, Sp100A overexpressing cells, co-transfected with either HP1α or HP1β (Fig. 27B, C). An

interaction between Sp100A and HP1β could not be detected. However; HP1α binding to Sp100A was significantly reduced in infected cells (Fig. 27B, lane 6).

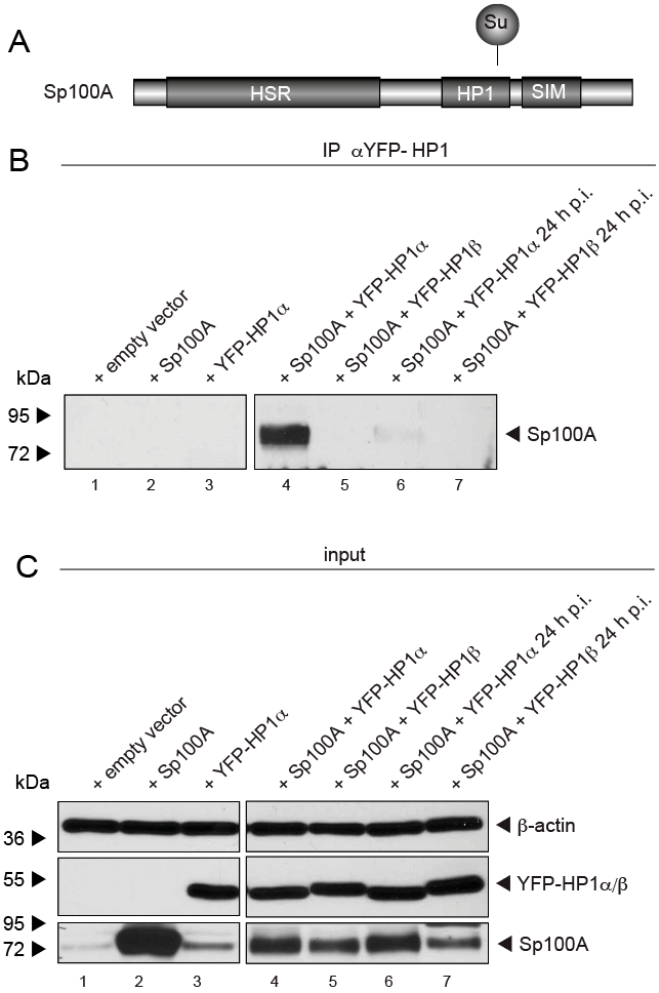

Figure 27: HP1α interaction with Sp100A is reduced during Ad infection. (A) Schematic representation of Sp100A with domain organization. (B, C) H1299 cells were superinfected with wt virus (H5*pg*4100) at a multiplicity of 20 ffu/cell 8 h after transfection of 2 µg of pflag-Sp100A and 3 µg of pYFP-HP1α/pYFP-HP1β, as indicated. Cells were harvested 24 h p.i., prior to preparation of total cell extracts and co-immunoprecipitation assays. Co-precipitated proteins (B) and input levels (C) of total cell lysates were detected using pAb GH3 (α-Sp100), mAb AC-15 (α-β-actin) and mAb GFP (α-YFP-HP1α/pYFP-HP1β). Molecular weights in kDa are indicated on the *left*, specific proteins on the *right*.

5.2.6 Sp100A-specific activation of Ad promoter activity

Recently, Newhart *et al.* reported that Sp100A promotes chromatin decondensation at CMV (Cytomegalovirus) promoter-regulated transcription sites. In contrast, Sp100B, containing an additional SAND domain, promotes chromatin condensation, and thus transcriptional repression (Newhart *et al.*, 2013).

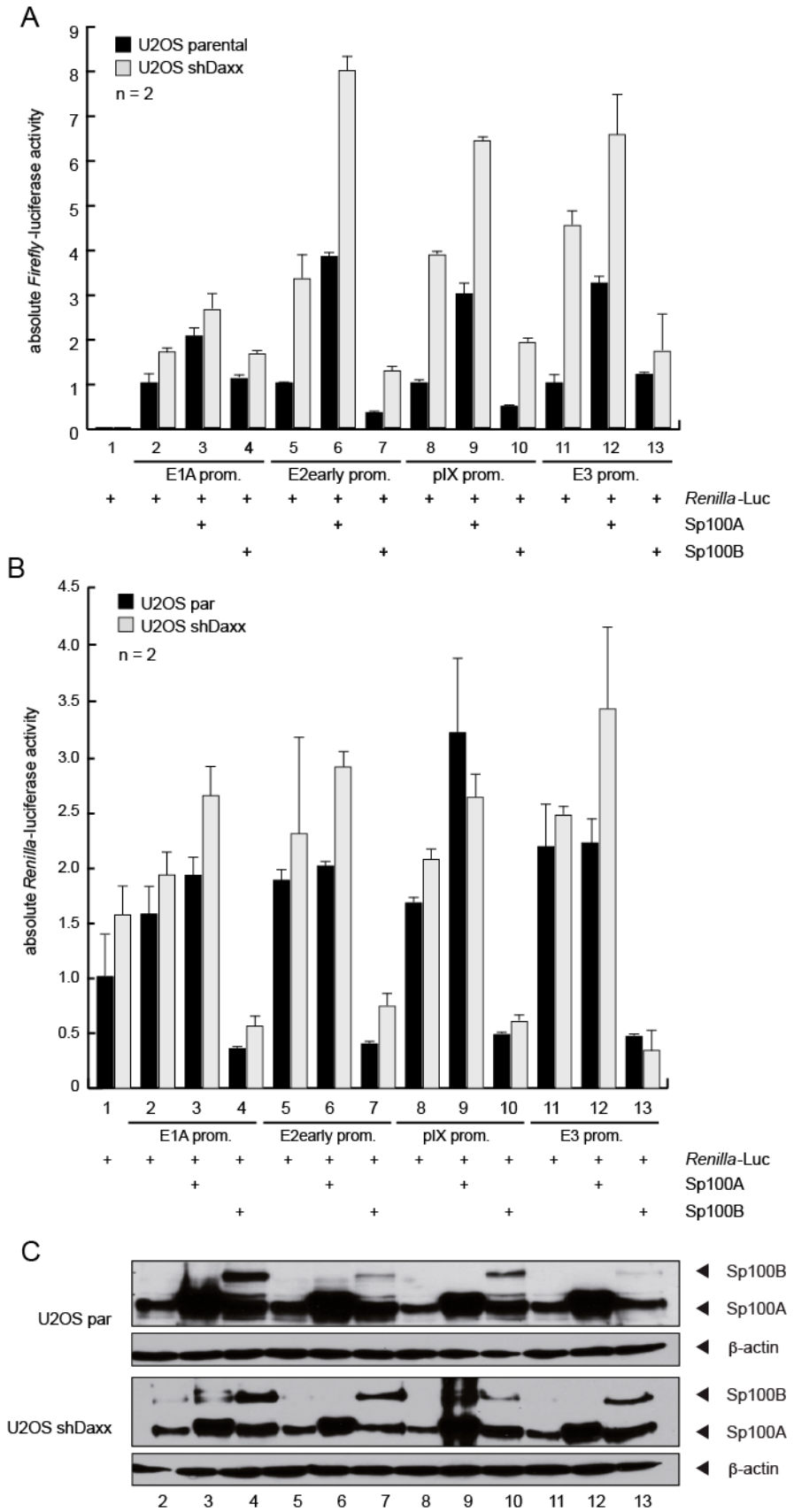

Figure 28: Sp100 isoform-specific regulation of Ad gene expression. (A) U2OS and U2OS shDaxx cells were transfected with 0.5 µg of pRL-TK (*Renilla*-Luc), 0.5 µg pGL3-Basic-Prom E1A

(E1A promoter), 0.5 µg pGL3-Basic-Prom E1E (E2early promoter), 0.5 µg pGL3-Basic-Prom E3 (E3 promoter), or 0.5 µg pGL3-Basic-Prom pIX (pIX promoter), plus 0.5 µg pflagSp100A or pflagSp100B in the combinations indicated (+). Total cell extracts were prepared and luciferase activity determined 24 h post transfection. Absolute *Firefly*-luciferase activity is shown. The mean and standard deviations are presented for two independent experiments. (B) The mean and standard deviations of the absolute *Renilla*-luciferase activity are presented for three independent experiments. (C) Input levels of total cell lysates were detected using pAb GH3 (α-Sp100) and mAb AC-15 (α-β-actin).

To investigate whether Sp100 also affects transcription from Ad5 promoters, E1A, E2early, pIX and E3 promoter activity in the presence of either Sp100A or Sp100B was investigated (Fig. 28). Since Sp100A was recently reported not to overcome Daxx/ATRX-mediated transcriptional repression, we used U2OS cells that have reduced ATRX expression to minimize additional effects mediated by these transcription factors. Furthermore, Daxx-depleted U2OS cells were employed to additionally diminish the repressive effect of the Daxx/ATRX chromatin remodeling complex.

Sp100A stimulated transcription from the Ad promoters by two- to three-fold in both cell lines. As anticipated, basal activity of the promoters was higher in Daxx-depleted cells, implying an additional repression mechanism of Daxx independently of the Daxx/ATRX complex. Contrary to Sp100A, the B isoform reduced E2early, pIX and E3 promoter activity 0.5 - to three–fold (Fig. 28A). To normalize transfection efficiencies we used *Renilla*-luciferase under the control of the HSV-TK (herpes simplex virus thymidine kinase) promoter. Since Sp100 also affected *Renilla*-luciferase expression, either transactivating via Sp100A, or repressing via Sp100B, the *Renilla* expression levels were depicted in separate bar charts (Fig. 28B).

To further confirm our data in a replication-competent virus-system, we measured Ad early and late mRNA expression in infected cells expressing either Sp100A or Sp100B (Fig. 29). Viral early E1A and E2A mRNA production was stimulated in infected cells expressing Sp100A compared to cells treated with the empty vector control (Fig. 29). Additionally, late Fiber transcript synthesis was enhanced in cells co-transfected with Sp100A, suggesting an impact of either enhanced synthesis of early viral gene products or direct stimulation of the late promoter (Fig. 29). Consistent with data obtained in reporter assays, Sp100B negatively affected viral early and late mRNA expression although the effect was not as strong as observed for Sp100A activation. Similar results were obtained for early and late mRNA stimulation by Sp100A in cells infected with a higher multiplicity of infection (Fig. 29, right panel).

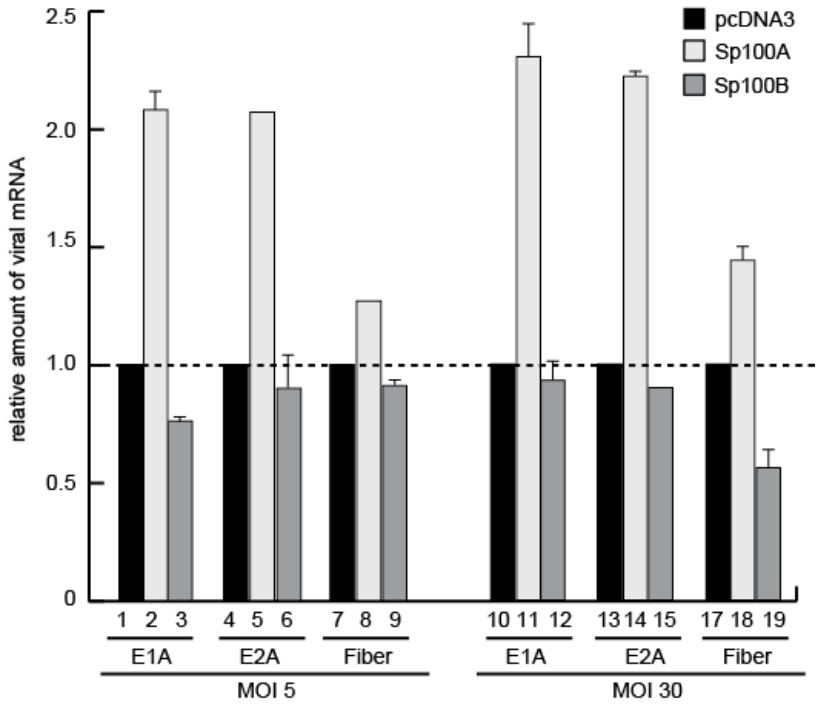

Figure 29: Sp100 isoform-specific regulation of Ad gene expression. Subconfluent U2OS cells were transfected with 5 µg pcDNA3, pflagSp100A or pflagSp100B and superinfected with wt virus H5*pg*4100 at a multiplicity of 5 or 30 ffu/cell 48 h post transfection. The cells were harvested 24 h p.i., total RNA was extracted, reverse transcribed, and quantified by RT-PCR analysis using primers specific for Ad5 E1A, E2A and Fiber. The data were normalized to 18S rRNA levels.

5.2.7 Sp100A-specific activation of E2F-1 and p53-dependent promoter activity

Next, we investigated whether Sp100 isoform-dependent effects on the cellular E2F-dependent H2A promoter (Fig. 30A) or p53-dependent Cyclin G promoter (Fig. 30B) can be detected. Consistent with the viral reporter constructs, co-expression of Sp100A stimulated (Fig. 30A, lane 4; 30B, lane 4), whereas the presence of Sp100B, C or HMG efficiently inhibited transcription from both cellular promoters (Fig. 30A, lanes 5, 6 and 7; 30B, lanes 5, 6 and 7). The inhibitory effect of Sp100B, C and HMG isoforms on Cyclin G promoter activity could not even be overcome by addition of its transcriptional activator p53 (Fig. 30B, lanes 5-7). The *Renilla* results were included in separate bar charts (Fig. 30C, D). Taken together, Sp100 efficiently regulates viral and cellular promoters in an isoform-dependent manner.

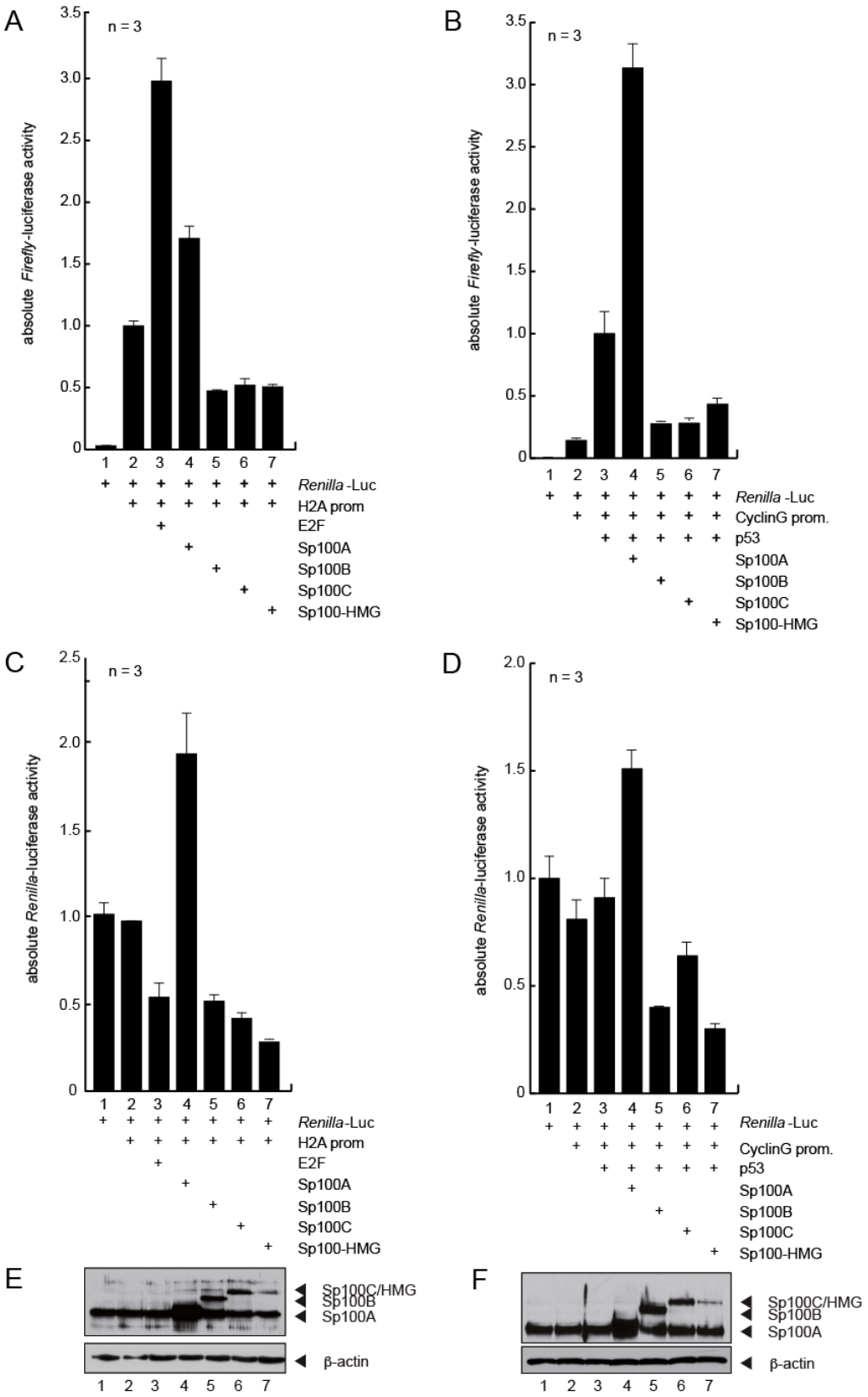

Figure 30: Sp100 isoform-specific regulation of transcription from E2F-1 and p53-dependent promoters. (A) U2OS cells were transfected with 0.5 µg of pRL-TK (*Renilla*-Luc), 0.5 µg pH2A-prom luc (H2A promoter) and 0.5 µg pE2F-1, pflag-Sp100A, pflag-Sp100B, pflag-Sp100C or pflag-Sp100HMG in the combinations indicated (+). Total cell extracts were prepared

and luciferase activity determined 24 h post transfection. Absolute *Firefly*-luciferase activity is shown with mean and standard deviations from three independent experiments. (B) U2OS cells were transfected as in (A), except now with 0.5 μg of pRL-TK (*Renilla*-Luc), 0.5 μg pCyclin G-Luc (Cyclin G promoter) and 0.5 μg pC53SN3 (p53), pflag-Sp100A, pflag-Sp100B, pflag-Sp100C or pflag-Sp100HMG in the combinations indicated (+). Luciferase activity was determined in total cell extracts 24 h post transfection. Absolute *Firefly*-luciferase activity is shown with mean and standard deviations for three independent experiments. (C, D) The mean and standard deviations of the absolute *Renilla*-luciferase activity are presented for three independent experiments. (E, F) Input levels of total cell lysates were detected using pAb GH3 (α-Sp100) and mAb AC-15 (α-β-actin).

5.2.8 Sp100-SIM promotes transcriptional activation and localization to track-like structures

The transactivating properties of Sp100 on transcription have previously been mapped to amino acids 333-407, a region immediately downstream of the HP1 interaction region. The SIM has been described to be important for Sp100 recruitment to HSV-1 (herpes simplex virus type 1) genomes. Given the fact that SIM is located within the transactivating region of Sp100 (Fig. 31A), we investigated the transcriptional properties of an Sp100A non-functional SIM derivative (Sp100A-I323I324K) on Ad5 promoters (Fig. 31B). Reporter gene assays with the Ad E2early promoter revealed that the Sp100A-SIM mutant was no longer able to efficiently stimulate transcription from the viral promoter (Fig 31B, lane 7), although Sp100A wt and Sp100A-SIM were expressed in similar amounts (Fig. 31F; *Renilla* is shown in Fig. 31D). The p300 protein possesses intrinsic acetyltransferase activity and is therefore an important transcriptional co-activator; it is recruited to gene promoters via its association with numerous DNA-binding transcription factors. We tested whether Sp100 variants affect p300 co-activator function in transcriptional regulation by performing luciferase reporter assays with a GAL4-responsive promoter and p300 fused to a GAL4 DNA-binding domain, in combination with Sp100 (Fig. 31C). Sp100A stimulated transcription from the GAL4 promoter three-fold, while the SIM mutant lost this ability. Consistent with our observations above, Sp100B, C, and HMG inhibited transcription, whereas co-expression of Sp100A with a functional SIM stimulated luciferase activity from the p300-responsive promoter (*Renilla* is shown in Fig. 31E). Next, we tested whether the SIM mutation alters Sp100A intracellular localization (Fig. 32). In non-infected cells, the Sp100A-SIM mutant localized to the PML-NBs (Fig. 32d). Co-staining with Ad E2A revealed that after PML track formation the Sp100A-SIM mutant was diffusely distributed in the host-cell nucleus, neither localizing to the tracks nor to the viral replication centers in 80 % of the cells investigated (n>50; Fig. 32i). However in 20 % of the cells, Sp100A-SIM mutant localized to PML tracks and/or viral replication centers, likely due to dimerization with endogenous wt Sp100 via the HSR domain (n>50; data not shown).

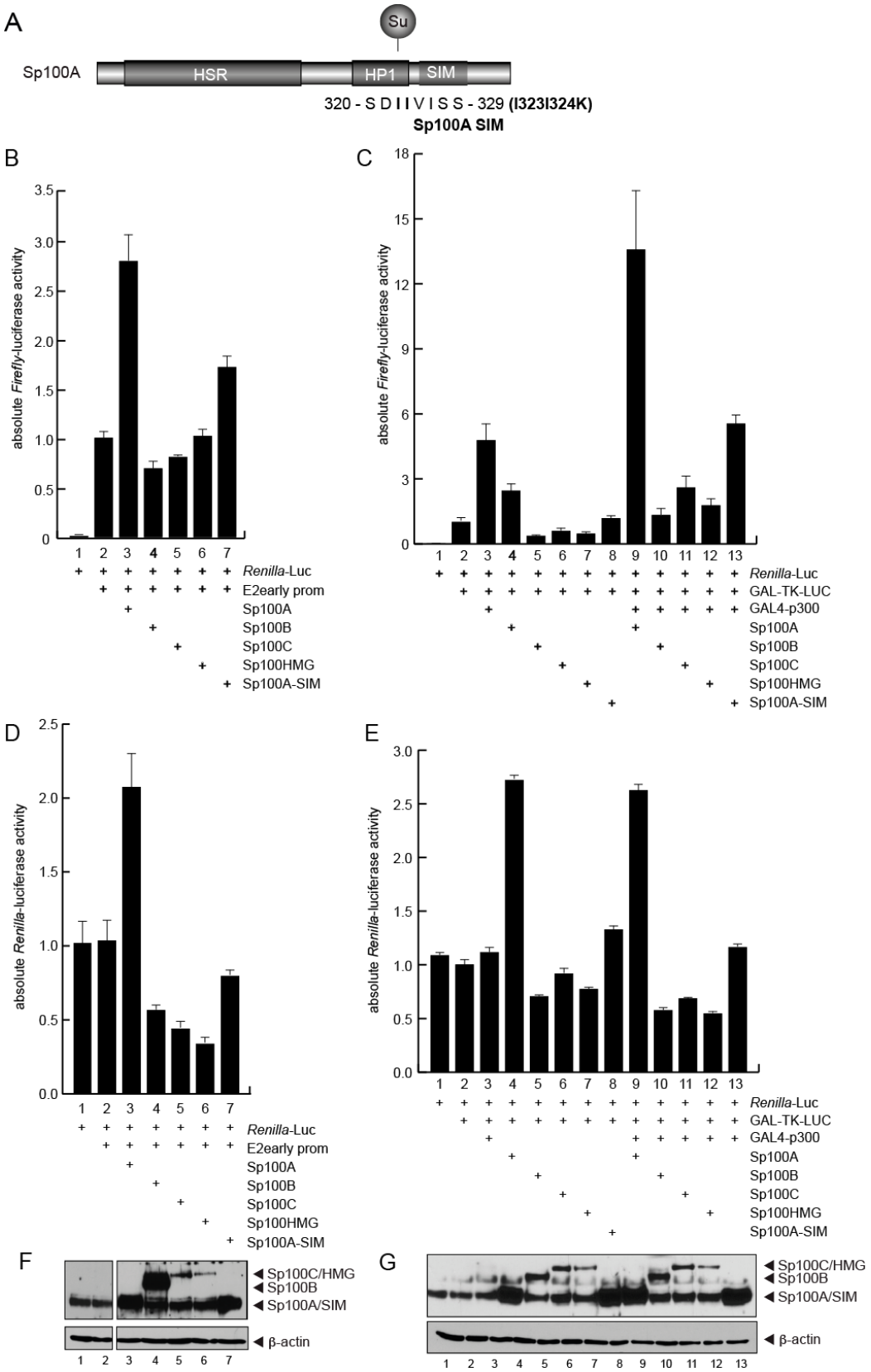

Figure 31: Sp100A transcriptional activation and localization depends on its functional SIM. (A) Schematic representation of Sp100A with SIM point mutations. (B) U2OS cells were transfected with 0.5 µg of pRL-TK (*Renilla*-Luc), 0.5 µg pGL3-Basic-Prom E2E (E2early promoter)

and 0.2 µg pHA-E1A-13S, pflag-Sp100A, pflag-Sp100B, pflag-Sp100C, pflag-Sp100HMG, and pflag-Sp100A-SIM in the combinations indicated (+). Luciferase activity was determined as in Fig. 30. The mean and standard deviations are presented for three independent experiments. (C) U2OS cells were transfected and assayed as in (B), but now with 0.5 µg pGL-GAL-TK-LUC, and 0.5 µg pG4-p300, in the combinations indicated (+). The mean and standard deviations are presented for three independent experiments. (D, E) The mean and standard deviations of the absolute *Renilla*-luciferase activity are presented for three independent experiments. (F, G) Input levels of total cell lysates were detected using pAb GH3 (α-Sp100) and mAb AC-15 (α-β-actin).

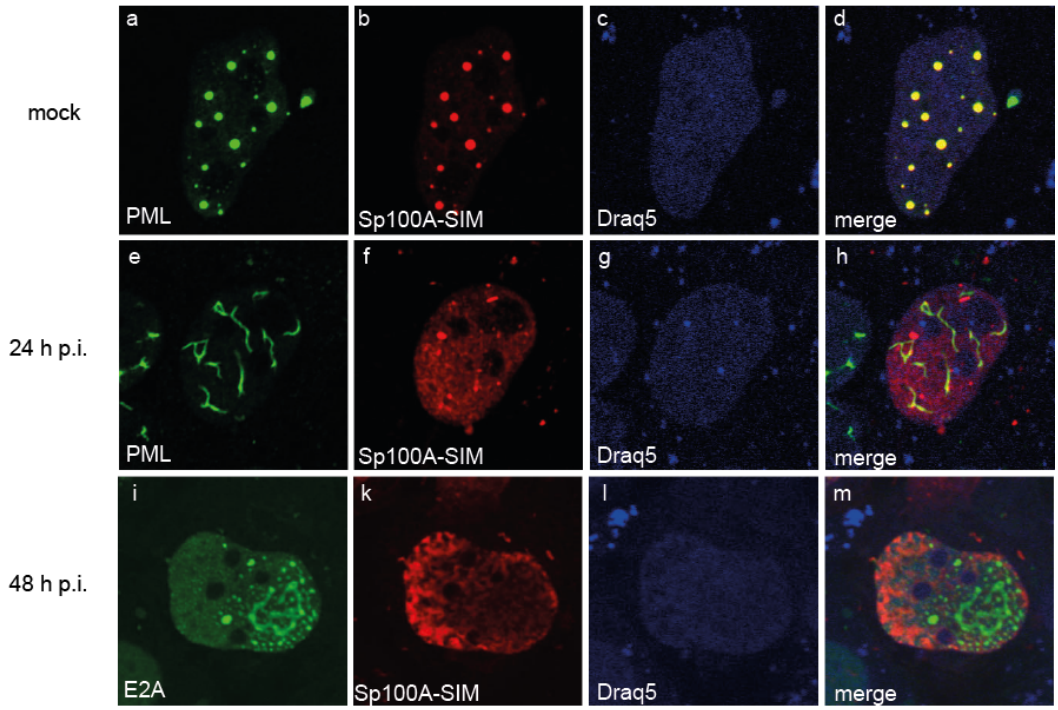

Figure 32: Sp100A-dependent transcriptional activation and localization depends on its functional SIM. HepaRG cells were transfected with 1.5 µg of pflag-Sp100A-SIM and superinfected with wt virus (H5*pg*4100) at a multiplicity of 50 ffu/cell 8 h post transfection. The cells were fixed with 4 % PFA 48 h p.i. and double-labeled with pAb NB 100-59787 (α-PML), mAb flag-M2 (α-flag) and rabbit mAb α-E2A. Primary Abs were detected with Cy3 (α-flag; red) and Alexa488 (α-E2A; green) conjugated secondary Abs. The DNA intercalating dye Draq5 (Biostatus) was used for nuclear staining. Representative α-PML (green; a, e), α-E2A (green; i) and α-flag-Sp100 (red; b, f, k) staining patterns of at least 50 analyzed cells are shown. Overlays of the single images (merge) are shown in d, f, m (magnification x 7600).

5.3 Interaction of E1B-55K with Sp100

5.3.1 E1B-55K specifically interacts with Sp100A in transiently transfected cells

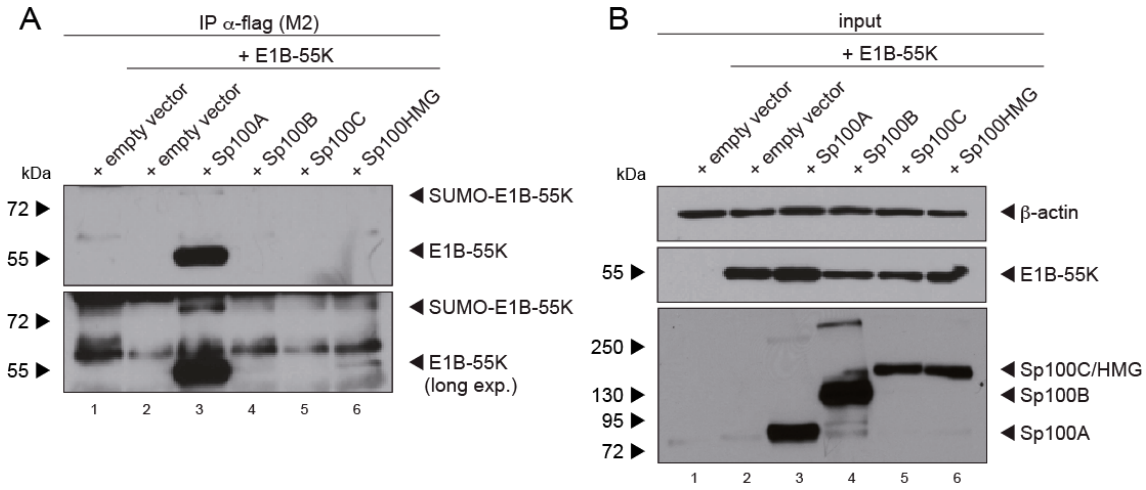

Figure 33: E1B-55K interacts specifically with Sp100A in transiently transfected cells. H1299 cells were transfected with 3 µg of pE1B-55K and 5 µg of different constructs encoding N-terminal flag-tagged human Sp100A, B, C and HMG, and harvested after 48 h to prepare total cell extracts. Immunoprecipitation of flag-Sp100 was performed using mAb flag-M2 (α-flag), and proteins resolved by SDS-PAGE were visualized by immunoblotting. Input levels of total cell lysates (B) and co-precipitated proteins (A) were detected using mAb 2A6 (α-E1B-55K), pAb GH3 (α-Sp100) and mAb AC-15 (α-β-actin). Molecular weight in kDa is indicated on the *left*, while the relevant proteins are labeled on the *right*.

E1B-55K has been shown to interact with different PML-NB residents such as Daxx/ATRX and PML isoforms IV and V (Schreiner *et al.*, 2013a; Schreiner *et al.*, 2010; Wimmer *et al.*, 2010). To ascertain whether E1B-55K also interacts with a specific Sp100 isoform, H1299 cells were transfected with E1B-55K and plasmids encoding human Sp100 A, B, C or HMG. Precipitating flag-Sp100 and subsequently staining for E1B-55K, revealed a specific interaction between E1B-55K and Sp100A (Fig. 33). A minor interaction with Sp100-HMG was visible after long exposure. Interestingly, the E1B-55K antibody also detected a comparably strong band of ~75 kDa. This band is most presumably corresponding to SUMO-modified E1B-55K. These observations imply that Sp100A interacts with both E1B-55K species and SUMO might be a regulator of this process.

5.3.2 E1B-55K SUMO modification and C-terminal domain is essential for Sp100A interaction

To more precisely identify the binding domain required for E1B-55K/Sp100A interaction, E1B-55K mutants were included in the co-immunoprecipitation analysis with Sp100A (Fig. 34). Although the E1B-55K mutants had slightly altered gel migration properties, input levels of E1B-55K and Sp100A were equal in the co-immunoprecipitation assays (Fig. 34C). These experiments revealed that E1B-55K mutated in the SUMO conjugation motif (SCM) exhibited strongly impaired Sp100A binding properties (Fig. 34B, lane 4). On the other hand, the nuclear export signal (NES) mutant of E1B-55K, mostly kept in the nucleus, exhibited a stronger affinity towards Sp100A (Fig. 34B, lane 5). Additionally, E1B-55K proteins with mutations of the C-terminal repression domains (RTR, R4433in, RF6 and E2) were highly deficient in binding of Sp100A (Fig. 34B, lanes 7 to 10). Interestingly, these mutants have previously been described as binding mutants for other PML-NB residents such as E1B-55K-RTR and -R443in for PML, E1B-55K-RF6 for Mre11 and E1B-55K-E2 for Daxx (Endter *et al.*, 2001; Hartl *et al.*, 2008; Schreiner *et al.*, 2011; Wimmer, 2010). More importantly, these mutants have been observed to lack SUMO modification (Wimmer, 2010). As the SUMOylation-deficient mutants are substantially impaired to co-immunoprecipitate Sp100A, we assume that SUMOylation of E1B-55K is an important determinant of Sp100A binding.

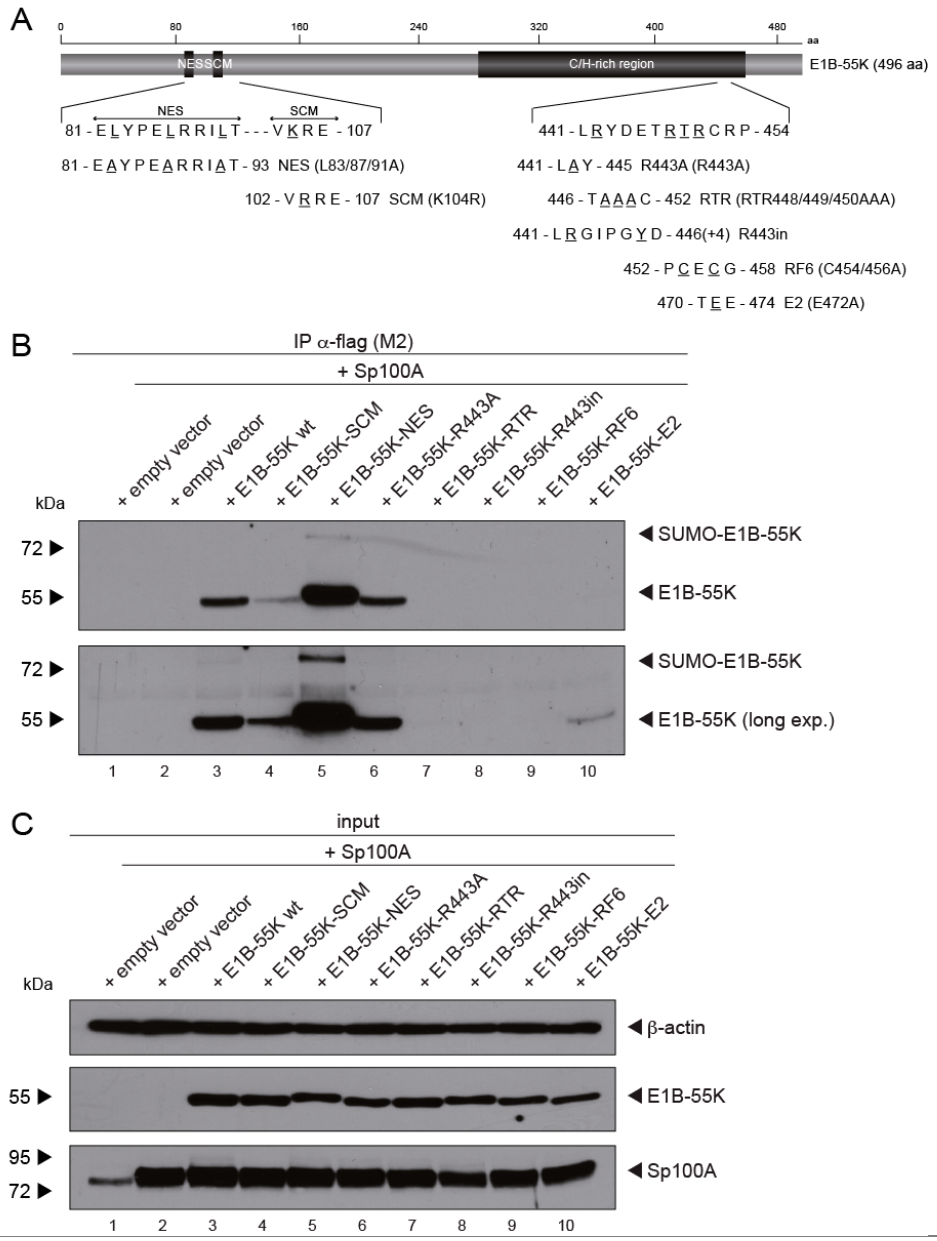

Figure 34: SUMO modification and C-terminal domain of E1B-55K are important for Sp100A interaction. (A) Schematic representation of E1B-55K protein structure and mutations are illustrated, showing previously published E1B-55K mutants, as well as the detailed aa substitutions (Endter *et al.*, 2005; Endter *et al.*, 2001; Kindsmuller *et al.*, 2007; Schreiner *et al.*, 2011; Yew & Berk, 1992). NES, nuclear export signal; SCM, SUMO conjugation motif. (B, C) H1299 cells were transfected with 3 µg of pE1B-55K mutants and 2 µg of pflag-Sp100A, harvested after 48 h, before preparing total cell extracts. Co-immunoprecipitation assays were performed as described in Fig. 33. Note the different E1B-55K mutants show different mobilities. Molecular weights in kDa are indicated on the *left*, relevant proteins on the *right*.

5.3.3 E1B-55K is colocalizing with Sp100A in transiently transfected cells

To evaluate whether the Sp100A isoform is colocalizing with E1B-55K, HepaRG cells were transfected with the E1B-55K wt, E1B-55K-SCM, or E1B-55K-NES together with flag-tagged Sp100A. Costaining with mAb 4E8 (α-E1B-55K) and mAb M2 (α-flag) revealed that E1B-55K wt and Sp100A are colocalizing within the nucleus in dot-like structures and in cytoplasmic aggregates (Fig. 35d). The E1B-55K-SCM mutant was not localizing to nuclear dot-like structures as previously described (Kindsmuller *et al.*, 2007), although Sp100A was still found almost completely within these structures, most presumably PML-NBs (Fig. 35h). Interestingly co-transfection of E1B-55K-NES caused a relocalization of Sp100A into track-like structures (Fig. 35l).

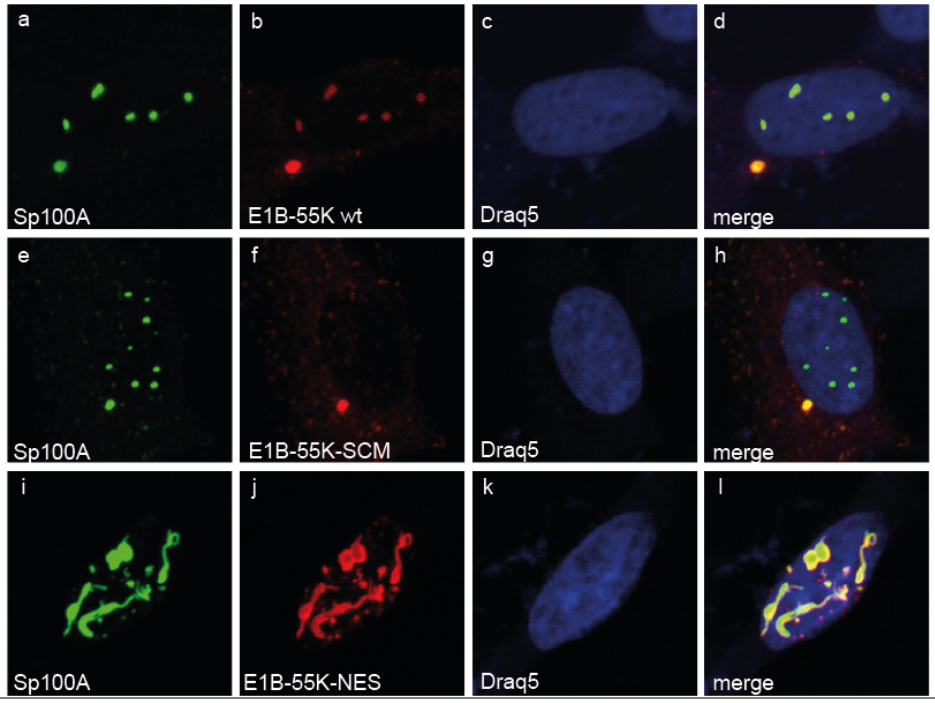

Figure 35: E1B-55K colocalizes with Sp100A in transiently transfected cells. HepaRG cells were transfected with 3 µg of pE1B-55K wt, pE1B-55K-K104R (E1B-55K-SCM) or pE1B-55K-NES and pflag-Sp100A, fixed with 4 % PFA 48 h post transfection and double-labeled with mAb 4E8 (α-E1B-55K) and mAb M2 (α-flag). Primary Abs were detected with Alexa488 (α-Sp100A; green) and Cy3 (α-E1B-55K; red) conjugated secondary Abs. For nuclear staining the DNA intercalating dye Draq5 (Biostatus) was used. Representative α-E1B-55K (b, f, j) and α-Sp100A (a, e, i) staining patterns of at least 50 analyzed cells are shown. Overlays of single images (merge) are shown in d, h, l (magnification x 7600).

It is known that the HSR domain of Sp100 is essential for the localization to PML-NBs (Sternsdorf *et al.*, 1999). To test whether this Sp100A domain is important for the massive accumulation of Sp100A and E1B-55K-NES within the track-like structures an Sp100A mutant with a deletion of aa 33-139 covering a large portion of the HSR domain was

constructed (Fig. 36A). Immunofluorescence analysis after transfection of Sp100A ΔHSR into HepaRG cells proved a complete diffuse localization of this Sp100A mutant and no localization to the PML-NBs (Fig. 36B). However, co-transfection with E1B-55K wt led to accumulation of both proteins in large cytoplasmic aggregates and nuclear dot-like structures (Fig. 36C, a-d). E1B-55K-NES however accumulated together with Sp100A in nuclear dot-and track-like structures (Fig. 36C, e-h) although these had a slightly different morphology compared with the structures resulting after co-transfection of E1B-55K-NES and Sp100A wt.

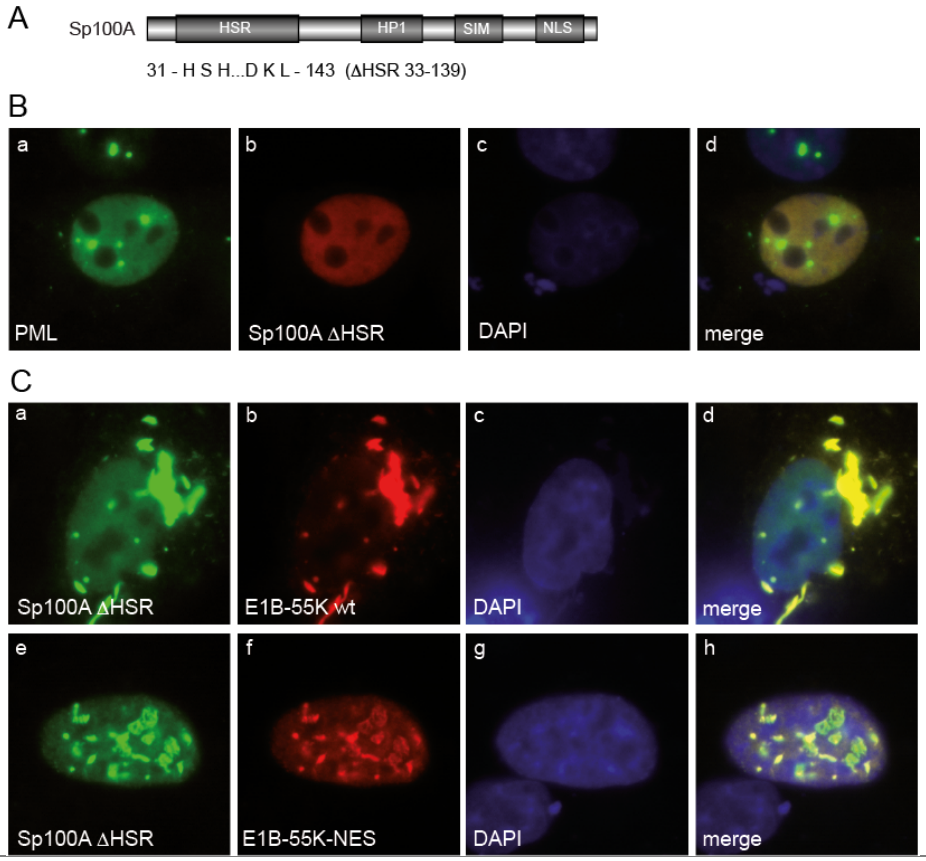

Figure 36: Sp100A HSR domain is not important for interaction with E1B-55K within PML tracks. (A) Schematic representation of Sp100A protein structure with position and detailed aa deletions of mutant Sp100A ΔHSR illustrated below. (B) HepaRG cells were transfected with 3 µg pflag-Sp100A ΔHSR, fixed with 4 % PFA 48 h post transfection and double-labeled with mAb pAb NB 100-59787 (α-PML) and mAb M2 (α-flag). (C) HepaRG cells were transfected with 3 µg of pE1B-55K wt or pE1B-55K-NES and pflag-Sp100A ΔHSR, fixed with 4 % PFA 48 h post transfection and double-labeled with mAb 4E8 (α-E1B-55K) and mAb M2 (α-flag). Primary Abs were detected with Alexa488 (green) and Cy3 (red) conjugated secondary Abs. DAPI was used for nuclear staining. Representative α-E1B-55K (Cb, f) and α-Sp100A (Ca, e) staining patterns of at least 50 analyzed cells are shown. Overlays of single images (merge) are shown in Cd, h (magnification x 7600).

6 Discussion

6.1 Ad regulatory proteins interacting with PML-NBs

To date several Ad regulatory proteins have been shown to interact with PML-NBs, substantiating their crucial role during Ad infection, although the functional consequences of this association are still largely elusive. E1A is the major transcriptional regulator of Ad5 and the first Ad protein to be expressed upon adenoviral infection. It orchestrates the temporally regulated expression of other viral proteins, resulting in the production of regulatory proteins, such as E1B-55K, E4orf3 and E4orf6 in the early phase of infection (Shenk, 2001). Already three hours after infection, E4orf3 induces the reorganization of PML-NBs via interaction with PML-II, leading to the formation of track-like structures in the nuclei of the host cells (Carvalho *et al.*, 1995; Doucas *et al.*, 1996; Hoppe *et al.*, 2006; Leppard *et al.*, 2009; Leppard & Everett, 1999). This reorganization of PML-NBs is highly conserved among most Ad species, suggesting an important function during Ad infection (Stracker *et al.*, 2005). This work demonstrates that the major Ad5 transcriptional activator E1A-13S but not E1A-12S, lacking the transactivating CR3, interacts with PML in transiently transfected as well as in infected cells. Interestingly, E1A-13S targets the same PML isoform as E4orf3, which seems to positively affect E1A-dependent transcription. Although the results imply that E1A-13S interacts with PML-II independently of E4orf3, the fact that both adenoviral proteins target the same PML isoform provides evidence for cooperation between E1A, E4orf3 and PML-II during productive adenoviral infection. Nevertheless, co-expression of E4orf3 with E1A and PML-II in the luciferase assays did not reveal a significant effect (data not shown), suggesting that this cooperation may not affect transcription, at least not under the reporter gene assay conditions applied here. Interestingly, localization of E1A-13S to PML-NBs was observed in only 30 % of the transfected cells, indicating that association of these proteins takes place in specific cells. As PML-NBs are dynamic structures and undergo profound biochemical changes during the cell cycle (Everett *et al.*, 1999), it is possible that E1A-13S targets PML only when the cell is in a specific cell cycle stage.

Figures 14 and 15 additionally show that PML isoforms, which do not interact with E1A-13S in co-immunoprecipitation experiments do activate E1A-13S-dependent transcription to some extend. PML isoforms form homo- and heterodimers via their RBCC/TRIM motif. As the reporter gene assays were not performed in PML knockout cells, endogenous PML-II could heterodimerize with the other PML isoforms. On the other hand, it is also

possible that the interaction of E1A and PML-II is more stable compared to the other PML isoforms and that those weak interactions could not be monitored in the co-immunoprecipitation assays due to the stringent RIPA lysis buffer.

In 1995 Carvalho and coworkers described for the first time that E1A colocalized with PML-NBs during virus infection and in transient transfection experiments (Carvalho *et al.*, 1995). Nevertheless, their results are somehow conflicting with this work as they assigned the interaction region of E1A and PML to the conserved LxCxE motif within CR2, which is present in both E1A isoforms. However, these observations could only be validated by immunofluorescence analysis and not by co-immunoprecipitation experiments. The contradictory results may be explained by the fact that the LxCxE motif is essential for interaction with pocket proteins such as pRb, which are also localizing to PML-NBs (Ferbeyre *et al.*, 2000; Whyte *et al.*, 1988). Therefore, it is likely that the LxCxE motif is additionally important for proper subnuclear localization while CR3 is necessary for physical interaction. Furthermore, cell type specific differences could play a role, as Carvalho and coworkers used HeLa cells instead of HepaRG cells.

E1B-55K targets PML-IV and PML-V, with the PML-IV interaction being dependent on the SUMO modification of E1B-55K (Wimmer *et al.*, 2010). Interestingly, different Ad regulatory proteins apparently target single PML isoforms implying a specific function for each isoform. Indeed, comparative studies with the PML isoforms have suggested increasing evidence that each PML isoform possesses distinct functions mediated by its unique C-terminal region (Nisole *et al.*, 2013).

Upon expression of E4orf6 with a delay of approximately 6 h in relation to E4orf3/E1B-55K, deSUMOylation of E1B-55K is initiated followed by the loss of PML interaction and relocalization of E1B-55K to the viral replication centers (Lethbridge *et al.*, 2003; Wimmer *et al.*, 2010). Subsequently, E1B-55K alone or E1B-55K in combination with E4orf6 then target repressive cellular factors such as p53, Daxx/ATRX or Mre11 for proteasomal degradation (Schreiner *et al.*, 2013a; Schreiner *et al.*, 2010; Stracker *et al.*, 2002). Interestingly, numerous interaction partners of E1B-55K are localizing to PML-NBs (Van Damme *et al.*, 2010) and many of these factors are targeted for proteasomal degradation. In contrast to Daxx, the interaction between E1B-55K and PML does not cause degradation of PML but seems to be important for induction of p53 SUMOylation thereby likely modulating its function (Muller & Dobner, 2008; Pennella *et al.*, 2010). Nevertheless, the functional consequences of enhanced p53 SUMOylation are still under debate (Muller & Dobner,

2008; Pennella *et al.*, 2010). While reports exist that SUMOylation of p53 activates its transcriptional response (Rodriguez *et al.*, 1999), others propose a negative impact on p53's transactivating properties (Pennella *et al.*, 2010) and another report shows both activation and repression of p53 target genes (Stindt *et al.*, 2011).

This work demonstrates that besides the constitutive factors PML and Daxx, E1B-55K additionally interacts with Sp100A, which seems to be a positive factor of adenoviral and cellular transcription. As Sp100A is almost identical to Sp100B, C and HMG except for a three aa stretch at the very C-terminus (Newhart *et al.*, 2013; Wasylyk *et al.*, 2002), it is likely that E1B-55K targets the C-terminal end of Sp100A. Immunofluorescence analysis showed that the sub-nuclear localization of Sp100A and E1B-55K does not depend on the HSR domain of Sp100, which has been shown to be required for PML-NB targeting (Sternsdorf *et al.*, 1999). Rather it seems as if E1B-55K is recruiting Sp100A to nuclear structures independently of the HSR domain, which may be enlarged PML-NBs. In this context, Sp100 self-association has been observed to promote formation of elongated PML-NBs. In this case it is possible that in the beginning of Ad5 infection soluble Sp100A is recruited and kept at PML-NBs where it would be able to promote adenoviral transcription. On the other hand, this recruitment may represent a means to spatially restrict Sp100A, thereby preventing it from activating cellular promoters as it seems to activate not only adenoviral transcription but also positively affects numerous cellular promoters. This idea is supported by the fact that Sp100A is bound by the C-terminal repression domain of E1B-55K, which has also been shown to bind and repress p53's transactivating domain (Yew *et al.*, 1994).

Taken together PML-II seems to be a positive regulator of E1A-13S-dependent transcription. However, it is clearly preliminary to speculate about the functional consequences of E1B-55K-Sp100A interaction. Nevertheless, the fact that that the major Ad regulatory proteins E1A, E1B-55K and E4orf3 interact and transiently localize to PML-NBs in transfection and infection highlight the importance of these nuclear subdomains.

6.2 PML track-like structures might be a positive microenvironment for Ad transcription

So far PML-NBs are mainly considered to be part of an intracellular anti-viral defense mechanism (Everett & Chelbi-Alix, 2007; Geoffroy & Chelbi-Alix, 2011; Tavalai & Stamminger, 2008). Most viruses, including Ad have evolved counteracting strategies to disrupt PML-NBs soon after initiation of the immediate early transcription, and the

absence of this ability can adversely affect the success of the infection, suggesting a negative role in virus infection. Furthermore, many PML-NB-associated factors are induced by interferons giving further credence to this assumption (Guldner *et al.*, 1992; Lavau *et al.*, 1995). Based on available data with different DNA viruses it is reasonable to conclude that diverse molecular mechanisms have evolved to counteract PML-NB-mediated antiviral activities. For instance, inactivation of PML-NBs during early stages of HSV-1 infection depends exclusively on the expression of the immediate-early protein ICP0, which rapidly localizes to these subnuclear structures and disrupts them completely (Chelbi-Alix & de The, 1999; Maul & Everett, 1994; Maul *et al.*, 1993). ICP0 leads to the rapid loss of high-molecular weight PML in a proteasome-dependent manner, and subsequently results in disintegration of PML-NB structures (Everett *et al.*, 1998; Muller & Dejean, 1999).

For Ad, the functional consequences of E4orf3-induced PML-NB reorganization prior to formation of track-like structures in the nucleus of cells still remain unclear. Nevertheless, the question remains why adenoviruses do not completely disrupt PML-NBs and target their components for proteasomal degradation similar to HSV-1 but reorganize them into unique track-like structures. These structures are maintained until the late stages of infection, providing evidence that preservation of these structures might be beneficial for the virus.

Indeed, indications of a pro-viral role of PML-NBs exist for several virus types. Particularly DNA viruses seem to require PML-NB-associated factors or the PML-NB microenvironment to ensure efficient viral transcription/replication, as their genomes and RNA synthesis sites are often located in the vicinity of these distinct nuclear regions (Everett, 2001; Maul, 1998; Maul *et al.*, 1996): Human papillomavirus (HPV) infection is enhanced by PML expression (Day *et al.*, 2004). Human cytomegalovirus (HCMV) and human herpes simplex virus type 1 (HSV-1) genome transcription exclusively takes place at PML-NBs (Ishov & Maul, 1996; Ishov *et al.*, 1997; Maul *et al.*, 1996). SV40 replication preferentially occurs in the vicinity of PML-NBs (Tang *et al.*, 2000) and similar observations were made for human polyomaviruses (Jul-Larsen *et al.*, 2004; Shishido-Hara *et al.*, 2008). Nevertheless, it is still under debate if viral DNA actively associates with PML-NBs to hijack and profit from their components or if PML-NBs are recruited to the incoming foreign DNA as part of the intracellular antiviral defense to counteract viral gene expression and replication (Everett, 2001; 2013; Everett & Chelbi-Alix, 2007; Moller &

Schmitz, 2003). Supportive for the first idea is that several lines of evidence propose a role for PML-NBs in cellular transcriptional regulation (Zhong *et al.*, 2000b), due to the association of newly synthesized RNA with the periphery of PML-NBs, and the recruitment of transcriptional regulators (Boisvert *et al.*, 2000; LaMorte *et al.*, 1998). In this context, over 50 % of the PML-NB-associated proteins are transcription factors and epigenetic regulators (Van Damme *et al.*, 2010), e. g. the histone acetyltransferases, cAMP-response element-binding protein (CBP) and the RNA polymerase II (von Mikecz *et al.*, 2000). Additionally, Xie and coworkers observed loss of PML-NB staining after DNaseI treatment of mammalian cells and proposed that PML-NB components directly or indirectly associate with nuclear DNA and that these factors may participate in the activation of transcription of specific regions of the genome (Xie *et al.*, 1993).

Numerous reports suggest that gene expression is regulated not only by the interaction between transcription factors and DNA but also by the higher-order architecture of the cell nucleus and/or the position of the genes within the nucleus (Carmo-Fonseca, 2002; Misteli, 2001; Tashiro *et al.*, 2004). However, other studies have found no association of nascent RNA and active transcription with these subdomains (Boisvert *et al.*, 2000; Wang *et al.*, 2004). Another report by Kießlich and coworkers confirmed that in non-synchronized cells the majority of nascent RNA was not associated with PML-NBs (Kiesslich *et al.*, 2002). However, it was found that active mRNA transcription sites overlapped with PML-NBs in cells traversing the G1 phase and after IFNγ treatment, suggesting that although basal activity may not require the presence of PML-NBs, upregulated transcription may. The authors argued that PML-NBs may be recruited to nuclear sites of induced or upregulated mRNA transcription, where they may serve as a scaffold for factors involved in expression of specific genes and that the introduction of viral DNA during viral infection may be an example of this induced activity.

This work shows for the first time an adenoviral protein, E1A-13S, taking direct advantage of PML. Overexpression of PML increased E1A-13S-dependent transcription in a dose-dependent manner and vice versa depletion of PML from MEFs decreased adenoviral gene expression (Figs. 14-17). Furthermore, interaction of E1A-13S and PML-II is dependent on the highly conserved transcription factor-binding region of E1A-13S. Since neither E1A nor PML have shown to possess DNA binding activity, it is likely that PML activates transcription through stabilizing co-activator/transcription factor complexes. Based on the

observation that PML-II enhances p300 co-activator function, it is also possible that PML acts as a platform for E1A-13S to interact with other co-activators or transcription factors.

Additionally to E1A-13S, it is demonstrated that Sp100A, which seems to be a positive factor of viral and cellular transcription (Figs. 28-29), is found within PML track-like structures, while the repressive factors Sp100B, C and HMG are relocalized from the tracks (Fig. 23). In the late stages of infection, Sp100A is still detected at the tracks, which are often associated with newly formed viral replication centers, giving the impression that they are surrounded by the tracks (Fig. 23, enlarged merge). A small fraction of Sp100A is then also found at the outer rim of the replication compartments, the designated sites of active transcription. It has been described that while compact viral DNA is mainly found in the interior of the Ad replication centers, nascent viral mRNAs are mainly detected at the outer rim (Pombo *et al.*, 1994; Puvion-Dutilleul & Puvion, 1991). This observation again supports the idea of the tracks being positive structures, providing a scaffold for adenoviral transcription.

Recently Newhardt and coworkers proposed that Sp100A is able to promote the recruitment of histone acetyltransferases (HAT) and acetyllysine binding factors, increasing chromatin decondensation at a CMV promoter regulated transgene, while Sp100B, C and HMG repressed HAT recruitment (Newhart *et al.*, 2013). In line with this, it has also been observed that depletion of all Sp100 proteins enhanced the acetylation levels of histone H4 -associated with an HCMV promoter (Kim *et al.*, 2011).

Taken together our data support the idea that PML-NBs may possess antiviral properties due to the large number of repressive proteins localizing to these compartments. However upon infection and E4orf3 expression, redistribution may cause the release of negative factors with positive factors remaining associated with the track-like structures as illustrated in Figure 37A. PML-II may function as a scaffold and serve to recruit E1A-13S and its coactivators. Under these conditions, Sp100A, which is held back at the PML tracks, may be able to recruit HATs, creating a favorable microenvironment for activation of Ad promoters.

6.3 Relocalization of PML track-like structures and changes of SUMO modification as alternatives to counteract repressive factors

According to the data of this work, depletion of Sp100 results in significantly increased Ad progeny production. This effect is likely attributed to the depletion of repressive Sp100

isoforms B, C and HMG, which repressed transcription from Ad promoters in reporter gene assays (Figs. 28-31). Sp100 has been reported to modulate the replication program of several DNA viruses: HCMV and HVS (Herpesvirus Saimiri) target Sp100 for proteasomal degradation, thus depletion of Sp100 by RNA interference enhances HCMV replication and gene expression (Full *et al.*, 2012; Kim *et al.*, 2011). Similar to our findings, Maul and coworkers previously demonstrated that Sp100 isoforms B, C, and HMG suppressed HSV-1 IE gene expression and repressed the ICP0 promoter-dependent on their SAND domains (Negorev *et al.*, 2006; Newhart *et al.*, 2013). Concerning Ad, in 1995 Doucas and colleagues reported relocalization of endogenous Sp100 into the E4orf3-induced PML track-like structures early post infection. During late stages, PML and Sp100 segregation was observed, with Sp100 relocalizing from these Ad induced tracks to the early viral replication centers (Doucas *et al.*, 1996). This work now illustrates that the transactivating isoform Sp100A is mainly found in the tracks, while only the repressive Sp100 proteins B, C and HMG are completely displaced from these nuclear structures (Fig. 23).

It is possible that Ad-dependent loss of PML-NB integrity by redistribution into track-like structures serves the dispersal of associated repressive factors in the nucleus. Consequently, these antivirals would become accessible for targeting by newly synthesized viral gene products such as Ad5 E1B-55K and E4orf6 (illustrated in Figure 37). Recently, our group showed that the constitutive PML-NB factor Daxx represses Ad5 gene expression and productive infection. This inhibition is counteracted by capsid protein pVI-dependent Daxx relocalization from the NBs in immediate early times of infection, followed by E1B-55K-dependent proteasomal degradation (Schreiner *et al.*, 2012; Schreiner *et al.*, 2010). The relocalization of Daxx suggests a detrimental effect when it is kept within PML-NBs. In this context, it is conceivable that this may also be the case for the repressive Sp100 isoforms B, C and HMG. Although, the reduction of the high molecular weight Sp100 species seems to depend on E1B-55K and E4orf6 in infection, E1B-55K could not be co-precipitated with Sp100 B, C and HMG. As E1B-55K has been described as the target recognition unit of the classical Ad ubiquitin ligase complex it is likely that other viral proteins participate in the loss of the high molecular weight Sp100. The fact that complete loss of these isoforms is efficiently achieved in the late stages of Ad5 infection implies an involvement of late adenoviral proteins in this process. Clearly, further studies have to elucidate the fate of the repressive Sp100 isoforms.

As infection progresses, overexpressed Sp100 B, C and HMG accumulate at viral replication compartments (Fig. 23). Besides the Sp100 variants, other repressive factors and proteins participating in DNA damage response (DDR) have shown recruitment to viral replication centers, suggesting a common phenomenon during Ad infection. Examples are RPA32, ATR, ATRIP, Rad9, TOPBP1, Rad17 and hnRNPUL1 (Turnell & Grand, 2012). Recently SPOC1, a novel regulator of the DDR and chromatin structure has been shown to restrict adenoviral replication/transcription and is similarly recruited to these nuclear viral compartments before E1B-55K/E4orf6 induced proteasomal degradation (Schreiner *et al.*, 2013b). Another study showed that the Bloom Helicase, another PML-NB resident factor which is implicated in resection of DNA breaks, is localized at distinct foci close to the DBP staining early during Ad infection and is degraded later (Orazio *et al.*, 2011). The Mre11, Rad50 and NBS1 (MRN) complex, participating in sensing and repair of DNA damage, represents a particular case. Early after infection, E4orf3 causes its components to relocalize to track-like structures. As infection progresses, Mre11 levels decline, Rad50 is maintained in association with the tracks and NBS1 is completely relocalized into viral replication centers (Evans & Hearing, 2005). It has been proposed that the relocalization into viral replication compartments may inhibit the functions of these DDR factors. However, also positive factors, such as proteins involved in DNA replication and RNA synthesis, are recruited to viral replication centers to promote viral DNA replication and transcription (de Jong & van der Vliet, 1999; Hindley *et al.*, 2007; Lawrence *et al.*, 2006). Therefore, it appears possible that some apparently negative factors may play a beneficial role early during infection and are degraded, as they are no more useful, to prevent adverse functions during the late stages of infection. The viral replication cycle requires a precise regulation of viral gene expression. Consequently, virus-induced changes in cellular regulators, such as Sp100, are likely to be critical to the viral life cycle. In this context it seems plausible that differential transcriptional properties of the Sp100 isoforms may help to establish a chronologically regulated viral gene expression.

In addition to relocalization, similar to herpes viruses (Kim *et al.*, 2011; Muller & Dejean, 1999; Tavalai *et al.*, 2011), modulation of SUMOylated Sp100 forms is also observed during Ad5 infection. In HSV-1 infection, ICP0-mediated proteasomal depletion of SUMO modified PML and Sp100, has suggested that counteraction occurs via interference with a common SUMOylation pathway rather than by specific targeting of individual proteins (Everett *et al.*, 2006; Muller & Dejean, 1999). Another study provides evidence that the

formation of repressive PML-NB-like structures in association with incoming viral DNA depends on the respective SIMs of antiviral proteins such as PML, Sp100 and Daxx (Cuchet-Lourenco *et al.*, 2011). This observation provides a convincing explanation of how early viral proteins may inhibit the antiviral functions of these proteins by depleting PML-SUMO conjugates and, consequently, eliminating of their SIM-dependent recruitment.

During Ad infection, loss of SUMOylation was observed for all Sp100 isoforms. In line with this, reduced stability of the repressive Sp100 isoforms may be attributed to the lack of stable association between PML-NB factors via a SUMO bridge. Interestingly, while SUMO-2 modification of Sp100A is significantly reduced upon Ad5 infection, SUMO-1 modified Sp100A is not affected at this time point, suggesting that SUMO-2 deconjugation is initiated earlier. The PML-NB is defined by a spherical shell consisting of PML and Sp100, stabilized via non-covalent SUMO-SIM interactions between PML and Sp100 (Lang *et al.*, 2010). While SUMO-1 modifications are preferably found within the shell or adjacent to it, Poly-SUMO-2/3 chains have been shown to protrude into the interior of the PML-NB where they represent binding sites for proteins, such as HP1 or Daxx, located inside the PML-NB. Therefore, considering the architecture of PML-NBs provides a plausible explanation why Ad preferentially abolishes/suppresses SUMO-2 modification. The observation that mutation of the SIM in PML-II further enhanced E1A-dependent transactivation (Fig. 18B) supports this model. Assuming that the PML-SIM mediates non-covalent interactions with other SUMOylated proteins, it is tempting to speculate that protein interactions within PML-NBs, mediated by the SIM, may inhibit transcriptional stimulation by PML itself and that Ad induced deSUMOylation of Sp100 and likely other factors may relieve from this inhibitory interactions.

The fact that SUMO-1 modification of Sp100A is comparably stable supports the observation that Sp100 stays associated with PML tracks. Although it was shown that SUMO modification is not absolutely prerequisite for the localization of Sp100 to the PML-NBs, it may help stabilizing the interaction of Sp100A and PML during Ad infection (Lang *et al.*, 2010; Shen *et al.*, 2006; Sternsdorf *et al.*, 1999). Interestingly, the SIM defective Sp100A mutant fails to efficiently stimulate transcription as well as to localize to the Ad5 induced PML-tracks, despite of a functional HSR domain, which is essential for the localization to PML-NBs (Sternsdorf *et al.*, 1999). Apparently, upon relocalization of the PML-NBs SUMO-SIM interactions have a stronger impact on the localization of Sp100 compared to the HSR domain. As inactivation of the SIM negatively affects Sp100A's

transcription activity, it is tempting to speculate that Sp100A activates transcription from Ad promoters, most likely when it is kept in the PML tracks, where it may recruit histone deacetylases to create a favorable environment for Ad gene expression (Fig. 37).

It has been proposed that HP1 and Sp100 form a complex to regulate chromatin remodeling (Lehming *et al.*, 1998), although the exact functionality of the complex is still unknown. Another study demonstrated that HP1 proteins are phosphorylated in response to DNA damage, and appear to be important for recruiting DDR factors and dynamically reorganizing chromatin (Baldeyron *et al.*, 2011; Dinant & Luijsterburg, 2009). Furthermore, SUMOylation of Sp100 has been shown to stabilize the interaction with HP1 *in vitro* (Seeler *et al.*, 2001; Seeler *et al.*, 1998). Consequently, Ad disrupts the Sp100-HP1α interaction suggesting that this cellular chromatin-remodeling complex is repressive for virus replication, providing evidence for the general model that Ad promotes deSUMOylation of PML-NB-associated proteins to prevent recruitment of certain repressive factors to the PML track-like structures in infected cells (Fig. 37). Consistent with this observation, EBV (Epstein-Barr Virus) EBNA-LP, the coactivator of the EBV transactivator EBNA2, has been shown to interact with Sp100 and displace the Sp100/HP1α complex from PML-NBs (Ling *et al.*, 2005).

In sum, considering the data of this thesis and the actual literature, it appears plausible that NBs possess antiviral properties due to the large number of repressive proteins localizing to these compartments, such as Daxx/ATRX, p53 or HP1. Therefore, during evolution Ads have apparently acquired a mechanism to counteract this PML-NB function, disrupting the integrity of PML-NBs by expressing early viral E4orf3, which causes PML-NB components to redistribute into track-like structures. Intrinsic to this idea is the notion that while in the NBs, the PML-NB residents are functionally inaccessible and thus, in case of the positive factors, are unable to participate in the viral program and in case of repressive factors cannot be reached and counteracted by adenoviral proteins. Thus, the aim of the virus would be to expose and release of the virus promoting factors to active sites of viral transcription and replication as illustrated in Figure 37A. Counteraction of repressive factors by Ad proteins may take place at different levels, as already described for several cellular targets, and may involve direct interaction (e. g. p53), relocalization (e. g. Daxx), change of posttranslational modification, such as SUMOylation (e. g. p53) and targeting for degradation (e. g. p53, Daxx, ATRX; Fig. 37B). Apparently Ad5 uses relocalization, changes in SUMOylation and interaction with E1B-55K to cope with the

different functions of Sp100; however the fate of the different Sp100 isoforms during the late stages of infection and involvement of other Ad proteins are still subjects for further investigations.

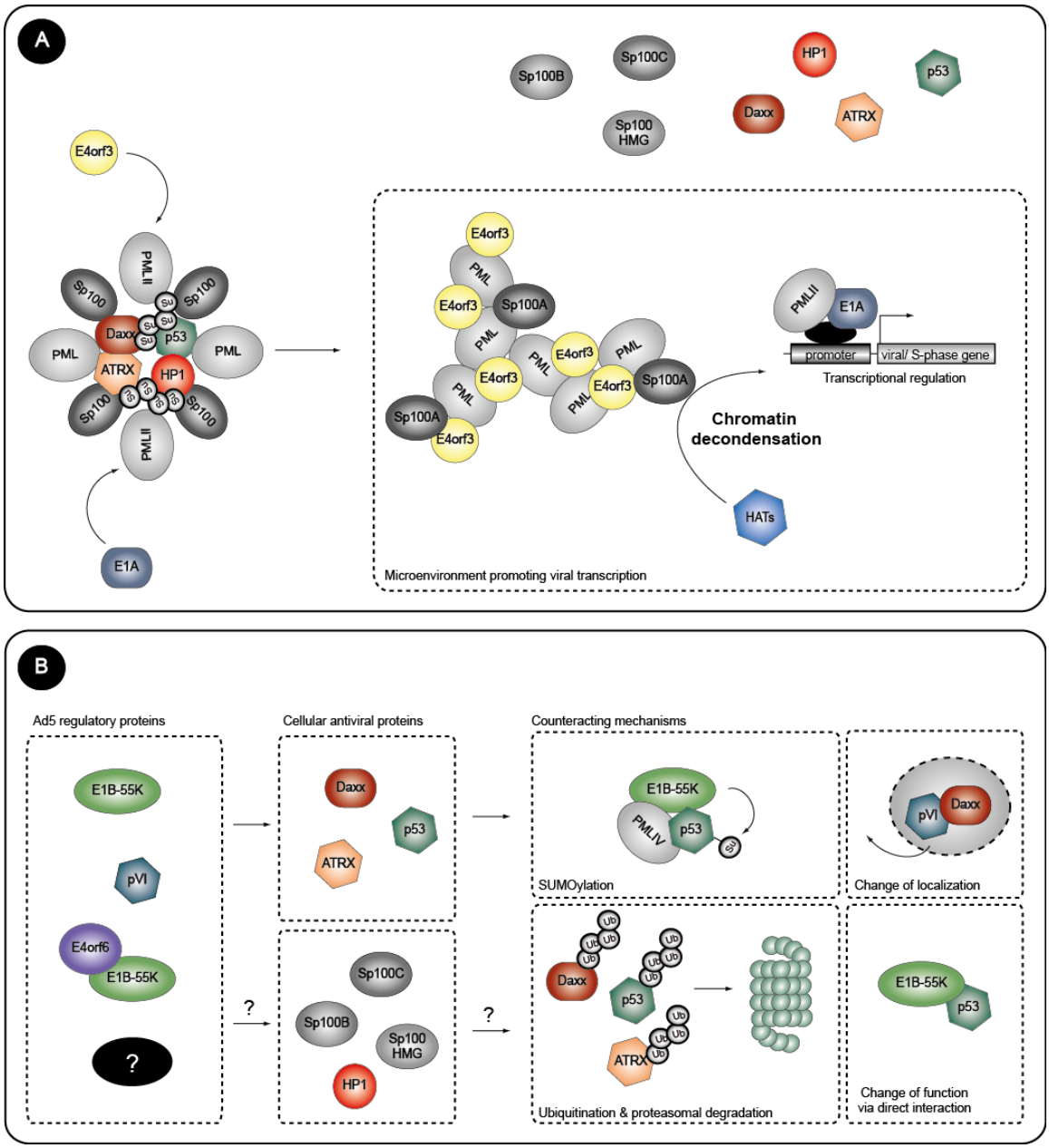

Figure 37: Model of selective modulation of PML-NBs by Ad5 regulatory proteins. A schematic representation highlighting the proposed model of Ad mediated relocalization of antiviral factors-associated to PML-NBs. A) In non-infected cells transcriptional activators and repressors, such as PML, the Sp100 isoforms, HP1, Daxx, ATRX or p53 are united within the PML-NBs. Sp100A promotes chromatin decondensation and HAT (Histone acetyltransferase) recruitment. In contrast Sp100B, Sp100C and Sp100HMG prevent these events. HP1 and the Daxx/ATRX complex function in gene silencing by organizing higher-order chromatin structures. Poly-SUMO-2/3 chains protrude into the interior of the PML-NB to mediate interactions with HP1, Daxx or ATRX, which are enriched in the interior of the PML-NB. In early time points after infection E4orf3 targets PML isoform II to reorganize PML-NB into track-like structures. SUMO-2/3 chains are abolished, causing release of the repressive factors HP1, Daxx and ATRX from the PML-NBs. Under these conditions, Sp100A, which is held back at the PML tracks, is able to recruit HATs, creating a favorable microenvironment for activation of Ad promoters. (B) Repressive factors are dispersed into the nucleoplasm, increasing accessibility by Ad counteracting proteins, such as E1B-55K, E4orf6 or pVI.

7 Literature

Abe, S., Miyamura, K., Oba, T., Terakura, S., Kasai, M., Kitaori, K., Sasaki, T. & Kodera, Y. (2003). Oral ribavirin for severe adenovirus infection after allogeneic marrow transplantation. *Bone Marrow Transplant* 32, 1107-1108.

Adamson, A. L. & Kenney, S. (2001). Epstein-barr virus immediate-early protein BZLF1 is SUMO-1 modified and disrupts promyelocytic leukemia bodies. *J Virol* 75, 2388-2399.

Ahn, J. H., Brignole, E. J., 3rd & Hayward, G. S. (1998). Disruption of PML subnuclear domains by the acidic IE1 protein of human cytomegalovirus is mediated through interaction with PML and may modulate a RING finger-dependent cryptic transactivator function of PML. *Mol Cell Biol* 18, 4899-4913.

Amon, W., White, R. E. & Farrell, P. J. (2006). Epstein-Barr virus origin of lytic replication mediates association of replicating episomes with promyelocytic leukaemia protein nuclear bodies and replication compartments. *J Gen Virol* 87, 1133-1137.

Anderson, C. W. (1990). The proteinase polypeptide of adenovirus serotype 2 virions. *Virology* 177, 259-272.

Araujo, F. D., Stracker, T. H., Carson, C. T., Lee, D. V. & Weitzman, M. D. (2005). Adenovirus type 5 E4orf3 protein targets the Mre11 complex to cytoplasmic aggresomes. *J Virol* 79, 11382-11391.

Ascoli, C. A. & Maul, G. G. (1991). Identification of a novel nuclear domain. *J Cell Biol* 112, 785-795.

Asper, M., Sternsdorf, T., Hass, M., Drosten, C., Rhode, A., Schmitz, H. & Gunther, S. (2004). Inhibition of different Lassa virus strains by alpha and gamma interferons and comparison with a less pathogenic arenavirus. *J Virol* 78, 3162-3169.

Babich, A., Feldman, L. T., Nevins, J. R., Darnell, J. E., Jr. & Weinberger, C. (1983). Effect of adenovirus on metabolism of specific host mRNAs: transport control and specific translational discrimination. *Mol Cell Biol* 3, 1212-1221.

Babiss, L. E. & Ginsberg, H. S. (1984). Adenovirus type 5 early region 1b gene product is required for efficient shutoff of host protein synthesis. *J Virol* 50, 202-212.

Babiss, L. E., Ginsberg, H. S. & Darnell, J. E., Jr. (1985). Adenovirus E1B proteins are required for accumulation of late viral mRNA and for effects on cellular mRNA translation and transport. *Mol Cell Biol* 5, 2552-2558.

Bailey, A. & Mautner, V. (1994). Phylogenetic relationships among adenovirus serotypes. *Virology* 205, 438-452.

Baker, A., Rohleder, K. J., Hanakahi, L. A. & Ketner, G. (2007). Adenovirus E4 34k and E1b 55k oncoproteins target host DNA ligase IV for proteasomal degradation. *J Virol* 81, 7034-7040.

Baker, L. A., Allis, C. D. & Wang, G. G. (2008). PHD fingers in human diseases: disorders arising from misinterpreting epigenetic marks. *Mutat Res* 647, 3-12.

Baldeyron, C., Soria, G., Roche, D., Cook, A. J. & Almouzni, G. (2011). HP1alpha recruitment to DNA damage by p150CAF-1 promotes homologous recombination repair. *J Cell Biol* 193, 81-95.

Bell, P., Lieberman, P. M. & Maul, G. G. (2000). Lytic but not latent replication of epstein-barr virus is associated with PML and induces sequential release of nuclear domain 10 proteins. *J Virol* 74, 11800-11810.

Beltz, G. A. & Flint, S. J. (1979). Inhibition of HeLa cell protein synthesis during adenovirus infection. Restriction of cellular messenger RNA sequences to the nucleus. *J Mol Biol* 131, 353-373.

Benko, M. & Harrach, B. (1998). A proposal for a new (third) genus within the family Adenoviridae. *Arch Virol* 143, 829-837.

Bergelson, J. M., Cunningham, J. A., Droguett, G., Kurt-Jones, E. A., Krithivas, A., Hong, J. S., Horwitz, M. S., Crowell, R. L. & Finberg, R. W. (1997). Isolation of a common receptor for Coxsackie B viruses and adenoviruses 2 and 5. *Science* 275, 1320-1323.

Berk, A. J. (2005). Recent lessons in gene expression, cell cycle control, and cell biology from adenovirus. *Oncogene* 24, 7673-7685.

Berk, A. J. (2007). Adenoviridae: The Viruses and Their Replication. In *Fields Virology*, 5th edn, pp. 2355-2394.

Bernardi, R. & Pandolfi, P. P. (2007). Structure, dynamics and functions of promyelocytic leukaemia nuclear bodies. *Nat Rev Mol Cell Biol* 8, 1006-1016.

Berthoux, L., Towers, G. J., Gurer, C., Salomoni, P., Pandolfi, P. P. & Luban, J. (2003). As(2)O(3) enhances retroviral reverse transcription and counteracts Ref1 antiviral activity. *J Virol* 77, 3167-3180.

Bischof, O., Nacerddine, K. & Dejean, A. (2005). Human papillomavirus oncoprotein E7 targets the promyelocytic leukemia protein and circumvents cellular senescence via the Rb and p53 tumor suppressor pathways. *Mol Cell Biol* 25, 1013-1024.

Bjorndal, A. S., Szekely, L. & Elgh, F. (2003). Ebola virus infection inversely correlates with the overall expression levels of promyelocytic leukaemia (PML) protein in cultured cells. *BMC Microbiol* 3, 6.

Blanchette, P., Cheng, C. Y., Yan, Q., Ketner, G., Ornelles, D. A., Dobner, T., Conaway, R. C., Conaway, J. W. & Branton, P. E. (2004). Both BC-box motifs of adenovirus protein E4orf6 are required to efficiently assemble an E3 ligase complex that degrades p53. *Mol Cell Biol* 24, 9619-9629.

Blanchette, P., Kindsmuller, K., Groitl, P., Dallaire, F., Speiseder, T., Branton, P. E. & Dobner, T. (2008). Control of mRNA export by adenovirus E4orf6 and E1B55K proteins during productive infection requires E4orf6 ubiquitin ligase activity. *J Virol* 82, 2642-2651.

Blondel, D., Kheddache, S., Lahaye, X., Dianoux, L. & Chelbi-Alix, M. K. (2010). Resistance to rabies virus infection conferred by the PMLIV isoform. *J Virol* 84, 10719-10726.

Blondel, D., Regad, T., Poisson, N., Pavie, B., Harper, F., Pandolfi, P. P., De The, H. & Chelbi-Alix, M. K. (2002). Rabies virus P and small P products interact directly with PML and reorganize PML nuclear bodies. *Oncogene* 21, 7957-7970.

Boisvert, F. M., Hendzel, M. J. & Bazett-Jones, D. P. (2000). Promyelocytic leukemia (PML) nuclear bodies are protein structures that do not accumulate RNA. *J Cell Biol* 148, 283-292.

Bonilla, W. V., Pinschewer, D. D., Klenerman, P., Rousson, V., Gaboli, M., Pandolfi, P. P., Zinkernagel, R. M., Salvato, M. S. & Hengartner, H. (2002). Effects of promyelocytic leukemia protein on virus-host balance. *J Virol* 76, 3810-3818.

Borden, K. L., Campbelldwyer, E. J., Carlile, G. W., Djavani, M. & Salvato, M. S. (1998). Two RING finger proteins, the oncoprotein PML and the arenavirus Z protein, colocalize with the nuclear fraction of the ribosomal P proteins. *J Virol* 72, 3819-3826.

Borden, K. L. & Freemont, P. S. (1996). The RING finger domain: a recent example of a sequence-structure family. *Curr Opin Struct Biol* 6, 395-401.

Bos, J. L., Polder, L. J., Bernards, R., Schrier, P. I., van den Elsen, P. J., van der Eb, A. J. & van Ormondt, H. (1981). The 2.2 kb E1b mRNA of human Ad12 and Ad5 codes for two tumor antigens starting at different AUG triplets. *Cell* 27, 121-131.

Bossis, G. & Melchior, F. (2006). SUMO: regulating the regulator. *Cell Div* 1, 13.

Bottomley, M. J., Collard, M. W., Huggenvik, J. I., Liu, Z., Gibson, T. J. & Sattler, M. (2001). The SAND domain structure defines a novel DNA-binding fold in transcriptional regulation. *Nat Struct Biol* 8, 626-633.

Boyer, J., Rohleder, K. & Ketner, G. (1999). Adenovirus E4 34k and E4 11k inhibit double strand break repair and are physically associated with the cellular DNA-dependent protein kinase. *Virology* 263, 307-312.

Bradford, M. M. (1976). A rapid and sensitive method for the quantitation of microgram quantities of protein utilizing the principle of protein-dye binding. *Anal Biochem* 72, 248-254.

Bridge, E. & Pettersson, U. (1995). Nuclear organization of replication and gene expression in adenovirus-infected cells. *Curr Top Microbiol Immunol* 199 (Pt 1), 99-117.

Buckwalter, S. P., Teo, R., Espy, M. J., Sloan, L. M., Smith, T. F. & Pritt, B. S. (2012). Real-time qualitative PCR for 57 human adenovirus types from multiple specimen sources. *J Clin Microbiol* 50, 766-771.

Burkham, J., Coen, D. M., Hwang, C. B. & Weller, S. K. (2001). Interactions of herpes simplex virus type 1 with ND10 and recruitment of PML to replication compartments. *J Virol* 75, 2353-2367.

Burkham, J., Coen, D. M. & Weller, S. K. (1998). ND10 protein PML is recruited to herpes simplex virus type 1 prereplicative sites and replication compartments in the presence of viral DNA polymerase. *J Virol* 72, 10100-10107.

Burnett, E., Christensen, J. & Tattersall, P. (2001). A consensus DNA recognition motif for two KDWK transcription factors identifies flexible-length, CpG-methylation sensitive cognate binding sites in the majority of human promoters. *J Mol Biol* 314, 1029-1039.

Carmo-Fonseca, M. (2002). The contribution of nuclear compartmentalization to gene regulation. *Cell* 108, 513-521.

Carrigan, D. R. (1997). Adenovirus infections in immunocompromised patients. *Am J Med* 102, 71-74.

Carvalho, T., Seeler, J. S., Ohman, K., Jordan, P., Pettersson, U., Akusjarvi, G., Carmo-Fonseca, M. & Dejean, A. (1995). Targeting of adenovirus E1A and E4-ORF3 proteins to nuclear matrix-associated PML bodies. *J Cell Biol* 131, 45-56.

Cathomen, T. & Weitzman, M. D. (2000). A functional complex of adenovirus proteins E1B-55kDa and E4orf6 is necessary to modulate the expression level of p53 but not its transcriptional activity. *J Virol* 74, 11407-11412.

Cerec, V., Glaise, D., Garnier, D., Morosan, S., Turlin, B., Drenou, B., Gripon, P., Kremsdorf, D., Guguen-Guillouzo, C. & Corlu, A. (2007). Transdifferentiation of hepatocyte-like cells from the human hepatoma HepaRG cell line through bipotent progenitor. *Hepatology* 45, 957-967.

Chang, K. S., Stass, S. A., Chu, D. T., Deaven, L. L., Trujillo, J. M. & Freireich, E. J. (1992). Characterization of a fusion cDNA (RARA/myl) transcribed from the t(15;17) translocation breakpoint in acute promyelocytic leukemia. *Mol Cell Biol* 12, 800-810.

Chee, A. V., Lopez, P., Pandolfi, P. P. & Roizman, B. (2003). Promyelocytic leukemia protein mediates interferon-based anti-herpes simplex virus 1 effects. *J Virol* 77, 7101-7105.

Chelbi-Alix, M. K. & de The, H. (1999). Herpes virus induced proteasome-dependent degradation of the nuclear bodies-associated PML and Sp100 proteins. *Oncogene* 18, 935-941.

Chelbi-Alix, M. K., Quignon, F., Pelicano, L., Koken, M. H. & de The, H. (1998). Resistance to virus infection conferred by the interferon-induced promyelocytic leukemia protein. *J Virol* 72, 1043-1051.

Condemine, W., Takahashi, Y., Zhu, J., Puvion-Dutilleul, F., Guegan, S., Janin, A. & de The, H. (2006). Characterization of endogenous human promyelocytic leukemia isoforms. *Cancer Res* 66, 6192-6198.

Cress, W. D. & Nevins, J. R. (1996). Use of the E2F transcription factor by DNA tumor virus regulatory proteins. *Curr Top Microbiol Immunol* 208, 63-78.

Cuchet, D., Sykes, A., Nicolas, A., Orr, A., Murray, J., Sirma, H., Heeren, J., Bartelt, A. & Everett, R. D. (2011). PML isoforms I and II participate in PML-dependent restriction of HSV-1 replication. *J Cell Sci* 124, 280-291.

Cuchet-Lourenco, D., Boutell, C., Lukashchuk, V., Grant, K., Sykes, A., Murray, J., Orr, A. & Everett, R. D. (2011). SUMO pathway dependent recruitment of cellular repressors to herpes simplex virus type 1 genomes. *PLoS Pathog* 7, e1002123.

Cuchet-Lourenco, D., Vanni, E., Glass, M., Orr, A. & Everett, R. D. (2012). Herpes simplex virus 1 ubiquitin ligase ICP0 interacts with PML isoform I and induces its SUMO-independent degradation. *J Virol* 86, 11209-11222.

Dallaire, F., Blanchette, P., Groitl, P., Dobner, T. & Branton, P. E. (2009). Identification of integrin alpha3 as a new substrate of the adenovirus E4orf6/E1B 55-kilodalton E3 ubiquitin ligase complex. *J Virol* 83, 5329-5338.

Davison, A. J., Benko, M. & Harrach, B. (2003). Genetic content and evolution of adenoviruses. *J Gen Virol* 84, 2895-2908.

Day, P. M., Baker, C. C., Lowy, D. R. & Schiller, J. T. (2004). Establishment of papillomavirus infection is enhanced by promyelocytic leukemia protein (PML) expression. *Proc Natl Acad Sci U S A* 101, 14252-14257.

De Jong, J. C., Wermenbol, A. G., Verweij-Uijterwaal, M. W., Slaterus, K. W., Wertheim-Van Dillen, P., Van Doornum, G. J., Khoo, S. H. & Hierholzer, J. C. (1999). Adenoviruses from human immunodeficiency virus-infected individuals, including two strains that represent new candidate serotypes Ad50 and Ad51 of species B1 and D, respectively. *J Clin Microbiol* 37, 3940-3945.

de Jong, R. N. & van der Vliet, P. C. (1999). Mechanism of DNA replication in eukaryotic cells: cellular host factors stimulating adenovirus DNA replication. *Gene* 236, 1-12.

de Stanchina, E., Querido, E., Narita, M., Davuluri, R. V., Pandolfi, P. P., Ferbeyre, G. & Lowe, S. W. (2004). PML is a direct p53 target that modulates p53 effector functions. *Mol Cell* 13, 523-535.

de The, H., Lavau, C., Marchio, A., Chomienne, C., Degos, L. & Dejean, A. (1991). The PML-RAR alpha fusion mRNA generated by the t(15;17) translocation in acute promyelocytic leukemia encodes a functionally altered RAR. *Cell* 66, 675-684.

Debbas, M. & White, E. (1993). Wild-type p53 mediates apoptosis by E1A, which is inhibited by E1B. *Genes Dev* 7, 546-554.

Dellaire, G. & Bazett-Jones, D. P. (2004). PML nuclear bodies: dynamic sensors of DNA damage and cellular stress. *Bioessays* 26, 963-977.

Dent, A. L., Yewdell, J., Puvion-Dutilleul, F., Koken, M. H., de The, H. & Staudt, L. M. (1996). LYSP100-associated nuclear domains (LANDs): description of a new class of subnuclear structures and their relationship to PML nuclear bodies. *Blood* 88, 1423-1426.

Desbois, C., Rousset, R., Bantignies, F. & Jalinot, P. (1996). Exclusion of Int-6 from PML nuclear bodies by binding to the HTLV-I Tax oncoprotein. *Science* 273, 951-953.

Deshaies, R. J. & Joazeiro, C. A. (2009). RING domain E3 ubiquitin ligases. *Annu Rev Biochem* 78, 399-434.

Desterro, J. M., Rodriguez, M. S., Kemp, G. D. & Hay, R. T. (1999). Identification of the enzyme required for activation of the small ubiquitin-like protein SUMO-1. *J Biol Chem* 274, 10618-10624.

Desterro, J. M., Thomson, J. & Hay, R. T. (1997). Ubch9 conjugates SUMO but not ubiquitin. *FEBS Lett* 417, 297-300.

Dinant, C. & Luijsterburg, M. S. (2009). The emerging role of HP1 in the DNA damage response. *Mol Cell Biol* 29, 6335-6340.

Djavani, M., Rodas, J., Lukashevich, I. S., Horejsh, D., Pandolfi, P. P., Borden, K. L. & Salvato, M. S. (2001). Role of the promyelocytic leukemia protein PML in the interferon sensitivity of lymphocytic choriomeningitis virus. *J Virol* 75, 6204-6208.

Dobbelstein, M., Roth, J., Kimberly, W. T., Levine, A. J. & Shenk, T. (1997). Nuclear export of the E1B 55-kDa and E4 34-kDa adenoviral oncoproteins mediated by a rev-like signal sequence. *Embo J* 16, 4276-4284.

Dobner, T., Horikoshi, N., Rubenwolf, S. & Shenk, T. (1996). Blockage by adenovirus E4orf6 of transcriptional activation by the p53 tumor suppressor. *Science* 272, 1470-1473.

Doucas, V., Ishov, A. M., Romo, A., Juguilon, H., Weitzman, M. D., Evans, R. M. & Maul, G. G. (1996). Adenovirus replication is coupled with the dynamic properties of the PML nuclear structure. *Genes Dev* 10, 196-207.

Duprez, E., Saurin, A. J., Desterro, J. M., Lallemand-Breitenbach, V., Howe, K., Boddy, M. N., Solomon, E., de The, H., Hay, R. T. & Freemont, P. S. (1999). SUMO-1 modification of the acute promyelocytic leukaemia protein PML: implications for nuclear localisation. *J Cell Sci* 112 (Pt 3), 381-393.

Dyck, J. A., Maul, G. G., Miller, W. H., Jr., Chen, J. D., Kakizuka, A. & Evans, R. M. (1994). A novel macromolecular structure is a target of the promyelocyte-retinoic acid receptor oncoprotein. *Cell* 76, 333-343.

Dyson, N., Guida, P., McCall, C. & Harlow, E. (1992). Adenovirus E1A makes two distinct contacts with the retinoblastoma protein. *J Virol* 66, 4606-4611.

Echendu, C. W. & Ling, P. D. (2008). Regulation of Sp100A subnuclear localization and transcriptional function by EBNA-LP and interferon. *J Interferon Cytokine Res* 28, 667-678.

El McHichi, B., Regad, T., Maroui, M. A., Rodriguez, M. S., Aminev, A., Gerbaud, S., Escriou, N., Dianoux, L. & Chelbi-Alix, M. K. (2010). SUMOylation promotes PML degradation during encephalomyocarditis virus infection. *J Virol* 84, 11634-11645.

Enders, J. F., Bell, J. A., Dingle, J. H., Francis, T., Jr., Hilleman, M. R., Huebner, R. J. & Payne, A. M. (1956). Adenoviruses: group name proposed for new respiratory-tract viruses. *Science* 124, 119-120.

Endter, C., Hartl, B., Spruss, T., Hauber, J. & Dobner, T. (2005). Blockage of CRM1-dependent nuclear export of the adenovirus type 5 early region 1B 55-kDa protein augments oncogenic transformation of primary rat cells. *Oncogene* 24, 55-64.

Endter, C., Kzhyshkowska, J., Stauber, R. & Dobner, T. (2001). SUMO-1 modification required for transformation by adenovirus type 5 early region 1B 55-kDa oncoprotein. *Proc Natl Acad Sci U S A* 98, 11312-11317.

Eskiw, C. H., Dellaire, G. & Bazett-Jones, D. P. (2004). Chromatin contributes to structural integrity of promyelocytic leukemia bodies through a SUMO-1-independent mechanism. *J Biol Chem* 279, 9577-9585.

Eskiw, C. H., Dellaire, G., Mymryk, J. S. & Bazett-Jones, D. P. (2003). Size, position and dynamic behavior of PML nuclear bodies following cell stress as a paradigm for supramolecular trafficking and assembly. *J Cell Sci* 116, 4455-4466.

Evans, J. D. & Hearing, P. (2005). Relocalization of the Mre11-Rad50-Nbs1 complex by the adenovirus E4 ORF3 protein is required for viral replication. *J Virol* 79, 6207-6215.

Everett, R. D. (2001). DNA viruses and viral proteins that interact with PML nuclear bodies. *Oncogene* 20, 7266-7273.

Everett, R. D. (2013). The spatial organization of DNA virus genomes in the nucleus. *PLoS Pathog* 9, e1003386.

Everett, R. D. & Chelbi-Alix, M. K. (2007). PML and PML nuclear bodies: implications in antiviral defence. *Biochimie* 89, 819-830.

Everett, R. D., Freemont, P., Saitoh, H., Dasso, M., Orr, A., Kathoria, M. & Parkinson, J. (1998). The disruption of ND10 during herpes simplex virus infection correlates with the Vmw110- and proteasome-dependent loss of several PML isoforms. *J Virol* 72, 6581-6591.

Everett, R. D., Lomonte, P., Sternsdorf, T., van Driel, R. & Orr, A. (1999). Cell cycle regulation of PML modification and ND10 composition. *J Cell Sci* 112 (Pt 24), 4581-4588.

Everett, R. D. & Maul, G. G. (1994). HSV-1 IE protein Vmw110 causes redistribution of PML. *Embo J* 13, 5062-5069.

Everett, R. D., Parada, C., Gripon, P., Sirma, H. & Orr, A. (2008). Replication of ICP0-null mutant herpes simplex virus type 1 is restricted by both PML and Sp100. *J Virol* 82, 2661-2672.

Everett, R. D., Rechter, S., Papior, P., Tavalai, N., Stamminger, T. & Orr, A. (2006). PML contributes to a cellular mechanism of repression of herpes simplex virus type 1 infection that is inactivated by ICP0. *J Virol* 80, 7995-8005.

Everett, R. D. & Zafiropoulos, A. (2004). Visualization by live-cell microscopy of disruption of ND10 during herpes simplex virus type 1 infection. *J Virol* 78, 11411-11415.

Everitt, E., Lutter, L. & Philipson, L. (1975). Structural proteins of adenoviruses. XII. Location and neighbor relationship among proteins of adenovirion type 2 as revealed by enzymatic iodination, immunoprecipitation and chemical cross-linking. *Virology* 67, 197-208.

Everitt, E., Sundquist, B., Pettersson, U. & Philipson, L. (1973). Structural proteins of adenoviruses. X. Isolation and topography of low molecular weight antigens from the virion of adenovirus type 2. *Virology* 52, 130-147.

Fagioli, M., Alcalay, M., Pandolfi, P. P., Venturini, L., Mencarelli, A., Simeone, A., Acampora, D., Grignani, F. & Pelicci, P. G. (1992). Alternative splicing of PML transcripts predicts coexpression of several carboxy-terminally different protein isoforms. *Oncogene* 7, 1083-1091.

Fattaey, A. R., Harlow, E. & Helin, K. (1993). Independent regions of adenovirus E1A are required for binding to and dissociation of E2F-protein complexes. *Mol Cell Biol* 13, 7267-7277.

Ferbeyre, G., de Stanchina, E., Querido, E., Baptiste, N., Prives, C. & Lowe, S. W. (2000). PML is induced by oncogenic ras and promotes premature senescence. *Genes Dev* 14, 2015-2027.

Ferrari, R., Berk, A. J. & Kurdistani, S. K. (2009). Viral manipulation of the host epigenome for oncogenic transformation. *Nat Rev Genet* 10, 290-294.

Ferrari, R., Pellegrini, M., Horwitz, G. A., Xie, W., Berk, A. J. & Kurdistani, S. K. (2008). Epigenetic reprogramming by adenovirus e1a. *Science* 321, 1086-1088.

Fish, P. V., Filippakopoulos, P., Bish, G., Brennan, P. E., Bunnage, M. E., Cook, A. S., Federov, O., Gerstenberger, B. S., Jones, H., Knapp, S., Marsden, B., Nocka, K., Owen, D. R., Philpott, M., Picaud, S., Primiano, M. J., Ralph, M. J., Sciammetta, N. & Trzupek, J. D. (2012). Identification of a chemical probe for bromo and extra C-terminal bromodomain inhibition through optimization of a fragment-derived hit. *J Med Chem* 55, 9831-9837.

Flint, J. & Shenk, T. (1989). Adenovirus E1A protein paradigm viral transactivator. *Annu Rev Genet* 23, 141-161.

Florin, L., Schafer, F., Sotlar, K., Streeck, R. E. & Sapp, M. (2002). Reorganization of nuclear domain 10 induced by papillomavirus capsid protein l2. *Virology* 295, 97-107.

Forrester, N. A., Patel, R. N., Speiseder, T., Groitl, P., Sedgwick, G. G., Shimwell, N. J., Seed, R. I., Catnaigh, P. O., McCabe, C. J., Stewart, G. S., Dobner, T., Grand, R. J., Martin, A. & Turnell, A. S. (2012). Adenovirus E4orf3 targets Transcriptional Intermediary Factor 1gamma for proteasome-dependent degradation during infection. *J Virol.*

Frisch, S. M. & Mymryk, J. S. (2002). Adenovirus-5 E1A: paradox and paradigm. *Nat Rev Mol Cell Biol* 3, 441-452.

Full, F., Reuter, N., Zielke, K., Stamminger, T. & Ensser, A. (2012). Herpesvirus saimiri antagonizes nuclear domain 10-instituted intrinsic immunity via an ORF3-mediated selective degradation of cellular protein Sp100. *J Virol* 86, 3541-3553.

Gaggar, A., Shayakhmetov, D. M. & Lieber, A. (2003). CD46 is a cellular receptor for group B adenoviruses. *Nat Med* 9, 1408-1412.

Gallimore, P. H. & Turnell, A. S. (2001). Adenovirus E1A: remodelling the host cell, a life or death experience. *Oncogene* 20, 7824-7835.

Garcia, C. C., Topisirovic, I., Djavani, M., Borden, K. L., Damonte, E. B. & Salvato, M. S. (2010). An antiviral disulfide compound blocks interaction between arenavirus Z protein and cellular promyelocytic leukemia protein. *Biochem Biophys Res Commun* 393, 625-630.

Gasparovic, M. L., Maginnis, M. S., O'Hara, B. A., Dugan, A. S. & Atwood, W. J. (2009). Modulation of PML protein expression regulates JCV infection. *Virology* 390, 279-288.

Gaydos, C. A. & Gaydos, J. C. (1995). Adenovirus vaccines in the U.S. military. *Mil Med* 160, 300-304.

Geiss-Friedlander, R. & Melchior, F. (2007). Concepts in sumoylation: a decade on. *Nat Rev Mol Cell Biol* 8, 947-956.

Geoffroy, M. C. & Chelbi-Alix, M. K. (2011). Role of promyelocytic leukemia protein in host antiviral defense. *J Interferon Cytokine Res* 31, 145-158.

Geoffroy, M. C., Jaffray, E. G., Walker, K. J. & Hay, R. T. (2010). Arsenic-induced SUMO-dependent recruitment of RNF4 into PML nuclear bodies. *Mol Biol Cell* 21, 4227-4239.

Glass, M. & Everett, R. D. (2013). Components of promyelocytic leukemia nuclear bodies (ND10) act cooperatively to repress herpesvirus infection. *J Virol* 87, 2174-2185.

Goodman, R. H. & Smolik, S. (2000). CBP/p300 in cell growth, transformation, and development. *Genes Dev* 14, 1553-1577.

Goodrum, F. D., Shenk, T. & Ornelles, D. A. (1996). Adenovirus early region 4 34-kilodalton protein directs the nuclear localization of the early region 1B 55-kilodalton protein in primate cells. *J Virol* 70, 6323-6335.

Gorisch, S. M., Wachsmuth, M., Ittrich, C., Bacher, C. P., Rippe, K. & Lichter, P. (2004). Nuclear body movement is determined by chromatin accessibility and dynamics. *Proc Natl Acad Sci U S A* 101, 13221-13226.

Graham, F. L., Smiley, J., Russell, W. C. & Nairn, R. (1977). Characteristics of a human cell line transformed by DNA from human adenovirus type 5. *J Gen Virol* 36, 59-74.

Gray, G. C., Goswami, P. R., Malasig, M. D., Hawksworth, A. W., Trump, D. H., Ryan, M. A. & Schnurr, D. P. (2000). Adult adenovirus infections: loss of orphaned vaccines precipitates military respiratory disease epidemics. For the Adenovirus Surveillance Group. *Clin Infect Dis* 31, 663-670.

Greber, U. F., Willetts, M., Webster, P. & Helenius, A. (1993). Stepwise dismantling of adenovirus 2 during entry into cells. *Cell* 75, 477-486.

Gripon, P., Rumin, S., Urban, S., Le Seyec, J., Glaise, D., Cannie, I., Guyomard, C., Lucas, J., Trepo, C. & Guguen-Guillouzo, C. (2002). Infection of a human hepatoma cell line by hepatitis B virus. *Proc Natl Acad Sci U S A* 99, 15655-15660.

Grotzinger, T., Sternsdorf, T., Jensen, K. & Will, H. (1996). Interferon-modulated expression of genes encoding the nuclear-dot-associated proteins Sp100 and promyelocytic leukemia protein (PML). *Eur J Biochem* 238, 554-560.

Guccione, E., Lethbridge, K. J., Killick, N., Leppard, K. N. & Banks, L. (2004). HPV E6 proteins interact with specific PML isoforms and allow distinctions to be made between different POD structures. *Oncogene* 23, 4662-4672.

Guldner, H. H., Szostecki, C., Grotzinger, T. & Will, H. (1992). IFN enhance expression of Sp100, an autoantigen in primary biliary cirrhosis. *J Immunol* 149, 4067-4073.

Guldner, H. H., Szostecki, C., Schroder, P., Matschl, U., Jensen, K., Luders, C., Will, H. & Sternsdorf, T. (1999). Splice variants of the nuclear dot-associated Sp100 protein contain homologies to HMG-1 and a human nuclear phosphoprotein-box motif. *J Cell Sci* 112 (Pt 5), 733-747.

Gupta, A., Jha, S., Engel, D. A., Ornelles, D. A. & Dutta, A. (2013). Tip60 degradation by adenovirus relieves transcriptional repression of viral transcriptional activator EIA. *Oncogene* 32, 5017-5025.

Gurrieri, C., Capodieci, P., Bernardi, R., Scaglioni, P. P., Nafa, K., Rush, L. J., Verbel, D. A., Cordon-Cardo, C. & Pandolfi, P. P. (2004). Loss of the tumor suppressor PML in human cancers of multiple histologic origins. *J Natl Cancer Inst* 96, 269-279.

Halbert, D. N., Cutt, J. R. & Shenk, T. (1985). Adenovirus early region 4 encodes functions required for efficient DNA replication, late gene expression, and host cell shutoff. *J Virol* 56, 250-257.

Hamamori, Y., Sartorelli, V., Ogryzko, V., Puri, P. L., Wu, H. Y., Wang, J. Y., Nakatani, Y. & Kedes, L. (1999). Regulation of histone acetyltransferases p300 and PCAF by the bHLH protein twist and adenoviral oncoprotein E1A. *Cell* 96, 405-413.

Hanahan, D. & Meselson, M. (1983). Plasmid screening at high colony density. *Methods Enzymol* 100, 333-342.

Harada, J. N., Shevchenko, A., Pallas, D. C. & Berk, A. J. (2002). Analysis of the adenovirus E1B-55K-anchored proteome reveals its link to ubiquitination machinery. *J Virol* 76, 9194-9206.

Harlow, E., Franza, B. R., Jr. & Schley, C. (1985). Monoclonal antibodies specific for adenovirus early region 1A proteins: extensive heterogeneity in early region 1A products. *J Virol* 55, 533-546.

Harpst, J. A., Ennever, J. F. & Russell, W. C. (1977). Physical properties of nucleoprotein cores from adenovirus type 5. *Nucleic Acids Res* 4, 477-490.

Hartl, B., Zeller, T., Blanchette, P., Kremmer, E. & Dobner, T. (2008). Adenovirus type 5 early region 1B 55-kDa oncoprotein can promote cell transformation by a mechanism independent from blocking p53-activated transcription. *Oncogene* 27, 3673-3684.

Hay, R. T. (2005). SUMO: a history of modification. *Mol Cell* 18, 1-12.

Hay, R. T. (2006). Role of ubiquitin-like proteins in transcriptional regulation. *Ernst Schering Res Found Workshop*, 173-192.

Hay, R. T. (2007). SUMO-specific proteases: a twist in the tail. *Trends Cell Biol* 17, 370-376.

Herzer, K., Weyer, S., Krammer, P. H., Galle, P. R. & Hofmann, T. G. (2005). Hepatitis C virus core protein inhibits tumor suppressor protein promyelocytic leukemia function in human hepatoma cells. *Cancer Res* 65, 10830-10837.

Heun, P. (2007). SUMOrganization of the nucleus. *Curr Opin Cell Biol* 19, 350-355.

Hilleman, M. R. & Werner, J. H. (1954). Recovery of new agent from patients with acute respiratory illness. *Proc Soc Exp Biol Med* 85, 183-188.

Hindley, C. E., Davidson, A. D. & Matthews, D. A. (2007). Relationship between adenovirus DNA replication proteins and nucleolar proteins B23.1 and B23.2. *J Gen Virol* 88, 3244-3248.

Hodges, M., Tissot, C., Howe, K., Grimwade, D. & Freemont, P. S. (1998). Structure, organization, and dynamics of promyelocytic leukemia protein nuclear bodies. *Am J Hum Genet* 63, 297-304.

Hofmann, H., Sindre, H. & Stamminger, T. (2002). Functional interaction between the pp71 protein of human cytomegalovirus and the PML-interacting protein human Daxx. *J Virol* 76, 5769-5783.

Hoppe, A., Beech, S. J., Dimmock, J. & Leppard, K. N. (2006). Interaction of the adenovirus type 5 E4 Orf3 protein with promyelocytic leukemia protein isoform II is required for ND10 disruption. *J Virol* 80, 3042-3049.

Houweling, A., van den Elsen, P. J. & van der Eb, A. J. (1980). Partial transformation of primary rat cells by the leftmost 4.5% fragment of adenovirus 5 DNA. *Virology* 105, 537-550.

Huang, M. M. & Hearing, P. (1989). Adenovirus early region 4 encodes two gene products with redundant effects in lytic infection. *J Virol* 63, 2605-2615.

Ikeda, M. A. & Nevins, J. R. (1993). Identification of distinct roles for separate E1A domains in disruption of E2F complexes. *Mol Cell Biol* 13, 7029-7035.

Iki, S., Yokota, S., Okabayashi, T., Yokosawa, N., Nagata, K. & Fujii, N. (2005). Serum-dependent expression of promyelocytic leukemia protein suppresses propagation of influenza virus. *Virology* 343, 106-115.

Isaac, A., Wilcox, K. W. & Taylor, J. L. (2006). SP100B, a repressor of gene expression preferentially binds to DNA with unmethylated CpGs. *J Cell Biochem* 98, 1106-1122.

Ishov, A. M. & Maul, G. G. (1996). The periphery of nuclear domain 10 (ND10) as site of DNA virus deposition. *J Cell Biol* 134, 815-826.

Ishov, A. M., Sotnikov, A. G., Negorev, D., Vladimirova, O. V., Neff, N., Kamitani, T., Yeh, E. T., Strauss, J. F., 3rd & Maul, G. G. (1999). PML is critical for ND10 formation and recruits the

PML-interacting protein daxx to this nuclear structure when modified by SUMO-1. *J Cell Biol* 147, 221-234.

Ishov, A. M., Stenberg, R. M. & Maul, G. G. (1997). Human cytomegalovirus immediate early interaction with host nuclear structures: definition of an immediate transcript environment. *J Cell Biol* 138, 5-16.

Izumiya, Y., Kobayashi, K., Kim, K. Y., Pochampalli, M., Izumiya, C., Shevchenko, B., Wang, D. H., Huerta, S. B., Martinez, A., Campbell, M. & Kung, H. J. (2013). Kaposi's Sarcoma-Associated Herpesvirus K-Rta Exhibits SUMO-Targeting Ubiquitin Ligase (STUbL) Like Activity and Is Essential for Viral Reactivation. *PLoS Pathog* 9, e1003506.

Jawetz, E. (1959). The story of shipyard eye. *Br Med J* 1, 873-876.

Jensen, K., Shiels, C. & Freemont, P. S. (2001). PML protein isoforms and the RBCC/TRIM motif. *Oncogene* 20, 7223-7233.

Jiang, M., Entezami, P., Gamez, M., Stamminger, T. & Imperiale, M. J. (2011). Functional reorganization of promyelocytic leukemia nuclear bodies during BK virus infection. *MBio* 2, e00281-00210.

Jiang, W. Q., Szekely, L., Klein, G. & Ringertz, N. (1996). Intranuclear redistribution of SV40T, p53, and PML in a conditionally SV40T-immortalized cell line. *Exp Cell Res* 229, 289-300.

Johnson, E. S. & Blobel, G. (1997). Ubc9p is the conjugating enzyme for the ubiquitin-like protein Smt3p. *J Biol Chem* 272, 26799-26802.

Johnson, E. S., Schwienhorst, I., Dohmen, R. J. & Blobel, G. (1997). The ubiquitin-like protein Smt3p is activated for conjugation to other proteins by an Aos1p/Uba2p heterodimer. *Embo J* 16, 5509-5519.

Jul-Larsen, A., Visted, T., Karlsen, B. O., Rinaldo, C. H., Bjerkvig, R., Lonning, P. E. & Boe, S. O. (2004). PML-nuclear bodies accumulate DNA in response to polyomavirus BK and simian virus 40 replication. *Exp Cell Res* 298, 58-73.

Kakizuka, A., Miller, W. H., Jr., Umesono, K., Warrell, R. P., Jr., Frankel, S. R., Murty, V. V., Dmitrovsky, E. & Evans, R. M. (1991). Chromosomal translocation t(15;17) in human acute promyelocytic leukemia fuses RAR alpha with a novel putative transcription factor, PML. *Cell* 66, 663-674.

Kao, C. C., Yew, P. R. & Berk, A. J. (1990). Domains required for in vitro association between the cellular p53 and the adenovirus 2 E1B 55K proteins. *Virology* 179, 806-814.

Katano, H., Ogawa-Goto, K., Hasegawa, H., Kurata, T. & Sata, T. (2001). Human-herpesvirus-8-encoded K8 protein colocalizes with the promyelocytic leukemia protein (PML) bodies and recruits p53 to the PML bodies. *Virology* 286, 446-455.

Kaukinen, P., Vaheri, A. & Plyusnin, A. (2005). Hantavirus nucleocapsid protein: a multifunctional molecule with both housekeeping and ambassadorial duties. *Arch Virol* 150, 1693-1713.

Kentsis, A., Gordon, R. E. & Borden, K. L. (2002). Self-assembly properties of a model RING domain. *Proc Natl Acad Sci U S A* 99, 667-672.

Kerscher, O., Felberbaum, R. & Hochstrasser, M. (2006). Modification of proteins by ubiquitin and ubiquitin-like proteins. *Annu Rev Cell Dev Biol* 22, 159-180.

Kiesslich, A., von Mikecz, A. & Hemmerich, P. (2002). Cell cycle-dependent association of PML bodies with sites of active transcription in nuclei of mammalian cells. *J Struct Biol* 140, 167-179.

Kim, Y. E., Lee, J. H., Kim, E. T., Shin, H. J., Gu, S. Y., Seol, H. S., Ling, P. D., Lee, C. H. & Ahn, J. H. (2011). Human cytomegalovirus infection causes degradation of Sp100 proteins that suppress viral gene expression. *J Virol* 85, 11928-11937.

Kimelman, D., Miller, J. S., Porter, D. & Roberts, B. E. (1985). E1a regions of the human adenoviruses and of the highly oncogenic simian adenovirus 7 are closely related. *J Virol* 53, 399-409.

Kindsmuller, K., Groitl, P., Hartl, B., Blanchette, P., Hauber, J. & Dobner, T. (2007). Intranuclear targeting and nuclear export of the adenovirus E1B-55K protein are regulated by SUMO1 conjugation. *Proc Natl Acad Sci U S A* 104, 6684-6689.

Kindsmuller, K., Schreiner, S., Leinenkugel, F., Groitl, P., Kremmer, E. & Dobner, T. (2009). A 49-kilodalton isoform of the adenovirus type 5 early region 1B 55-kilodalton protein is sufficient to support virus replication. *J Virol* 83, 9045-9056.

Koken, M. H., Puvion-Dutilleul, F., Guillemin, M. C., Viron, A., Linares-Cruz, G., Stuurman, N., de Jong, L., Szostecki, C., Calvo, F., Chomienne, C. & et al. (1994). The t(15;17) translocation alters a nuclear body in a retinoic acid-reversible fashion. *Embo J* 13, 1073-1083.

Konig, C., Roth, J. & Dobbelstein, M. (1999). Adenovirus type 5 E4orf3 protein relieves p53 inhibition by E1B-55-kilodalton protein. *J Virol* 73, 2253-2262.

Korioth, F., Maul, G. G., Plachter, B., Stamminger, T. & Frey, J. (1996). The nuclear domain 10 (ND10) is disrupted by the human cytomegalovirus gene product IE1. *Exp Cell Res* 229, 155-158.

Kratzer, F., Rosorius, O., Heger, P., Hirschmann, N., Dobner, T., Hauber, J. & Stauber, R. H. (2000). The adenovirus type 5 E1B-55K oncoprotein is a highly active shuttle protein and shuttling is independent of E4orf6, p53 and Mdm2. *Oncogene* 19, 850-857.

Kyratsous, C. A. & Silverstein, S. J. (2009). Components of nuclear domain 10 bodies regulate varicella-zoster virus replication. *J Virol* 83, 4262-4274.

Lallemand-Breitenbach, V., Jeanne, M., Benhenda, S., Nasr, R., Lei, M., Peres, L., Zhou, J., Zhu, J., Raught, B. & de The, H. (2008). Arsenic degrades PML or PML-RARalpha through a SUMO-triggered RNF4/ubiquitin-mediated pathway. *Nat Cell Biol* 10, 547-555.

LaMorte, V. J., Dyck, J. A., Ochs, R. L. & Evans, R. M. (1998). Localization of nascent RNA and CREB binding protein with the PML-containing nuclear body. *Proc Natl Acad Sci U S A* 95, 4991-4996.

Lang, M., Jegou, T., Chung, I., Richter, K., Munch, S., Udvarhelyi, A., Cremer, C., Hemmerich, P., Engelhardt, J., Hell, S. W. & Rippe, K. (2010). Three-dimensional organization of promyelocytic leukemia nuclear bodies. *J Cell Sci* 123, 392-400.

Lavau, C., Marchio, A., Fagioli, M., Jansen, J., Falini, B., Lebon, P., Grosveld, F., Pandolfi, P. P., Pelicci, P. G. & Dejean, A. (1995). The acute promyelocytic leukaemia-associated PML gene is induced by interferon. *Oncogene* 11, 871-876.

Lawrence, F. J., McStay, B. & Matthews, D. A. (2006). Nucleolar protein upstream binding factor is sequestered into adenovirus DNA replication centres during infection without affecting RNA polymerase I location or ablating rRNA synthesis. *J Cell Sci* 119, 2621-2631.

Ledl, A., Schmidt, D. & Muller, S. (2005). Viral oncoproteins E1A and E7 and cellular LxCxE proteins repress SUMO modification of the retinoblastoma tumor suppressor. *Oncogene* 24, 3810-3818.

Lee, H. R., Kim, D. J., Lee, J. M., Choi, C. Y., Ahn, B. Y., Hayward, G. S. & Ahn, J. H. (2004). Ability of the human cytomegalovirus IE1 protein to modulate sumoylation of PML correlates with its functional activities in transcriptional regulation and infectivity in cultured fibroblast cells. *J Virol* 78, 6527-6542.

Lehming, N., Le Saux, A., Schuller, J. & Ptashne, M. (1998). Chromatin components as part of a putative transcriptional repressing complex. *Proc Natl Acad Sci U S A* 95, 7322-7326.

Leppard, K. N., Emmott, E., Cortese, M. S. & Rich, T. (2009). Adenovirus type 5 E4 Orf3 protein targets promyelocytic leukaemia (PML) protein nuclear domains for disruption via a sequence in PML isoform II that is predicted as a protein interaction site by bioinformatic analysis. *J Gen Virol* 90, 95-104.

Leppard, K. N. & Everett, R. D. (1999). The adenovirus type 5 E1b 55K and E4 Orf3 proteins associate in infected cells and affect ND10 components. *J Gen Virol* 80 (Pt 4), 997-1008.

Lethbridge, K. J., Scott, G. E. & Leppard, K. N. (2003). Nuclear matrix localization and SUMO-1 modification of adenovirus type 5 E1b 55K protein are controlled by E4 Orf6 protein. *J Gen Virol* 84, 259-268.

Li, X. D., Makela, T. P., Guo, D., Soliymani, R., Koistinen, V., Vapalahti, O., Vaheri, A. & Lankinen, H. (2002). Hantavirus nucleocapsid protein interacts with the Fas-mediated apoptosis enhancer Daxx. *J Gen Virol* 83, 759-766.

Lin, Z., Yemelyanova, A. V., Gambhira, R., Jagu, S., Meyers, C., Kirnbauer, R., Ronnett, B. M., Gravitt, P. E. & Roden, R. B. (2009). Expression pattern and subcellular localization of human papillomavirus minor capsid protein L2. *Am J Pathol* 174, 136-143.

Ling, P. D., Peng, R. S., Nakajima, A., Yu, J. H., Tan, J., Moses, S. M., Yang, W. H., Zhao, B., Kieff, E., Bloch, K. D. & Bloch, D. B. (2005). Mediation of Epstein-Barr virus EBNA-LP transcriptional coactivation by Sp100. *Embo J* 24, 3565-3575.

Liu, F. & Green, M. R. (1994). Promoter targeting by adenovirus E1a through interaction with different cellular DNA-binding domains. *Nature* 368, 520-525.

Liu, Y., Colosimo, A. L., Yang, X. J. & Liao, D. (2000). Adenovirus E1B 55-kilodalton oncoprotein inhibits p53 acetylation by PCAF. *Mol Cell Biol* 20, 5540-5553.

Liu, Y., Shevchenko, A. & Berk, A. J. (2005). Adenovirus exploits the cellular aggresome response to accelerate inactivation of the MRN complex. *J Virol* 79, 14004-14016.

Louie, J. K., Kajon, A. E., Holodniy, M., Guardia-LaBar, L., Lee, B., Petru, A. M., Hacker, J. K. & Schnurr, D. P. (2008). Severe pneumonia due to adenovirus serotype 14: a new respiratory threat? *Clin Infect Dis* 46, 421-425.

Louria-Hayon, I., Alsheich-Bartok, O., Levav-Cohen, Y., Silberman, I., Berger, M., Grossman, T., Matentzoglu, K., Jiang, Y. H., Muller, S., Scheffner, M., Haupt, S. & Haupt, Y. (2009). E6AP promotes the degradation of the PML tumor suppressor. *Cell Death Differ* 16, 1156-1166.

Lukashchuk, V. & Everett, R. D. (2010). Regulation of ICP0-null mutant herpes simplex virus type 1 infection by ND10 components ATRX and hDaxx. *J Virol* 84, 4026-4040.

Marcos-Villar, L., Lopitz-Otsoa, F., Gallego, P., Munoz-Fontela, C., Gonzalez-Santamaria, J., Campagna, M., Shou-Jiang, G., Rodriguez, M. S. & Rivas, C. (2009). Kaposi's sarcoma-associated herpesvirus protein LANA2 disrupts PML oncogenic domains and inhibits PML-mediated transcriptional repression of the survivin gene. *J Virol* 83, 8849-8858.

Maroui, M. A., Pampin, M. & Chelbi-Alix, M. K. (2011). Promyelocytic leukemia isoform IV confers resistance to encephalomyocarditis virus via the sequestration of 3D polymerase in nuclear bodies. *J Virol* 85, 13164-13173.

Martin, M. E. & Berk, A. J. (1998). Adenovirus E1B 55K represses p53 activation in vitro. *J Virol* 72, 3146-3154.

Marton, M. J., Baim, S. B., Ornelles, D. A. & Shenk, T. (1990). The adenovirus E4 17-kilodalton protein complexes with the cellular transcription factor E2F, altering its DNA-binding properties and stimulating E1A-independent accumulation of E2 mRNA. *J Virol* 64, 2345-2359.

Mathias, P., Wickham, T., Moore, M. & Nemerow, G. (1994). Multiple adenovirus serotypes use alpha v integrins for infection. *J Virol* 68, 6811-6814.

Maul, G. G. (1998). Nuclear domain 10, the site of DNA virus transcription and replication. *Bioessays* 20, 660-667.

Maul, G. G. & Everett, R. D. (1994). The nuclear location of PML, a cellular member of the C3HC4 zinc-binding domain protein family, is rearranged during herpes simplex virus infection by the C3HC4 viral protein ICP0. *J Gen Virol* 75 (Pt 6), 1223-1233.

Maul, G. G., Guldner, H. H. & Spivack, J. G. (1993). Modification of discrete nuclear domains induced by herpes simplex virus type 1 immediate early gene 1 product (ICP0). *J Gen Virol* 74 (Pt 12), 2679-2690.

Maul, G. G., Ishov, A. M. & Everett, R. D. (1996). Nuclear domain 10 as preexisting potential replication start sites of herpes simplex virus type-1. *Virology* 217, 67-75.

Mautner, V., Steinthorsdottir, V. & Bailey, A. (1995). Enteric adenoviruses. *Curr Top Microbiol Immunol* 199 (Pt 3), 229-282.

Melchior, F. (2000). SUMO--nonclassical ubiquitin. *Annu Rev Cell Dev Biol* 16, 591-626.

Melnick, A. & Licht, J. D. (1999). Deconstructing a disease: RARalpha, its fusion partners, and their roles in the pathogenesis of acute promyelocytic leukemia. *Blood* 93, 3167-3215.

Meredith, M., Orr, A., Elliott, M. & Everett, R. (1995). Separation of sequence requirements for HSV-1 Vmw110 multimerisation and interaction with a 135-kDa cellular protein. *Virology* 209, 174-187.

Misteli, T. (2001). Protein dynamics: implications for nuclear architecture and gene expression. *Science* 291, 843-847.

Mitsudomi, T., Oyama, T., Gazdar, A. F., Minna, J. D., Okabayashi, K. & Shirakusa, T. (1992). [Mutations of ras and p53 genes in human non-small cell lung cancer cell lines and their clinical significance]. *Nihon Geka Gakkai Zasshi* 93, 944-947.

Moller, A. & Schmitz, M. L. (2003). Viruses as hijackers of PML nuclear bodies. *Arch Immunol Ther Exp (Warsz)* 51, 295-300.

Muller, S. & Dejean, A. (1999). Viral immediate-early proteins abrogate the modification by SUMO-1 of PML and Sp100 proteins, correlating with nuclear body disruption. *J Virol* 73, 5137-5143.

Muller, S. & Dobner, T. (2008). The adenovirus E1B-55K oncoprotein induces SUMO modification of p53. *Cell Cycle* 7, 754-758.

Muller, S., Matunis, M. J. & Dejean, A. (1998). Conjugation with the ubiquitin-related modifier SUMO-1 regulates the partitioning of PML within the nucleus. *Embo J* 17, 61-70.

Nakahara, T. & Lambert, P. F. (2007). Induction of promyelocytic leukemia (PML) oncogenic domains (PODs) by papillomavirus. *Virology* 366, 316-329.

Nardozza, T. A., Quigley, M. M. & Getzenberg, R. H. (1996). Association of transcription factors with the nuclear matrix. *J Cell Biochem* 61, 467-477.

Negorev, D. & Maul, G. G. (2001). Cellular proteins localized at and interacting within ND10/PML nuclear bodies/PODs suggest functions of a nuclear depot. *Oncogene* 20, 7234-7242.

Negorev, D. G., Vladimirova, O. V., Ivanov, A., Rauscher, F., 3rd & Maul, G. G. (2006). Differential role of Sp100 isoforms in interferon-mediated repression of herpes simplex virus type 1 immediate-early protein expression. *J Virol* 80, 8019-8029.

Negorev, D. G., Vladimirova, O. V. & Maul, G. G. (2009). Differential functions of interferon-upregulated Sp100 isoforms: herpes simplex virus type 1 promoter-based immediate-early gene suppression and PML protection from ICP0-mediated degradation. *J Virol* 83, 5168-5180.

Nemerow, G. R., Pache, L., Reddy, V. & Stewart, P. L. (2009). Insights into adenovirus host cell interactions from structural studies. *Virology* 384, 380-388.

Netsawang, J., Noisakran, S., Puttikhunt, C., Kasinrerk, W., Wongwiwat, W., Malasit, P., Yenchitsomanus, P. T. & Limjindaporn, T. (2010). Nuclear localization of dengue virus capsid protein is required for DAXX interaction and apoptosis. *Virus Res* 147, 275-283.

Nevels, M., Rubenwolf, S., Spruss, T., Wolf, H. & Dobner, T. (1997). The adenovirus E4orf6 protein can promote E1A/E1B-induced focus formation by interfering with p53 tumor suppressor function. *Proc Natl Acad Sci U S A* 94, 1206-1211.

Nevels, M., Tauber, B., Kremmer, E., Spruss, T., Wolf, H. & Dobner, T. (1999). Transforming potential of the adenovirus type 5 E4orf3 protein. *J Virol* 73, 1591-1600.

Nevins, J. R. & Darnell, J. E. (1978). Groups of adenovirus type 2 mRNA's derived from a large primary transcript: probable nuclear origin and possible common 3' ends. *J Virol* 25, 811-823.

Nevins, J. R., Ginsberg, H. S., Blanchard, J. M., Wilson, M. C. & Darnell, J. E., Jr. (1979). Regulation of the primary expression of the early adenovirus transcription units. *J Virol* **32, 727-733.**

Newhart, A., Negorev, D. G., Rafalska-Metcalf, I. U., Yang, T., Maul, G. G. & Janicki, S. M. (2013). Sp100A promotes chromatin decondensation at a cytomegalovirus-promoter-regulated transcription site. *Mol Biol Cell* **24, 1454-1468.**

Nisole, S., Maroui, M. A., Mascle, X. H., Aubry, M. & Chelbi-Alix, M. K. (2013). Differential Roles of PML Isoforms. *Front Oncol* **3, 125.**

Nojima, T., Oshiro-Ideue, T., Nakanoya, H., Kawamura, H., Morimoto, T., Kawaguchi, Y., Kataoka, N. & Hagiwara, M. (2009). Herpesvirus protein ICP27 switches PML isoform by altering mRNA splicing. *Nucleic Acids Res* **37, 6515-6527.**

Okuma, T., Honda, R., Ichikawa, G., Tsumagari, N. & Yasuda, H. (1999). In vitro SUMO-1 modification requires two enzymatic steps, E1 and E2. *Biochem Biophys Res Commun* **254, 693-698.**

Orazio, N. I., Naeger, C. M., Karlseder, J. & Weitzman, M. D. (2011). The adenovirus E1b55K/E4orf6 complex induces degradation of the Bloom helicase during infection. *J Virol* **85, 1887-1892.**

Orlando, J. S. & Ornelles, D. A. (1999). An arginine-faced amphipathic alpha helix is required for adenovirus type 5 e4orf6 protein function. *J Virol* **73, 4600-4610.**

Ornelles, D. A. & Shenk, T. (1991). Localization of the adenovirus early region 1B 55-kilodalton protein during lytic infection: association with nuclear viral inclusions requires the early region 4 34-kilodalton protein. *J Virol* **65, 424-429.**

Owerbach, D., McKay, E. M., Yeh, E. T., Gabbay, K. H. & Bohren, K. M. (2005). A proline-90 residue unique to SUMO-4 prevents maturation and sumoylation. *Biochem Biophys Res Commun* **337, 517-520.**

Pampin, M., Simonin, Y., Blondel, B., Percherancier, Y. & Chelbi-Alix, M. K. (2006). Cross talk between PML and p53 during poliovirus infection: implications for antiviral defense. *J Virol* **80, 8582-8592.**

Pandolfi, P. P., Alcalay, M., Longo, L., Fagioli, M., Zangrilli, D., Grignani, F., Menccarelli, A., Biondi, A., Rambaldi, A., LoCoco, F. & et al. (1992). Molecular genetics of the t(15;17) of acute promyelocytic leukemia (APPL). *Leukemia* **6 Suppl 3, 120S-122S.**

Pelka, P., Ablack, J. N., Fonseca, G. J., Yousef, A. F. & Mymryk, J. S. (2008). Intrinsic structural disorder in adenovirus E1A: a viral molecular hub linking multiple diverse processes. *J Virol* **82, 7252-7263.**

Pelka, P., Ablack, J. N., Torchia, J., Turnell, A. S., Grand, R. J. & Mymryk, J. S. (2009). Transcriptional control by adenovirus E1A conserved region 3 via p300/CBP. *Nucleic Acids Res* **37, 1095-1106.**

Pennella, M. A., Liu, Y., Woo, J. L., Kim, C. A. & Berk, A. J. (2010). Adenovirus E1B 55-kilodalton protein is a p53-SUMO1 E3 ligase that represses p53 and stimulates its nuclear export through interactions with promyelocytic leukemia nuclear bodies. *J Virol* **84, 12210-12225.**

Percherancier, Y., Germain-Desprez, D., Galisson, F., Mascle, X. H., Dianoux, L., Estephan, P., Chelbi-Alix, M. K. & Aubry, M. (2009). Role of SUMO in RNF4-mediated promyelocytic leukemia protein (PML) degradation: sumoylation of PML and phospho-switch control of its SUMO binding domain dissected in living cells. *J Biol Chem* **284, 16595-16608.**

Perricaudet, M., Akusjarvi, G., Virtanen, A. & Pettersson, U. (1979). Structure of two spliced mRNAs from the transforming region of human subgroup C adenoviruses. *Nature* **281, 694-696.**

Pilder, S., Moore, M., Logan, J. & Shenk, T. (1986). The adenovirus E1B-55K transforming polypeptide modulates transport or cytoplasmic stabilization of viral and host cell mRNAs. *Mol Cell Biol* **6, 470-476.**

Pombo, A., Ferreira, J., Bridge, E. & Carmo-Fonseca, M. (1994). Adenovirus replication and transcription sites are spatially separated in the nucleus of infected cells. *Embo J* **13, 5075-5085.**

Ponten, J. & Saksela, E. (1967). Two established in vitro cell lines from human mesenchymal tumours. *Int J Cancer* 2, 434-447.

Puvion-Dutilleul, F., Chelbi-Alix, M. K., Koken, M., Quignon, F., Puvion, E. & de The, H. (1995). Adenovirus infection induces rearrangements in the intranuclear distribution of the nuclear body-associated PML protein. *Exp Cell Res* 218, 9-16.

Puvion-Dutilleul, F. & Puvion, E. (1991). Sites of transcription of adenovirus type 5 genomes in relation to early viral DNA replication in infected HeLa cells. A high resolution in situ hybridization and autoradiographical study. *Biol Cell* 71, 135-147.

Querido, E., Blanchette, P., Yan, Q., Kamura, T., Morrison, M., Boivin, D., Kaelin, W. G., Conaway, R. C., Conaway, J. W. & Branton, P. E. (2001). Degradation of p53 by adenovirus E4orf6 and E1B55K proteins occurs via a novel mechanism involving a Cullin-containing complex. *Genes Dev* 15, 3104-3117.

Querido, E., Marcellus, R. C., Lai, A., Charbonneau, R., Teodoro, J. G., Ketner, G. & Branton, P. E. (1997). Regulation of p53 levels by the E1B 55-kilodalton protein and E4orf6 in adenovirus-infected cells. *J Virol* 71, 3788-3798.

Reeves, M., Woodhall, D., Compton, T. & Sinclair, J. (2010). Human cytomegalovirus IE72 protein interacts with the transcriptional repressor hDaxx to regulate LUNA gene expression during lytic infection. *J Virol* 84, 7185-7194.

Regad, T. & Chelbi-Alix, M. K. (2001). Role and fate of PML nuclear bodies in response to interferon and viral infections. *Oncogene* 20, 7274-7286.

Regad, T., Saib, A., Lallemand-Breitenbach, V., Pandolfi, P. P., de The, H. & Chelbi-Alix, M. K. (2001). PML mediates the interferon-induced antiviral state against a complex retrovirus via its association with the viral transactivator. *Embo J* 20, 3495-3505.

Reich, N. C., Sarnow, P., Duprey, E. & Levine, A. J. (1983). Monoclonal antibodies which recognize native and denatured forms of the adenovirus DNA-binding protein. *Virology* 128, 480-484.

Reichelt, M., Wang, L., Sommer, M., Perrino, J., Nour, A. M., Sen, N., Baiker, A., Zerboni, L. & Arvin, A. M. (2011). Entrapment of viral capsids in nuclear PML cages is an intrinsic antiviral host defense against varicella-zoster virus. *PLoS Pathog* 7, e1001266.

Rodriguez, M. S., Dargemont, C. & Hay, R. T. (2001). SUMO-1 conjugation in vivo requires both a consensus modification motif and nuclear targeting. *J Biol Chem* 276, 12654-12659.

Rodriguez, M. S., Desterro, J. M., Lain, S., Midgley, C. A., Lane, D. P. & Hay, R. T. (1999). SUMO-1 modification activates the transcriptional response of p53. *Embo J* 18, 6455-6461.

Rosa-Calatrava, M., Puvion-Dutilleul, F., Lutz, P., Dreyer, D., de The, H., Chatton, B. & Kedinger, C. (2003). Adenovirus protein IX sequesters host-cell promyelocytic leukaemia protein and contributes to efficient viral proliferation. *EMBO Rep* 4, 969-975.

Roth, J., Konig, C., Wienzek, S., Weigel, S., Ristea, S. & Dobbelstein, M. (1998). Inactivation of p53 but not p73 by adenovirus type 5 E1B 55-kilodalton and E4 34-kilodalton oncoproteins. *J Virol* 72, 8510-8516.

Rowe, D. T., Graham, F. L. & Branton, P. E. (1983). Intracellular localization of adenovirus type 5 tumor antigens in productively infected cells. *Virology* 129, 456-468.

Rowe, W. P., Huebner, R. J., Gilmore, L. K., Parrott, R. H. & Ward, T. G. (1953). Isolation of a cytopathogenic agent from human adenoids undergoing spontaneous degeneration in tissue culture. *Proc Soc Exp Biol Med* 84, 570-573.

Ruley, H. E. (1983). Adenovirus early region 1A enables viral and cellular transforming genes to transform primary cells in culture. *Nature* 304, 602-606.

Russell, W. C. (2009). Adenoviruses: update on structure and function. *J Gen Virol* 90, 1-20.

Russell, W. C., McIntosh, K. & Skehel, J. J. (1971). The preparation and properties of adenovirus cores. *J Gen Virol* 11, 35-46.

Russell, W. C. & Precious, B. (1982). Nucleic acid-binding properties of adenovirus structural polypeptides. *J Gen Virol* 63 (Pt 1), 69-79.

Rux, J. J. & Burnett, R. M. (2004). Adenovirus structure. *Hum Gene Ther* 15, 1167-1176.

Sadowski, I. & Ptashne, M. (1989). A vector for expressing GAL4(1-147) fusions in mammalian cells. *Nucleic Acids Res* 17, 7539.

Saffert, R. T. & Kalejta, R. F. (2006). Inactivating a cellular intrinsic immune defense mediated by Daxx is the mechanism through which the human cytomegalovirus pp71 protein stimulates viral immediate-early gene expression. *J Virol* 80, 3863-3871.

Saitoh, H. & Hinchey, J. (2000). Functional heterogeneity of small ubiquitin-related protein modifiers SUMO-1 versus SUMO-2/3. *J Biol Chem* 275, 6252-6258.

Salomoni, P., Ferguson, B. J., Wyllie, A. H. & Rich, T. (2008). New insights into the role of PML in tumour suppression. *Cell Res* 18, 622-640.

Salomoni, P. & Pandolfi, P. P. (2002). The role of PML in tumor suppression. *Cell* 108, 165-170.

Salsman, J., Wang, X. & Frappier, L. (2011). Nuclear body formation and PML body remodeling by the human cytomegalovirus protein UL35. *Virology* 414, 119-129.

San Martin, C. & Burnett, R. M. (2003). Structural studies on adenoviruses. *Curr Top Microbiol Immunol* 272, 57-94.

Sarnow, P., Hearing, P., Anderson, C. W., Halbert, D. N., Shenk, T. & Levine, A. J. (1984). Adenovirus early region 1B 58,000-dalton tumor antigen is physically associated with an early region 4 25,000-dalton protein in productively infected cells. *J Virol* 49, 692-700.

Sarnow, P., Sullivan, C. A. & Levine, A. J. (1982). A monoclonal antibody detecting the adenovirus type 5-E1b-58Kd tumor antigen: characterization of the E1b-58Kd tumor antigen in adenovirus-infected and -transformed cells. *Virology* 120, 510-517.

Scaglioni, P. P., Yung, T. M., Cai, L. F., Erdjument-Bromage, H., Kaufman, A. J., Singh, B., Teruya-Feldstein, J., Tempst, P. & Pandolfi, P. P. (2006). A CK2-dependent mechanism for degradation of the PML tumor suppressor. *Cell* 126, 269-283.

Schreiner, S., Burck, C., Glass, M., Groitl, P., Wimmer, P., Kinkley, S., Mund, A., Everett, R. D. & Dobner, T. (2013a). Control of human adenovirus type 5 gene expression by cellular Daxx/ATRX chromatin-associated complexes. *Nucleic Acids Res* 41, 3532-3550.

Schreiner, S., Kinkley, S., Burck, C., Mund, A., Wimmer, P., Schubert, T., Groitl, P., Will, H. & Dobner, T. (2013b). SPOC1-Mediated Antiviral Host Cell Response Is Antagonized Early in Human Adenovirus Type 5 Infection. *PLoS Pathog* 9, e1003775.

Schreiner, S., Martinez, R., Groitl, P., Rayne, F., Vaillant, R., Wimmer, P., Bossis, G., Sternsdorf, T., Marcinowski, L., Ruzsics, Z., Dobner, T. & Wodrich, H. (2012). Transcriptional activation of the adenoviral genome is mediated by capsid protein VI. *PLoS Pathog* 8, e1002549.

Schreiner, S., Wimmer, P., Groitl, P., Chen, S. Y., Blanchette, P., Branton, P. E. & Dobner, T. (2011). Adenovirus type 5 early region 1B 55K oncoprotein-dependent degradation of cellular factor Daxx is required for efficient transformation of primary rodent cells. *J Virol* 85, 8752-8765.

Schreiner, S., Wimmer, P., Sirma, H., Everett, R. D., Blanchette, P., Groitl, P. & Dobner, T. (2010). Proteasome-dependent degradation of Daxx by the viral E1B-55K protein in human adenovirus-infected cells. *J Virol* 84, 7029-7038.

Seeler, J. S. & Dejean, A. (2003). Nuclear and unclear functions of SUMO. *Nat Rev Mol Cell Biol* 4, 690-699.

Seeler, J. S., Marchio, A., Losson, R., Desterro, J. M., Hay, R. T., Chambon, P. & Dejean, A. (2001). Common properties of nuclear body protein SP100 and TIF1alpha chromatin factor: role of SUMO modification. *Mol Cell Biol* 21, 3314-3324.

Seeler, J. S., Marchio, A., Sitterlin, D., Transy, C. & Dejean, A. (1998). Interaction of SP100 with HP1 proteins: a link between the promyelocytic leukemia-associated nuclear bodies and the chromatin compartment. *Proc Natl Acad Sci U S A* 95, 7316-7321.

Shen, T. H., Lin, H. K., Scaglioni, P. P., Yung, T. M. & Pandolfi, P. P. (2006). The mechanisms of PML-nuclear body formation. *Mol Cell* 24, 331-339.

Shenk, T. (2001). Adenoviridae: the viruses and their replication. In *Fields Virology*, 4th edn, pp. 2265-2300.

Shishido-Hara, Y., Higuchi, K., Ohara, S., Duyckaerts, C., Hauw, J. J. & Uchihara, T. (2008). Promyelocytic leukemia nuclear bodies provide a scaffold for human polyomavirus JC replication and are disrupted after development of viral inclusions in progressive multifocal leukoencephalopathy. *J Neuropathol Exp Neurol* 67, 299-308.

Shishido-Hara, Y., Ichinose, S. & Uchihara, T. (2012). JC virus intranuclear inclusions associated with PML-NBs: analysis by electron microscopy and structured illumination microscopy. *Am J Pathol* 180, 1095-1106.

Sides, M. D., Block, G. J., Chadwick, R. W., Shan, B., Flemington, E. K. & Lasky, J. A. (2011). Epstein - Barr virus Latent Membrane Protein 1 suppresses reporter activity through modulation of promyelocytic leukemia protein-nuclear bodies. *Virol J* 8, 461.

Sieber, T. & Dobner, T. (2007). Adenovirus type 5 early region 1B 156R protein promotes cell transformation independently of repression of p53-stimulated transcription. *J Virol* 81, 95-105.

Sivachandran, N., Sarkari, F. & Frappier, L. (2008). Epstein-Barr nuclear antigen 1 contributes to nasopharyngeal carcinoma through disruption of PML nuclear bodies. *PLoS Pathog* 4, e1000170.

Sivachandran, N., Wang, X. & Frappier, L. (2012). Functions of the Epstein-Barr virus EBNA1 protein in viral reactivation and lytic infection. *J Virol* 86, 6146-6158.

Stadler, M., Chelbi-Alix, M. K., Koken, M. H., Venturini, L., Lee, C., Saib, A., Quignon, F., Pelicano, L., Guillemin, M. C., Schindler, C. & et al. (1995). Transcriptional induction of the PML growth suppressor gene by interferons is mediated through an ISRE and a GAS element. *Oncogene* 11, 2565-2573.

Steegenga, W. T., Riteco, N., Jochemsen, A. G., Fallaux, F. J. & Bos, J. L. (1998). The large E1B protein together with the E4orf6 protein target p53 for active degradation in adenovirus infected cells. *Oncogene* 16, 349-357.

Stephens, C. & Harlow, E. (1987). Differential splicing yields novel adenovirus 5 E1A mRNAs that encode 30 kd and 35 kd proteins. *Embo J* 6, 2027-2035.

Stepp, W. H., Meyers, J. M. & McBride, A. A. (2013). Sp100 provides intrinsic immunity against human papillomavirus infection. *MBio* 4, e00845-00813.

Sternsdorf, T., Jensen, K., Reich, B. & Will, H. (1999). The nuclear dot protein sp100, characterization of domains necessary for dimerization, subcellular localization, and modification by small ubiquitin-like modifiers. *J Biol Chem* 274, 12555-12566.

Sternsdorf, T., Jensen, K. & Will, H. (1997). Evidence for covalent modification of the nuclear dot-associated proteins PML and Sp100 by PIC1/SUMO-1. *J Cell Biol* 139, 1621-1634.

Stindt, M. H., Carter, S., Vigneron, A. M., Ryan, K. M. & Vousden, K. H. (2011). MDM2 promotes SUMO-2/3 modification of p53 to modulate transcriptional activity. *Cell Cycle* 10, 3176-3188.

Stracker, T. H., Carson, C. T. & Weitzman, M. D. (2002). Adenovirus oncoproteins inactivate the Mre11-Rad50-NBS1 DNA repair complex. *Nature* 418, 348-352.

Stracker, T. H., Lee, D. V., Carson, C. T., Araujo, F. D., Ornelles, D. A. & Weitzman, M. D. (2005). Serotype-specific reorganization of the Mre11 complex by adenoviral E4orf3 proteins. *J Virol* 79, 6664-6673.

Stuurman, N., de Graaf, A., Floore, A., Josso, A., Humbel, B., de Jong, L. & van Driel, R. (1992). A monoclonal antibody recognizing nuclear matrix-associated nuclear bodies. *J Cell Sci* 101 (Pt 4), 773-784.

Szekely, L., Kiss, C., Mattsson, K., Kashuba, E., Pokrovskaja, K., Juhasz, A., Holmvall, P. & Klein, G. (1999). Human herpesvirus-8-encoded LNA-1 accumulates in heterochromatin-associated nuclear bodies. *J Gen Virol* 80 (Pt 11), 2889-2900.

Szostecki, C., Guldner, H. H., Netter, H. J. & Will, H. (1990). Isolation and characterization of cDNA encoding a human nuclear antigen predominantly recognized by autoantibodies from patients with primary biliary cirrhosis. *J Immunol* 145, 4338-4347.

Szostecki, C., Krippner, H., Penner, E. & Bautz, F. A. (1987). Autoimmune sera recognize a 100 kD nuclear protein antigen (sp-100). *Clin Exp Immunol* 68, 108-116.

Szostecki, C., Will, H., Netter, H. J. & Guldner, H. H. (1992). Autoantibodies to the nuclear Sp100 protein in primary biliary cirrhosis and associated diseases: epitope specificity and immunoglobulin class distribution. *Scand J Immunol* 36, 555-564.

Tang, Q., Bell, P., Tegtmeyer, P. & Maul, G. G. (2000). Replication but not transcription of simian virus 40 DNA is dependent on nuclear domain 10. *J Virol* 74, 9694-9700.

Tashiro, S., Muto, A., Tanimoto, K., Tsuchiya, H., Suzuki, H., Hoshino, H., Yoshida, M., Walter, J. & Igarashi, K. (2004). Repression of PML nuclear body-associated transcription by oxidative stress-activated Bach2. *Mol Cell Biol* 24, 3473-3484.

Tatham, M. H., Geoffroy, M. C., Shen, L., Plechanovova, A., Hattersley, N., Jaffray, E. G., Palvimo, J. J. & Hay, R. T. (2008). RNF4 is a poly-SUMO-specific E3 ubiquitin ligase required for arsenic-induced PML degradation. *Nat Cell Biol* 10, 538-546.

Tatham, M. H., Jaffray, E., Vaughan, O. A., Desterro, J. M., Botting, C. H., Naismith, J. H. & Hay, R. T. (2001). Polymeric chains of SUMO-2 and SUMO-3 are conjugated to protein substrates by SAE1/SAE2 and Ubc9. *J Biol Chem* 276, 35368-35374.

Tatham, M. H., Rodriguez, M. S., Xirodimas, D. P. & Hay, R. T. (2009). Detection of protein SUMOylation in vivo. *Nat Protoc* 4, 1363-1371.

Tauber, B. & Dobner, T. (2001a). Adenovirus early E4 genes in viral oncogenesis. *Oncogene* 20, 7847-7854.

Tauber, B. & Dobner, T. (2001b). Molecular regulation and biological function of adenovirus early genes: the E4 ORFs. *Gene* 278, 1-23.

Tavalai, N., Adler, M., Scherer, M., Riedl, Y. & Stamminger, T. (2011). Evidence for a dual antiviral role of the major nuclear domain 10 component Sp100 during the immediate-early and late phases of the human cytomegalovirus replication cycle. *J Virol* 85, 9447-9458.

Tavalai, N. & Stamminger, T. (2008). New insights into the role of the subnuclear structure ND10 for viral infection. *Biochim Biophys Acta* 1783, 2207-2221.

Taylor, J. L., Unverrich, D., O'Brien, W. J. & Wilcox, K. W. (2000). Interferon coordinately inhibits the disruption of PML-positive ND10 and immediate-early gene expression by herpes simplex virus. *J Interferon Cytokine Res* 20, 805-815.

Teodoro, J. G. & Branton, P. E. (1997). Regulation of p53-dependent apoptosis, transcriptional repression, and cell transformation by phosphorylation of the 55-kilodalton E1B protein of human adenovirus type 5. *J Virol* 71, 3620-3627.

Tsai, K., Thikmyanova, N., Wojcechowskyj, J. A., Delecluse, H. J. & Lieberman, P. M. (2011). EBV tegument protein BNRF1 disrupts DAXX-ATRX to activate viral early gene transcription. *PLoS Pathog* 7, e1002376.

Turelli, P., Doucas, V., Craig, E., Mangeat, B., Klages, N., Evans, R., Kalpana, G. & Trono, D. (2001). Cytoplasmic recruitment of INI1 and PML on incoming HIV preintegration complexes: interference with early steps of viral replication. *Mol Cell* 7, 1245-1254.

Turnell, A. S. & Grand, R. J. (2012). DNA viruses and the cellular DNA-damage response. *J Gen Virol* 93, 2076-2097.

Ulfendahl, P. J., Linder, S., Kreivi, J. P., Nordqvist, K., Sevensson, C., Hultberg, H. & Akusjarvi, G. (1987). A novel adenovirus-2 E1A mRNA encoding a protein with transcription activation properties. *Embo J* 6, 2037-2044.

Ullman, A. J. & Hearing, P. (2008). Cellular proteins PML and Daxx mediate an innate antiviral defense antagonized by the adenovirus E4 ORF3 protein. *J Virol* 82, 7325-7335.

Ullman, A. J., Reich, N. C. & Hearing, P. (2007). Adenovirus E4 ORF3 protein inhibits the interferon-mediated antiviral response. *J Virol* 81, 4744-4752.

Ulrich, H. D. (2009). The SUMO system: an overview. *Methods Mol Biol* 497, 3-16.

Van Damme, E., Laukens, K., Dang, T. H. & Van Ostade, X. (2010). A manually curated network of the PML nuclear body interactome reveals an important role for PML-NBs in SUMOylation dynamics. *Int J Biol Sci* 6, 51-67.

Van Damme, E. & Van Ostade, X. (2011). Crosstalk between viruses and PML nuclear bodies: a network-based approach. *Front Biosci* 17, 2910-2920.

van Ormondt, H., Maat, J. & Dijkema, R. (1980). Comparison of nucleotide sequences of the early E1a regions for subgroups A, B and C of human adenoviruses. *Gene* 12, 63-76.

Varga, M. J., Weibull, C. & Everitt, E. (1991). Infectious entry pathway of adenovirus type 2. *J Virol* 65, 6061-6070.

Vellinga, J., Van der Heijdt, S. & Hoeben, R. C. (2005). The adenovirus capsid: major progress in minor proteins. *J Gen Virol* 86, 1581-1588.

Verger, A., Perdomo, J. & Crossley, M. (2003). Modification with SUMO. A role in transcriptional regulation. *EMBO Rep* 4, 137-142.

Vertegaal, A. C. (2007). Small ubiquitin-related modifiers in chains. *Biochem Soc Trans* 35, 1422-1423.

von Mikecz, A., Zhang, S., Montminy, M., Tan, E. M. & Hemmerich, P. (2000). CREB-binding protein (CBP)/p300 and RNA polymerase II colocalize in transcriptionally active domains in the nucleus. *J Cell Biol* 150, 265-273.

Wadell, G. (1984). Molecular epidemiology of human adenoviruses. *Curr Top Microbiol Immunol* 110, 191-220.

Wang, G. & Berk, A. J. (2002). In vivo association of adenovirus large E1A protein with the human mediator complex in adenovirus-infected and -transformed cells. *J Virol* 76, 9186-9193.

Wang, J., Shiels, C., Sasieni, P., Wu, P. J., Islam, S. A., Freemont, P. S. & Sheer, D. (2004). Promyelocytic leukemia nuclear bodies associate with transcriptionally active genomic regions. *J Cell Biol* 164, 515-526.

Wang, L., Oliver, S. L., Sommer, M., Rajamani, J., Reichelt, M. & Arvin, A. M. (2011). Disruption of PML nuclear bodies is mediated by ORF61 SUMO-interacting motifs and required for varicella-zoster virus pathogenesis in skin. *PLoS Pathog* 7, e1002157.

Wang, Z. G., Delva, L., Gaboli, M., Rivi, R., Giorgio, M., Cordon-Cardo, C., Grosveld, F. & Pandolfi, P. P. (1998). Role of PML in cell growth and the retinoic acid pathway. *Science* 279, 1547-1551.

Wasylyk, C., Schlumberger, S. E., Criqui-Filipe, P. & Wasylyk, B. (2002). Sp100 interacts with ETS-1 and stimulates its transcriptional activity. *Mol Cell Biol* 22, 2687-2702.

Webster, A., Russell, S., Talbot, P., Russell, W. C. & Kemp, G. D. (1989). Characterization of the adenovirus proteinase: substrate specificity. *J Gen Virol* 70 (Pt 12), 3225-3234.

Webster, L. C. & Ricciardi, R. P. (1991). trans-dominant mutants of E1A provide genetic evidence that the zinc finger of the trans-activating domain binds a transcription factor. *Mol Cell Biol* 11, 4287-4296.

Weiden, M. D. & Ginsberg, H. S. (1994). Deletion of the E4 region of the genome produces adenovirus DNA concatemers. *Proc Natl Acad Sci U S A* 91, 153-157.

Weigel, S. & Dobbelstein, M. (2000). The nuclear export signal within the E4orf6 protein of adenovirus type 5 supports virus replication and cytoplasmic accumulation of viral mRNA. *J Virol* 74, 764-772.

Weinmann, R., Raskas, H. J. & Roeder, R. G. (1974). Role of DNA-dependent RNA polymerases II and III in transcription of the adenovirus genome late in productive infection. *Proc Natl Acad Sci U S A* 71, 3426-3439.

Weis, K., Rambaud, S., Lavau, C., Jansen, J., Carvalho, T., Carmo-Fonseca, M., Lamond, A. & Dejean, A. (1994). Retinoic acid regulates aberrant nuclear localization of PML-RAR alpha in acute promyelocytic leukemia cells. *Cell* 76, 345-356.

White, E. (1993). Regulation of apoptosis by the transforming genes of the DNA tumor virus adenovirus. *Proc Soc Exp Biol Med* 204, 30-39.

White, E. (2001). Regulation of the cell cycle and apoptosis by the oncogenes of adenovirus. *Oncogene* 20, 7836-7846.

Whyte, P., Buchkovich, K. J., Horowitz, J. M., Friend, S. H., Raybuck, M., Weinberg, R. A. & Harlow, E. (1988). Association between an oncogene and an anti-oncogene: the adenovirus E1A proteins bind to the retinoblastoma gene product. *Nature* 334, 124-129.

Wickham, T. J., Filardo, E. J., Cheresh, D. A. & Nemerow, G. R. (1994). Integrin alpha v beta 5 selectively promotes adenovirus mediated cell membrane permeabilization. *J Cell Biol* 127, 257-264.

Wickham, T. J., Mathias, P., Cheresh, D. A. & Nemerow, G. R. (1993). Integrins alpha v beta 3 and alpha v beta 5 promote adenovirus internalization but not virus attachment. *Cell* 73, 309-319.

Wiethoff, C. M., Wodrich, H., Gerace, L. & Nemerow, G. R. (2005). Adenovirus protein VI mediates membrane disruption following capsid disassembly. *J Virol* 79, 1992-2000.

Wilkinson, G. W., Kelly, C., Sinclair, J. H. & Rickards, C. (1998). Disruption of PML-associated nuclear bodies mediated by the human cytomegalovirus major immediate early gene product. *J Gen Virol* 79 (Pt 5), 1233-1245.

Wimmer, P. (2010). Analysis of the Modulation of Nuclear Domains by Human Adenovirus Type 5 Oncoproteins: PhD thesis. University of Hamburg.

Wimmer, P., Schreiner, S. & Dobner, T. (2012). Human pathogens and the host cell SUMOylation system. *J Virol* 86, 642-654.

Wimmer, P., Schreiner, S., Everett, R. D., Sirma, H., Groitl, P. & Dobner, T. (2010). SUMO modification of E1B-55K oncoprotein regulates isoform-specific binding to the tumour suppressor protein PML. *Oncogene* 29, 5511-5522.

Winberg, G. & Shenk, T. (1984). Dissection of overlapping functions within the adenovirus type 5 E1A gene. *Embo J* 3, 1907-1912.

Wu, E., Pache, L., Von Seggern, D. J., Mullen, T. M., Mikyas, Y., Stewart, P. L. & Nemerow, G. R. (2003). Flexibility of the adenovirus fiber is required for efficient receptor interaction. *J Virol* 77, 7225-7235.

Wu, F. Y., Ahn, J. H., Alcendor, D. J., Jang, W. J., Xiao, J., Hayward, S. D. & Hayward, G. S. (2001). Origin-independent assembly of Kaposi's sarcoma-associated herpesvirus DNA replication compartments in transient cotransfection assays and association with the ORF-K8 protein and cellular PML. *J Virol* 75, 1487-1506.

Xie, K., Lambie, E. J. & Snyder, M. (1993). Nuclear dot antigens may specify transcriptional domains in the nucleus. *Mol Cell Biol* 13, 6170-6179.

Yew, P. R. & Berk, A. J. (1992). Inhibition of p53 transactivation required for transformation by adenovirus early 1B protein. *Nature* 357, 82-85.

Yew, P. R., Liu, X. & Berk, A. J. (1994). Adenovirus E1B oncoprotein tethers a transcriptional repression domain to p53. *Genes Dev* 8, 190-202.

Yolken, R. H., Lawrence, F., Leister, F., Takiff, H. E. & Strauss, S. E. (1982). Gastroenteritis associated with enteric type adenovirus in hospitalized infants. *J Pediatr* 101, 21-26.

Yondola, M. A. & Hearing, P. (2007). The adenovirus E4 ORF3 protein binds and reorganizes the TRIM family member transcriptional intermediary factor 1 alpha. *J Virol* 81, 4264-4271.

Yousef, A. F., Fonseca, G. J., Pelka, P., Ablack, J. N., Walsh, C., Dick, F. A., Bazett-Jones, D. P., Shaw, G. S. & Mymryk, J. S. (2010). Identification of a molecular recognition feature in the E1A oncoprotein that binds the SUMO conjugase UBC9 and likely interferes with polySUMOylation. *Oncogene* 29, 4693-4704.

Zhang, W., Low, J. A., Christensen, J. B. & Imperiale, M. J. (2001). Role for the adenovirus IVa2 protein in packaging of viral DNA. *J Virol* **75, 10446-10454.**

Zhong, S., Muller, S., Ronchetti, S., Freemont, P. S., Dejean, A. & Pandolfi, P. P. (2000a). Role of SUMO-1-modified PML in nuclear body formation. *Blood* **95, 2748-2752.**

Zhong, S., Salomoni, P. & Pandolfi, P. P. (2000b). The transcriptional role of PML and the nuclear body. *Nat Cell Biol* **2, E85-90.**

Zhong, S., Salomoni, P., Ronchetti, S., Guo, A., Ruggero, D. & Pandolfi, P. P. (2000c). Promyelocytic leukemia protein (PML) and Daxx participate in a novel nuclear pathway for apoptosis. *J Exp Med* **191, 631-640.**

Zhu, Z., Zhang, Y., Xu, S., Yu, P., Tian, X., Wang, L., Liu, Z., Tang, L., Mao, N., Ji, Y., Li, C., Yang, Z., Wang, S., Wang, J., Li, D. & Xu, W. (2009). Outbreak of acute respiratory disease in China caused by B2 species of adenovirus type 11. *J Clin Microbiol* **47, 697-703.**

Publications

I. Publications in scientific journals

- Yip CK, **Berscheminski J**, Walz T. *Molecular architecture of the TRAPPII complex and implications for vesicle tethering.* Nat Struct Mol Biol. 2010 Nov; 17(11): 1298-304.
- **Berscheminski J**, Groitl P, Dobner T, Wimmer P & Schreiner S. *The adenoviral oncogene E1A-13S interacts with a specific isoform of the tumor suppressor PML to enhance viral transcription.* J Virol. 2013 Jan; 87(2): 965-77.
- Wimmer P, Blanchette P, Schreiner S, Ching W, Groitl P, **Berscheminski J**, Branton, PE, Will H & Dobner T. *Cross-talk between phosphorylation and SUMOylation regulates transforming activities of an adenoviral oncoprotein.* Oncogene 2013 Mar; 32(13): 1626-37.
- **Berscheminski, J.**, Wimmer P, Brun J, Ip, WH, Groitl P, Jaffray E, Hay RT, Dobner T & Schreiner S. *Sp100 isoform-specific regulation of human Adenovirus type 5 (Ad5) gene expression.* J Virol. under review.

II. Oral presentations at scientific meeting

- GfV-Workshop on the Cell Biology of Viral Infections, Deidesheim, Germany (2011)
- Small DNA Tumor Virus Meeting Montreal, Canada (2012)
- GfV-Workshop on the Cell Biology of Viral Infections, Deidesheim, Germany (2012)
- DNA Tumor Virus Meeting Birmingham, UK (2013)
- GfV-Workshop on the Cell Biology of Viral Infections, Deidesheim, Germany (2013)

III. Poster presentations at scientific meetings

- 21st Annual Meeting of the GfV (Society for Virology) and DVV, Freiburg, Germany (2011)
- 23st Annual Meeting of the GfV (Society for Virology) and DVV, Kiel, Germany (2013)

IV. Participation in scientific meetings/workshops

- Adenovirus workshop Regensburg, Germany (2011)
- Soft skill course: Communication & presentation in the academic context, Hamburg, Germany (2012)
- Soft skill course: Effective Scientific Writing, Hamburg, Germany (2012)
- Adenovirus workshop Hannover, Germany (2013)

Acknowledgements

First, I would like to thank my supervisor Thomas Dobner for giving me the opportunity to be part of the great Dobner lab as well as guidance and support.

Thank you to the members of the advisory committee for evaluating my thesis and my second supervisor Nicole Fischer for critical review of my work and suggestions. Furthermore, I want to thank Julia Kehr for kindly accepting to evaluate and chair my oral thesis defense.

I extend my gratitude to all people involved in this work and our collaborators for kindly providing reagents as well as for critical comments and scientific discussions. Thank you to Peter Groitl (HPI, Hamburg, Germany), Thomas Speiseder (HPI, Hamburg, Germany), Hans Will (HPI, Hamburg, Germany), Thomas Sternsdorf (Kinderkrebs-Zentrum Hamburg, Germany), Roger Everett (MRC Virology UNIT, Glasgow, UK), Roger Grand (Cancer Research, Birmingham, UK) and Andy Turnell (Cancer Research, Birmingham, UK).

I owe special thanks to Ron Hay (University of Dundee, UK) for giving me the opportunity to stay at his laboratory in Dundee. In this context, I would like to acknowledge the whole Ron Hay lab members for kindly taking me as a new short-time lab member and particularly Ellis Jaffray for constructive suggestions and training on methods and equipment.

I would also like to take this opportunity to acknowledge the people who helped me over the partly frustrating times and made the good days even more pleasant. Thank you to the whole Dobner lab, particularly the Dungeoneers: the Platoon Leader Sabrina Schreiner, Peter ("Bind's?") Wimmer, Carolin Bürck aka Dr. Bü, Remi Vaillant aka Jean-Claude and the Dungeon Joungsters Wing Hang Ip, Maggie Valdes-Aleman, Nora Freudenberger and Jana Kondrajew.

Additionally, I would like to acknowledge the Heinrich Pette Institute for the Mobility grant and funding of several scientific meetings and soft skill courses. Also thank you to the University Hamburg and the GlaxosmithKline Foundation for funding of scientific meetings.

Finally, I would like to thank my family and Bastian Gruhne for their support during my PhD time and for enduring my temper especially during the final part of my thesis.

Abstract (German)

PML Kerndomänen (PML-NBs) sind Matrix-gebundene, nukleäre Strukturen, die mit einer Vielzahl von Funktionen, einschließlich DNA Reparatur, transkriptionelle Regulation, Proteinabbau und Tumorsuppression verbunden sind. Diese Multiproteinkomplexe spielen außerdem eine essentielle Rolle bei der antiviralen Immunabwehr der Wirtszelle, welche durch Akkumulation von SUMO-abhängigen und Interferon-induzierten Wirtsfaktoren vermittelt wird. Um solchen immunmodulatorischen Vorgängen entgegenzuwirken, werden PML-NBs von zahlreichen viralen Regulatorproteinen manipuliert. Paradoxerweise dazu assoziieren hauptsächlich DNA-Virusgenome an den PML-NBs und virale Transkriptions-/Replikationszentren werden folglich in ihrer Nähe initiiert.

Da für einige Ad Regulatorproteine bereits eine enge Assoziation mit den PML-NBs beschrieben wurde, wird eine entscheidende Rolle dieser Kerndomänen im Ad Lebenszyklus vermutet, wobei die funktionellen Konsequenzen dieser Wechselwirkungen weitgehend unbekannt sind. Das frühe Ad5 Regulatorprotein E1B-55K scheint dabei einen zentralen Faktor darzustellen, da bereits SUMO-abhängige, funktionelle Interaktionen mit verschiedenen PML-NB-assoziierten Wirtsfaktoren beobachtet wurden. Ziel dieser Arbeit war die Aufklärung der feinregulierten Wechselwirkungen zwischen Ad Regulatorproteinen und Komponenten der zellulären PML-NBs, um das Verständnis dieser Wirtsstrukturen bezüglich ihrer Rolle in der Ad5 Infektion zu erweitern.

Im ersten Teil der Arbeit konnte gezeigt werden, dass der Ad5 Haupttransaktivator E1A-13S an den PML-NBs lokalisiert. Koimmunopräzipitationsexperimente belegten, dass E1A-13S bevorzugt mit PML-II, einer von mindesten sechs nukleären Isoformen des humanen PML Proteins interagiert. Genau diese PML-II Isoform ist ebenfalls an der Ad induzierten Umlokalisierung von PML-NBs in elongierte, fibrilläre Strukturen, den sogenannten *PML track-like structures*, beteiligt. Mit Hilfe von Deletionsmutanten konnte der Interaktionsbereich mit PML-II innerhalb der CR3 (*conserved region 3*) Region von E1A-13S lokalisiert werden. Diese Region im adenoviralen Protein wurde zuvor bereits als Bindestelle für zahlreiche andere Transkriptionsfaktoren beschrieben. Tatsächlich verstärkte die Kooperation mit PML-II die E1A-13S-vermittelte Aktivierung der zellulären sowie adenoviralen Transkription. Diese Ergebnisse deuten darauf hin, dass PML-II im Gegensatz zur zunächst postulierten antiviralen Funktion der PML-NBs, die virale Genexpression humaner Adenoviren positiv beeinflusst.

Der zweite Teil der Arbeit beschäftigt sich mit der Rolle des PML-NB-assoziierten, Transkriptionsfaktors Sp100 während der produktiven Ad5 Infektion. Die Abwesenheit von Sp100 mittels RNAi-basierten Techniken führte zur verstärkten Ad Replikation und zur gesteigerten viralen Genexpression. Die Sp100-vermittelte Repression der Virusvermehrung zeigte sich abhängig von der Expression der Sp100 Isoformen B, C und HMG, welche die virale Genexpression bereits auf der Transkriptionsebene inhibierten. Im Gegensatz dazu aktivierte Sp100A die Transkription von viralen und zellulären Promotoren in Reportergenversuchen.

Basierend auf den erhobenen Befunden nehmen wir an, dass humane Adenoviren der Sp100-vermittelten Restriktion entgegenwirken, um die effiziente virale Replikation sicherzustellen. Einerseits konnte eine Ad5-vermittelte Umlokalisierung von Sp100B, C und HMG von den PML-NBs weg beobachtet werden, wohingegen Sp100A an den *PML track-like structures* zurückgehalten wird, welche die neugebildeten viralen Replikationszentren, und somit die Orte der aktiven viralen Transkription darstellen. Der zusätzlich nachgewiesene Virus-induzierte Verlust der Sp100 SUMOylierung scheint einen weiteren Teil des viralen Repertoires zur Hemmung der intrinsischen Immunität darzustellen. Weitere Daten zeigen, dass die DeSUMOylierung von Sp100 zur verminderten Assoziation mit dem Heterochromatinprotein 1 (HP1) führt und vermutlich die Kondensation von Chromatin einschränkt. Zusätzliche Ergebnisse zeigen außerdem, dass E1B-55K mittels seiner C-terminalen Domäne in Abhängigkeit der eigenen SUMO Modifikation nur mit Sp100A interagiert, was zur Rekrutierung von Sp100A zu den PML-NBs führt.

Zusammengefasst liefert diese Arbeit wichtige Hinweise dafür, dass Ad antiviralen Immunantworten selektiv entgegenwirkt und gleichzeitig von proviralen PML-NB-assoziierten Transkriptionsfaktoren profitiert, indem positive Faktoren aktiv zu den *PML track-like structures* rekrutiert werden, um ein provirales Umfeld zur effizienten Genexpression an diesen nukleären Subdomänen zu schaffen.